



Université du Québec
à Rimouski

VERS UNE NOUVELLE VOIE DE VALORISATION DE LA DRÊCHE DE BRASSERIE

**Étude de la solubilisation de la drêche pour la production de produits
d'hygiène personnelle plus durables**

Mémoire présenté

dans le cadre du programme de maîtrise sur mesure (chimie)

en vue de l'obtention du grade de maître ès sciences

PAR

© Amy McMackin

Novembre 2022

Composition du jury :

Richard St-Louis, président du jury, Université du Québec à Rimouski

Sébastien Cardinal, directeur de recherche, Université du Québec à Rimouski

François Brouillette, examinateur externe, Université du Québec à Trois-Rivières

**Vincent Banville, examinateur externe, Centre de développement bioalimentaire du
Québec**

Dépôt initial le 14 août 2022

Dépôt final le 18 novembre 2022

UNIVERSITÉ DU QUÉBEC À RIMOUSKI
Service de la bibliothèque

Avertissement

La diffusion de ce mémoire ou de cette thèse se fait dans le respect des droits de son auteur, qui a signé le formulaire « *Autorisation de reproduire et de diffuser un rapport, un mémoire ou une thèse* ». En signant ce formulaire, l'auteur concède à l'Université du Québec à Rimouski une licence non exclusive d'utilisation et de publication de la totalité ou d'une partie importante de son travail de recherche pour des fins pédagogiques et non commerciales. Plus précisément, l'auteur autorise l'Université du Québec à Rimouski à reproduire, diffuser, prêter, distribuer ou vendre des copies de son travail de recherche à des fins non commerciales sur quelque support que ce soit, y compris Internet. Cette licence et cette autorisation n'entraînent pas une renonciation de la part de l'auteur à ses droits moraux ni à ses droits de propriété intellectuelle. Sauf entente contraire, l'auteur conserve la liberté de diffuser et de commercialiser ou non ce travail dont il possède un exemplaire.

Rien ne se perd, rien ne se crée, tout se transforme.

- *Antoine Lavoisier*

ACKNOWLEDGEMENTS

This work concludes several wonderful years of learning at the Université du Québec à Rimouski. I am eternally grateful for the opportunities this institution has provided me, both academically and otherwise. Notably, I would like to thank Professor Sébastien Cardinal, my graduate supervisor. I am so grateful for his precious expertise and guidance, and for his unfaltering belief in me from day one.

I am also incredibly appreciative to have had the chance to spend a year of my studies leaning from the professionals at the Centre de développement bioalimentaire du Québec (CDBQ). My time here was a unique and invaluable experience that allowed me to learn from a team of talented and motivated researchers. I am especially grateful for the guidance I received from Charles Emond, Vincent Banville, and Charles Lavigne.

Simple thanks do not suffice to acknowledge all the love and encouragement I've felt from my friends, family, and colleagues over the years. I am so very honoured to be surrounded by so many wonderful people who have made my years in the Lower-Saint-Lawrence so memorable. Of course, a very special thank you to my partner, Ciri, for his endless support throughout this project, no matter the many kilometers between us. *Merci.*

This research was conducted thanks to the financial support of the MITACS Accelerate program, the Partenariat canadien pour l'agriculture, the Fonds de recherche Nature et Technologies du Québec, and the Centre de développement bioalimentaire du Québec. I also wish to acknowledge the financial contributions of the Collectif de recherche appliquée aux bioprocédés et à la chimie de l'environnement (CRABE) at the Université du Québec à Rimouski, the Institut de nutrition et des aliments fonctionnels (INAF) at Université Laval, and the Programme de mobilité étudiante hors Québec (PMISCE) for the opportunity to present this research at local and international conferences. Finally, many thanks to the Le Bien le Malt (Rimouski) and Ras L'Bock (La Pocatière) microbreweries for providing me with more than enough brewer's spent grain to complete this project.

FORWARD

This dissertation is mostly presented in the form of two articles to be submitted to scientific journals (Chapters 2 and 3). A fourth chapter containing results complimentary to the information presented in the two articles will not be submitted for publication.

Contribution of the authors

While Sébastien Cardinal, Vincent Banville, and Charles Emond are co-authors of the articles, this manuscript must be considered as the student's thesis.

S. Cardinal, V. Banville, and C. Emond guided the student in planning the work in the laboratory, the scale-up process, and the technoeconomic assessment of the method. S. Cardinal also provided guidance during the preparation of the thesis. A. McMackin realized the laboratory and pilot-scale optimization, production, and analyses, and wrote the scientific articles and general manuscript presented herein.

RÉSUMÉ

Le nombre de microbrasseries au Québec a considérablement augmenté au cours des dernières années, augmentant de plus de 700 % de 2002 à 2020. En conséquence, une quantité de plus en plus importante de coproduits est générée. Notamment, la drêche de brasserie représente environ 85 % du total des coproduits, mais reste un résidu important et sous-évalué, sa principale utilisation actuelle étant comme composant de l'alimentation animale. D'ailleurs, la demande pour la drêche pour cette application est déjà inférieure à l'offre disponible et la distance entre les brasseries et les fermes d'élevage est un facteur limitant. Cette étude propose une nouvelle utilisation de la drêche comme matière première pour la production de microbilles biodégradables pour les produits d'hygiène personnelle. La méthodologie est inspirée d'un processus préexistant pour la production de microbilles à partir de solutions de 3 à 7 % massique en cellulose purifiée. Ce projet permet de réduire la teneur en cellulose purifiée à 2 % massique, obtenant plutôt la matière solide requise directement à partir de la matrice lignocellulosique de la drêche. La nature composite des billes résultantes leur confère de meilleures propriétés mécaniques, permettant leur utilisation comme particules exfoliantes dans les savons et gommages. Cette application envisagée est validée par la mise à l'échelle pilote du procédé et une évaluation technico-économique de la méthode (Chapitre 4). Au cours des dernières décennies, les produits d'hygiène personnelle ont été formulés avec des microbilles de plastique synthétiques, qui ont été liés à la pollution des écosystèmes aquatiques, à la bioaccumulation dans les organismes marins et au transfert vers des niveaux trophiques supérieurs de la chaîne alimentaire. En conséquence, leur production et leur vente ont récemment été interdites dans de nombreux pays, dont le Canada, d'où l'intérêt de développer des microbilles biodégradables à partir de la drêche (Chapitre 2). Autrement, une deuxième méthode permet la mise en solution complète de la drêche. Le produit final de cette méthode a aussi le potentiel d'être utilisé comme exfoliant physique dans les produits d'hygiène personnelle, même si les particules obtenues comme produit final manquent de sphéricité et d'uniformité (Chapitre 3). Globalement, cette étude permet de faire d'une pierre deux coups en offrant une nouvelle utilisation au principal résidu de l'industrie brassicole en développant une solution alternative aux microbilles de plastique conventionnelles.

Mots-clés : *drêche de brasserie, cellulose, microbilles, biodégradable, chimie verte*

ABSTRACT

The number of microbreweries in Quebec has grown significantly over the past several years, increasing by more than 700% from 2002 to 2020. Consequently, an increasing quantity of co-products is generated. Brewer's spent grain (BSG) represents approximately 85% of the total co-products but is an undervalued residue, as it is primarily used as an animal feedstock. This use is logistically challenging, as wet BSG has a short shelf-life and breweries are often at an inconvenient distance from animal husbandry farms. Moreover, the demand for BSG as an animal feedstock is lower than the supply available. This project proposes a novel use for BSG as the starting material for biodegradable, exfoliating microbeads. The methodology is inspired by a process for the production of cellulose microbeads, which uses 3 to 7 wt% purified, pretreated cellulose in the beads' formulation. The protocol presented herein reduces this to 2 wt% and the remaining required solid matter is directly obtained from the lignocellulosic matrix of humid BSG. The resulting composite nature of the beads grants their superior mechanical strength and stability, allowing for their use as exfoliating particles in soap and other personal hygiene products. This envisioned application for the microbeads is further validated by the scale-up of the protocol and a techno-economic assessment of the method (Chapter 4). Over the past few decades, exfoliating personal hygiene products have been formulated with synthetic plastic microbeads, which have been linked to the pollution of aqueous ecosystems, bioaccumulation in marine organisms, and transfer to superior trophic levels of the food chain. As a result, their production and sale have recently been banned in many countries, including Canada; hence the interest in developing a biodegradable alternative for exfoliating microbeads from BSG (Chapter 2). Otherwise, a second method described herein allows for the one-pot complete dissolution of BSG. The final product of this method has the potential to be used as a physical exfoliant in personal hygiene products, even though these particles lack sphericity and batch uniformity (Chapter 3). Overall, this study simultaneously yields a novel use for the primary residue of an ever-growing industry and provides an ecological alternative to conventional plastic microbeads.

Keywords: *Brewer's Spent Grain, Cellulose, Microbeads, Biodegradable, Green Chemistry*

TABLE OF CONTENTS

ACKNOWLEDGEMENTS.....	ix
FORWARD	xi
RÉSUMÉ	xiii
ABSTRACT.....	xv
TABLE OF CONTENTS.....	xvii
LIST OF TABLES.....	xxi
LIST OF FIGURES	xxiii
LIST OF ABBREVIATIONS AND ACRONYMS	xxviii
LIST OF SYMBOLS	xxx
CHAPTER 1 GENERAL INTRODUCTION	1
1.1 CONTEXT	1
1.1.1 A brief history of beer consumption and production.....	1
1.1.2 Situation in Quebec – a local perspective.....	5
1.1.3 Composition of brewer’s spent grain	7
1.1.4 Previously reported applications of brewer’s spent grain	12
1.1.5 Complete valorization of brewer’s spent grain	14
1.2 NATURAL POLYMERS	17
1.3 EXFOLIATING MICROBEADS IN PERSONAL HYGIENE PRODUCTS	19
1.3.1 Plastic pollution and microbeads.....	19
1.3.2 Nature and fate of microbeads in personal hygiene products.....	20
1.3.3 Current alternatives for microbeads in personal hygiene products	22
1.3.4 Microbeads in personal hygiene products – required characteristics	24
1.4 OBJECTIVES	25
1.4.1 Objective 1.....	25
1.4.2 Objective 2.....	26

1.4.3 Objective 3	26
1.5 METHODOLOGY AND PRECEDENTS	27
1.5.1 General.....	27
1.5.2 Pretreatment methods.....	28
1.5.3 Solubilization systems	31
1.5.4 Microbead production.....	38
1.5.5 Characterization methods adapted to microbeads and microparticles	47
1.6 ORGANIZATION OF THE CHAPTERS.....	52
CHAPTER 2 BIODEGRADABLE SPHERICAL MICROBEADS FROM BREWER’S SPENT GRAIN FOR SUSTAINABLE PERSONAL HYGIENE PRODUCTS.....	56
2.1 FRENCH ABSTRACT AND CONTEXT OF THE FIRST ARTICLE.....	56
2.1.1 Résumé.....	56
2.1.2 Contexte du projet.....	57
2.2 CONTENT OF THE MANUSCRIPT	58
2.2.1 Introduction.....	59
2.2.2 Results & Discussion	62
2.2.3 Conclusion	81
2.2.4 Experimental Section	82
2.2.5 Acknowledgements.....	90
2.2.6 Supporting Information.....	91
CHAPTER 3 COMPLETE SOLUBILIZATION OF BREWER’S SPENT GRAIN FOR THE PRODUCTION OF SUSTAINABLE LIGNOCELLULOSIC MATERIALS	100
3.1 FRENCH ABSTRACT AND CONTEXT OF THE SECOND ARTICLE.....	100
3.1.1 Résumé.....	100
3.1.2 Contexte du projet.....	101
3.2 CONTENT OF THE MANUSCRIPT	102
3.2.1 Introduction.....	103
3.2.2 Results & Discussion	106
3.2.3 Conclusion	126
3.2.4 Experimental Section	127
3.2.5 Acknowledgements.....	133
3.2.6 Supporting Information.....	134

CHAPTER 4 INDUSTRIAL FEASIBILITY OF THE METHODS	144
4.1 SCALE-UP OF THE PROTOCOL FOR BSG-BASED MICROBEAD PRODUCTION	144
4.1.1 Introduction	144
4.1.2 Results & Discussion.....	145
4.1.3 Conclusion.....	149
4.1.4 Experimental Section.....	150
4.2 TECHNOECONOMIC ASSESSMENT OF THE METHODS	152
CHAPTER 5 GENERAL CONCLUSION.....	161
5.1 REVIEW OF THE OBJECTIVES	161
5.2 FUTURE WORK.....	163
5.3 FINAL REMARKS	166
BIBLIOGRAPHY	168

LIST OF TABLES

Table 1. Previously reported data on the composition of brewer's spent grain.	8
Table 2. Amino acids that compose brewer's spent grain's protein content.	10
Table 3. Vitamin and mineral content of brewer's spent grain.	11
Table 4. Complete normalized data for BSG batches and according to pretreatment conditions.	91
Table 5. Select experimental data for the relationship between pretreatment conditions, BSG recovery, and BSG solubility.....	92
Table 6. Complete CMC results for the maximum penetration depth, indentation modulus, and indentation hardness of 15 CMC tests.	97
Table 7. Screen analysis of the various cellulose powders used, as provided by the manufacturers.	98
Table 8. Complete normalized data of the composition of BSG batches.	134
Table 9. Average mass yields and associated standard deviations for stability testing of gelled and regenerated BSG-derived particles ($n = 3$).....	135
Table 10. Average total area yields and associated standard deviations for stability testing of gelled and regenerated BSG-derived particles ($n = 3$).	136
Table 11. Screen analysis of the various cellulose powders used, as provided by the manufacturers.	142
Table 12. Raw materials associated with producing 1 kg of BSG-based microbead production.....	153
Table 13. Raw materials associated with producing 1 kg of BSG-based gelled particles.	154
Table 14. Raw materials associated with producing 1 kg of BSG-based regenerated particles.	155
Table 15. Raw materials associated with producing 1 kg of cellulose microbeads, according to Mohamed <i>et al.</i> (2015).	156

LIST OF FIGURES

Figure 1. Photograph of the collective Niagara Falls.	2
Figure 2. Visual representation of the modern beer brewing process.	4
Figure 3. Locations of Quebec's breweries in 2021.	6
Figure 4. Representation of the barley grain structure.	8
Figure 5. Schematization of some of the products resulting from the controlled processing of lignocellulosic biomass.	9
Figure 6. Macro photograph of brewer's spent grain.	15
Figure 7. Schematization of plant cellulose in biomass.	16
Figure 8. Typical life cycle of conventional plastic microbeads versus biodegradable alternatives when used in personal care products.	22
Figure 9. Molecular structure of cellulose.	33
Figure 10. Schematic representation of cellulose's solubilization in aqueous NaOH. Cellulose I (above) is complexed by Na ⁺ and OH ⁻ ions in solution (Na-Cell, below).	34
Figure 11. Phase diagram for aqueous NaOH-cellulose systems with encircled "Q-state".	36
Figure 12. Representation of variants of the dropping/extrusion technique: a) simple, b) jet cutting, c) spinning drop atomization, and d) spinning disc atomization.	39
Figure 13. Representation of membrane emulsification techniques: a) traditional membrane emulsification and b) coarse membrane emulsification.	41
Figure 14. Schematization of common fluidic device configurations: a) T-junction, b) flow-focusing, and c) co-flow.	42
Figure 15. Representation of microbead production through complex coacervation.	43

Figure 16. Representation of a) ionic and b) covalent crosslinking. This example demonstrates crosslinking bond formation across deprotonated carboxyl groups.	45
Figure 17. Schematization of the mechanisms of a) external gelation and b) internal gelation (with CaCO ₃ as the gelation agent).....	46
Figure 18. Representation of the mechanism of an ATR device used in FTIR spectroscopy.	52
Figure 19. Humid microbeads prepared from BSG solutions using various needle sizes: 21 G (left), 22 G (center), and 26 G (right).	67
Figure 20. Percent composition of the samples of raw BSG used throughout this project.	68
Figure 21. Percent composition of BSG after dilute acid hydrolysis pretreatment.....	70
Figure 22. SEM images of a BSG microbead at 200 X magnification (left) and 1000 X magnification (right).	73
Figure 23. SEM imaging of the interior of a BSG microbead at 1000 X magnification (left) and an individual cellulose fibril at 20,000 X magnification (right).	73
Figure 24. FITR spectra for raw BSG (purple), purified cellulose (blue), and BSG-based microbeads (red).	75
Figure 25. Average mass yield of dried BSG microbeads after soaking in shower gels or water for a specified time period ($n = 3$).	76
Figure 26. Average total area yield (%) of BSG microbeads after soaking in shower gels or water for a specified time period ($n = 3$).	77
Figure 27. Cleansing efficiency of solid soap, with or without physical exfoliating particles ($n = 3$).	79
Figure 28. Cleansing efficiency of solid soap, with or without physical exfoliating particles ($n = 5$).	80
Figure 29. Appearance of BSG during microbead production: raw BSG (left), pretreated BSG (center), and dissolved BSG (right).	93
Figure 30. HPLC chromatogram of BSG hydrolysate with UV detection at 276 nm.....	94
Figure 31. Eye pencil on skin before (left) and after (right) washing with a soap containing no exfoliating particles.....	96

Figure 32. Eye pencil on skin before (left) and after (right) washing with a soap containing small BSG microbeads (1.25 mm average diameter).....	96
Figure 33. Dried gelled (left) and regenerated (right) particles cut from BSG films.	110
Figure 34. Percent composition of the samples of raw BSG used throughout this project.....	111
Figure 35. SEM images of dried gelled BSG particles at 200 X magnification: "smooth" side (left) and "rough" side (right).....	114
Figure 36. SEM images of dried regenerated BSG particles at 200 X magnification: "smooth" side (left) and "rough" side (right).	115
Figure 37. SEM images of dried BSG particles at 1000 X magnification: gelled (left) and regenerated (right).	115
Figure 38. FTIR spectra for raw BSG (red), purified cellulose (purple), gelled BSG particles (pink), and regenerated BSG particles (turquoise).	118
Figure 39. Average mass yield of dried gelled and regenerated BSG particles after soaking in shower gels and water for a specified time period ($n = 3$).....	119
Figure 40. Average total area yield of dried gelled and regenerated BSG particles after soaking in shower gels and water for a specified time period ($n = 3$).	120
Figure 41. Cleansing efficiency of solid soap, with or without physical exfoliating particles ($n = 3$).	122
Figure 42. Cleansing efficiency of solid soap, with or without physical exfoliating particles ($n = 5$).	123
Figure 43. Comparison of onion plants (<i>Allium fistulosum</i>) grown in plain soil (control) or soil containing either gelled or regenerated BSG-particles.	124
Figure 44. Comparison of tomato plants (<i>Lycopersicon esculentum</i>) grown in plain soil (control) or soil containing either gelled or regenerated BSG-particles.....	124
Figure 45. Eye pencil on skin before (left) and after (right) washing with a soap containing no exfoliating particles.	138
Figure 46. Eye pencil on skin before (left) and after (right) washing with a soap containing gelled BSG particles.	138
Figure 47. Example photographs of onion (<i>Allium fistulosum</i>) plants after phytotoxicity tests: control (left), gelled particles (center), and regenerated particles (right).	140

Figure 48. Example photographs of tomato (<i>Lycopersicon esculentum</i>) plants after phytotoxicity tests: control (left), gelled particles (center), and regenerated particles (right).....	140
Figure 49. Temperature (red) and humidity (blue) tracking throughout phytotoxicity testing.....	141
Figure 50. Photographs of various scale-up tests in the stainless-steel reservoir: lot 1, 100 L (left); lot 2, 25 L (center left); lot 3, 25 L (center right); lot 4, 50 L (right).	147
Figure 51. Photographs of various scale-up tests in the stand mixer: stand mixer placed in the blast chiller (left), 1 L of “whipped” BSG solution (center), 1 L of BSG solution (right).....	148
Figure 52. Costs (\$ CAD) associated with the raw materials required for the production of 1 kg of BSG- and cellulose-based microbeads and particles.	157

LIST OF ABBREVIATIONS AND ACRONYMS

AGU	Anhydroglucose unit
ASTM	American Society for Testing and Materials
ATR	Attenuated total reflectance
BCE	Before the common era
BOD	Biochemical Oxygen Demand
BSG	Brewer's spent grain
CAD	Canadian dollars
CMC	Continuous Multi-Cycle
CNC	Cellulose nanocrystal
CNF	Cellulose nanofiber
CoV	Coefficient of variation
C₁₈	Octadecylsilane stationary phase
DMA	<i>N,N</i> -dimethylacetamide
DNA	Deoxyribonucleic acid
DP	Degree of polymerization
EDS	Energy-dispersive X-ray spectroscopy
EDX	Energy-dispersive X-ray spectroscopy
FTIR	Fourier-transform infrared spectroscopy
HPLC	High-performance liquid chromatography
ID	Internal diameter
IR	Infrared spectroscopy

KRICT	Korea Research Institute of Chemical Technology
LDP	Lignin degradation product
Na-Cell	Sodium-cellulose (cellulose dissolved in aqueous NaOH)
NIH	National Institutes of Health
NMMO	<i>N</i> -oxide monohydrate
NREL	National Renewable Energy Laboratory
PCL	Polycaprolactone
PE	Polyethylene
PES	Polyester
PLA	Polylactic acid
PP	Polypropylene
PS	Polystyrene
PVC	Polyvinyl chloride
SEM	Scanning electron microscopy
TAPPI	Technical Association of the Pulp and Paper Industry
USD	American dollars
5-HMF	5-Hydroxymethylfurfural

LIST OF SYMBOLS

A_f	Final area (mm ²)
A_i	Initial area (mm ²)
A_n	Area (mm ²) after n days
A_0	Initial area (mm ²)
A_r	Residual indentation area
cm	Centimeter
cP	Centipoise (1 mPa·s ⁻¹)
eV	Electron volt
g	Gram
G	Gauge
GPa	Gigapascal
h	Hour
H	Hardness
h_{max}	Maximum indentation depth
Hz	Hertz (1 cycle·s ⁻¹)
kg	Kilogram
kV	Kilovolt
K lux.	Illuminance (lumen·m ⁻²)
L	Liter
M	Molar (mol · L ⁻¹)
M	Indentation modulus (GPa)
mg	Milligram

MJ	Megajoule
mm	Millimeter
mN	Millinewtons
MPa	Megapascal (1 N·mm ⁻²)
<i>n</i>	Number
nm	Nanometer
pH	Power of hydrogen
pKa	Negative base-10 logarithm of the acid dissociation constant (Ka)
<i>P_{max}</i>	Maximum loading
<i>S</i>	Unloading slope
<i>S_A</i>	Stability (area)
<i>S_W</i>	Stability (weight)
<i>v</i>	Volume
<i>W_n</i>	Weight (grams) after <i>n</i> days
<i>W₀</i>	Initial weight (grams)
wt%	Percent weight
X	Times
α	Alpha
β	Beta
μm	Micrometer
μl	Microliter
©	Copyright
®	Registered trademark
™	Trademark
\$	Dollar
°C	Degrees Celsius
○	Circularity

CHAPTER 1

GENERAL INTRODUCTION

1.1 CONTEXT

1.1.1 A brief history of beer consumption and production

To beer, or not to beer, that is the question regularly posed by millions of people around the world. Although beer consumption has significantly varied across cultures and over time, the beverage plays an important role in social engagement and the dietary preferences of many. Globally, beer consumption is more important than that of any other alcoholic beverage, including wine.¹ The beverage seemingly transcends cultural differences and can be used as an economic indicator of the human experience.

In 2020, Asia was the world's largest beer-consuming region for the 13th consecutive year, representing 31.2% of the global market.² The Middle East and Northern Africa consume the least amount of alcohol in general, with the large majority of people from these regions' countries reporting complete alcohol abstinence.³ These regions represent 8% of the global beer market.² Although most adults in Oceania consume alcohol, their beer consumption accounts for only 1.3% of the global market.^{2, 3} Central and South American countries consume 18.1% of the beer produced worldwide, and North American countries are only slightly behind at 14.7%. Europe accounts for the remaining 26.8% of the global total, in large part due to beer consumption in Central European countries. Leading all other nations, the average adult in the Czech Republic consumes 181.9 L of beer per year. Despite occupying second through fifth place in the ranking, the average Austrian, Polish, Romanian, or German adult consumes significantly less per year, between 96.8 and 92.4 L per capita.²

In total, global beer consumption stood at approximately 177.50 billion liters in 2020.² To put this in perspective, 2.8 million liters of water flow over the collective Niagara Falls per second (Horseshoe, American, and Bridal Veil waterfalls, Figure 1).⁴ If this water were replaced by all the beer consumed worldwide in 2020 alone, the falls would flow at a steady pace for 17.6 hours.



Figure 1. Photograph of the collective Niagara Falls.

© Saffron Blaze, 2011. Creative Commons Attribution.

The relationship between humans and beer is a long one, dating back to 6000 BCE to the Sumerians of ancient Mesopotamia (present-day Iraq).⁵ Nomadic peoples in this area likely stumbled across a fermentation process for wild barley around 10,000 BCE, when rain-soaked grains were collected in jars containing wild yeast.⁶ Historians believe that the discovery motivated people to settle in the area and develop agricultural practices to cultivate barley, which became the area's most important crop, alongside wheat.⁷ Beer became a staple in the Sumerian diet as a safer and more nutritious alternative to often-contaminated drinking water sources. By 3200 to 3000 BCE, the sweet liquid belonged "to the products subjected to the centralized economy of Sumerian states" as a commercialized, traded, and taxed commodity.⁵

Beer consumption steadily grew in popularity across the Middle East and Northern Africa over the following centuries. The Babylonian Code of Hammurabi ordained a daily

beer ration, where labourers were allotted two liters per day, civil servants were allowed to indulge in three, and citizens of higher social standing, such as priests and administrators, were awarded five.⁶ In ancient Egypt, daily beer consumption began in early childhood, and labourers were commonly paid in barley. Public beer-drinking places, the precursors to modern pubs and bars, flourished. Beer was also exported to other regions across the Mediterranean Sea.⁵

Beer production began in Europe around 3600 BCE. Initially, it was seen as the drink of peasants, while the upper classes continued to favour wine and mead. This tendency continued across Europe for most of the Roman Empire, except amongst Germanic and Celtic peoples, who took a particular liking to beer. In the Middle Ages, as Christianity spread to Northern Europe, monks developed their own brewing processes, similar to those used today. German monks are also responsible for the flavour profile of modern beer, favouring brews seasoned with locally-produced hops in lieu of Mediterranean dates, olives, and bitter spices.^{5,6}

The modern beer brewing process (Figure 2) begins with producing malt, most commonly prepared from barley. Wheat is another common grain choice for beer production, which also requires malting. During malting, the grain is steeped in water for six to nine days, or until germination,⁸ which activates hydrolytic enzymes present in its aleurone layer. These enzymes, activated as a function of specific malting temperatures, hydrolyze the starchy endosperm of the grain into fermentable sugars. Complex proteins within the grain are also broken down into their amino acid building blocks, which help nourish the yeasts used during the fermentation process.⁹ Next, these sprouted grains are dry-roasted in a process known as kilning, halting germination.⁸ The duration and temperature of the dry-roast, as well as the moisture content in the grain, influence the flavour profile and colour of the resulting beer by controlling the reactions through which different flavour volatiles are produced (i.e., Maillard reaction, caramelization, pyrolysis).¹⁰

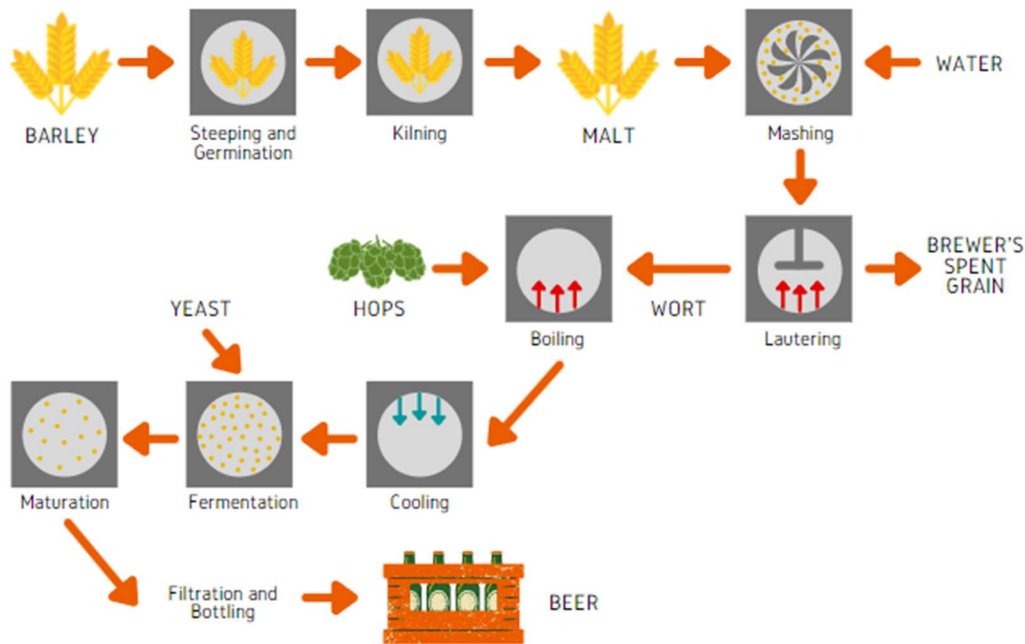


Figure 2. Visual representation of the modern beer brewing process.

Once the desired grain blend has been malted and dried, they are mashed and soaked in hot water, which effectively extracts fermentable sugars and flavour volatiles from the grain through maceration. If other grains are to be used in the beer – such as rice, corn, oats, or rye – they are added during this step.⁸ Similarly to malting conditions and grain choice, water pH, alkalinity, hardness, and mineralization influence the organoleptic profile of the final product. Historically, natural variations in geohydrology gave rise to the different beer varieties commonly associated with different locations. The flavour profile associated with Bavarian beers (Germany) is due to the high carbonate content in the region’s water, and pale ales from Burton-on-Trent (England) are due to higher sulfate and chloride concentrations.⁶

After maceration, the resulting sugary liquid (wort) is separated from the residual solid grain in a process called lautering. Next comes sparging, where the residual grain is rinsed to remove as much of the remaining wort as possible. Hops and other seasonings are

added to the wort, which is subsequently boiled to extract their unique polyphenolic compounds. The mixture is filtered to remove the solids and rapidly cooled.⁸ Finally, yeast is added to the wort, which ferments the liquid's sugars into alcohol. The species of yeast used for fermentation is chosen as a function of the desired final product, considering wort pH, mineralization, and total sugar content.¹¹ After fermentation comes maturation, the conditions of which also influence the nature of the beer. As an example, lagering is a specific maturation process that occurs at near-freezing temperatures, which causes yeasts to settle at the bottom of the liquid (as opposed to collecting at its surface). The resulting beer is known as a lager.⁶

Besides beer, the brewing process yields several other coproducts. Yeast, hops, other seasonings, and residual solid grain are all separated from the liquid at various steps throughout the process. Of these, the residual solid grain – otherwise known as brewer's spent grain (BSG) – is the primary residue of the brewery industry, representing 85% of the total co-products generated throughout the beer brewing process.¹² For each hectolitre of beer, an average of 20 kg of humid BSG is produced, which represents a total of ≈ 39 million tonnes of BSG produced worldwide annually.¹³

1.1.2 Situation in Quebec – a local perspective

Beer brewing in Quebec began with the first colonialists in 1647. Settlers in New France (whose borders fluctuated throughout the 17th and 18th centuries, often extending beyond the territory of present-day Quebec) relied upon beer for hydration and nutrition, as water and milk were often contaminated with harmful microorganisms. However, their consumption was out of necessity rather than a genuine taste for the product. As new technologies assured cleaner drinking water and safer milk, anglophone immigrants revitalized Quebec's beer brewing industry after the British Conquest in 1759.¹⁴

John Molson founded his namesake brewery in Montreal in 1786, which remains one of Canada’s largest breweries to this day (Molson Coors Brewing Company).¹⁵ Throughout the 18th and 19th centuries, other prospective Canadian brewers followed suit, including John Kinder Labatt (Labatt Breweries, London, Ontario) and Susannah Oland (Moosehead Breweries, Saint John, New Brunswick). These major breweries managed to survive prohibition in Canada and emerged stronger than ever after World War II.¹⁴

Since the mid-1980s, Quebec’s brewery industry has been experiencing a phenomenon known as ‘neolocalism’ or a “microbrewing renaissance”.¹⁶ Craft brewers orientate their products to local, niche markets and use artisanal brewing techniques. In 1985, in all of Canada, there were only ten breweries, all of which were owned by the same three major companies.¹⁷ As of April 2022, there are 302 breweries in Quebec alone. Artisanal microbreweries account for 89 of these, and the remaining 213 are classified as industrial brewers. The locations of these breweries, as of 2021, are shown in Figure 3. Fifteen additional breweries were established in the province over the following year.

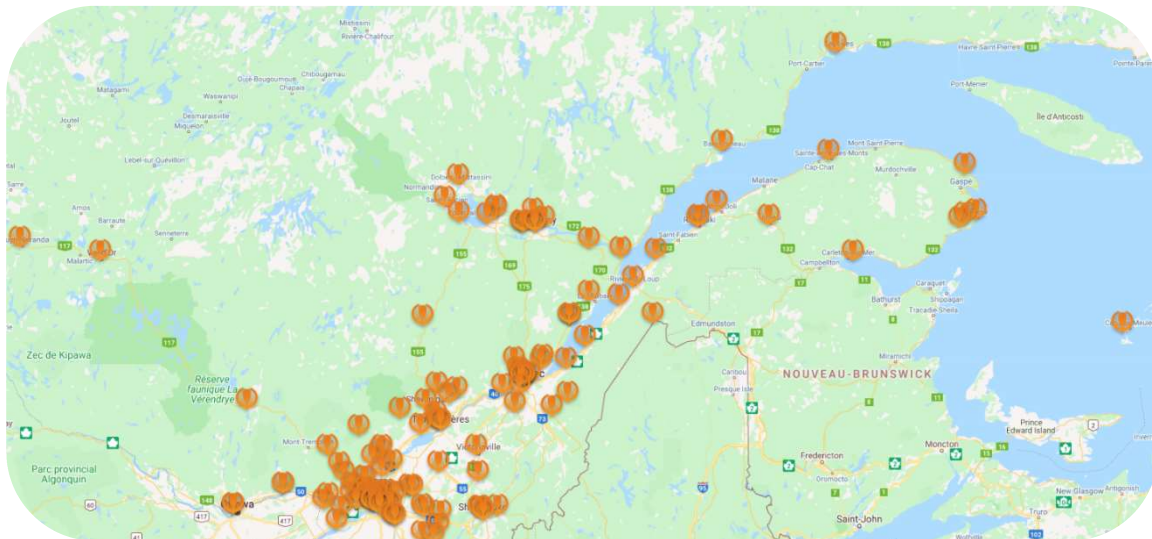


Figure 3. Locations of Quebec's breweries in 2021.

© Association des Microbrasseries du Québec, 2021. Permission to reproduce figure pending.

Although Quebec only accounts for a small fraction of the global beer market and the province's overall beer consumption has stagnated in recent years, Quebec's microbrewery industry is increasingly expanding. Valorizing BSG generated from small-scale operations has proved to be a challenge for brewers,¹⁸ while larger breweries export most of their co-products to farms in the neighboring American states.¹⁹ In 2017, Quebec's 60 artisanal microbreweries, responsible for only 8% of the province's beer consumption at the time, generated 13,376 tonnes of BSG alone, which is mainly recuperated by local farmers for animal feed or compost.^{18, 20} Ensuring BSG's valorization is increasingly logistically difficult for small-scale breweries, and provincial legislation prevents breweries from sending this organic food waste to landfills.²¹ Consequently, there is an increasing push to explore new high added value applications for BSG, providing an added economic incentive to valorize BSG within the province and facilitating the growth of small brewery businesses.

1.1.3 Composition of brewer's spent grain

When BSG is separated from the liquid wort during the brewing process, the biomass is wet. Humidity commonly represents between 77 and 85% of the grain's total weight.^{22, 23} The solid fraction generally contains 16-25 % cellulose, 19-42% hemicellulose, 11-27% lignin, 15-24% proteins, 1-4% ash, and 1-6% of soluble matter.¹² Previously reported data on the composition of BSG, compiled in Table 1, demonstrate the biomass's variable composition. Brewing conditions affect the composition of BSG, with the mashing step having the greatest influence. The more the grain is mashed, the more the starchy endosperm can be solubilized during lautering,¹³ which represents a lesser proportion of water-soluble extractables in BSG. The structure of barley, with soluble sugars encapsulated within a fiber-protein husk, can be seen in Figure 4. The use of grains other than barley, cereal type, time of harvesting, and malting conditions may also affect biomass composition, to varying extents.¹³

Table 1. Previously reported data on the composition of brewer's spent grain.

Components (% dry wt)	Kanauchi <i>et al.</i> (2001)	Carvalho <i>et al.</i> (2004)	Silva <i>et al.</i> (2004)	Russ <i>et al.</i> (2005)	Mussatto, Roberto (2006)	Adeniran <i>et al.</i> (2008)	Waters <i>et al.</i> (2012)	Meneses <i>et al.</i> (2013)
Cellulose	25.4	21.9	25.3	23-25	16.8		26.0	21.7
Hemicellulose	-	29.6	41.9	30-35	28.4	79.9 ± 0.6 ^b	22.2	19.2
Lignin	11.9	21.7	16.9	7-8	27.8		-	19.4
Proteins	24	24.6	-	19-23	15.3	2.4 ± 0.2	22.1	24.7
Ashes	2.4	1.2	4.6	4-4.5	4.6	7.9 ± 0.1	1.1	4.2
Extractives	-	-	9.5	-	5.8	-	-	10.7
Others	21.8 ^a	-	-	-	-	6.4 ± 0.2 ^c	-	-

a- Arabinoxylan

b- Total carbohydrates

c- Residual moisture

Source: Mussatto, 2014, and Aliyu & Bala, 2011.

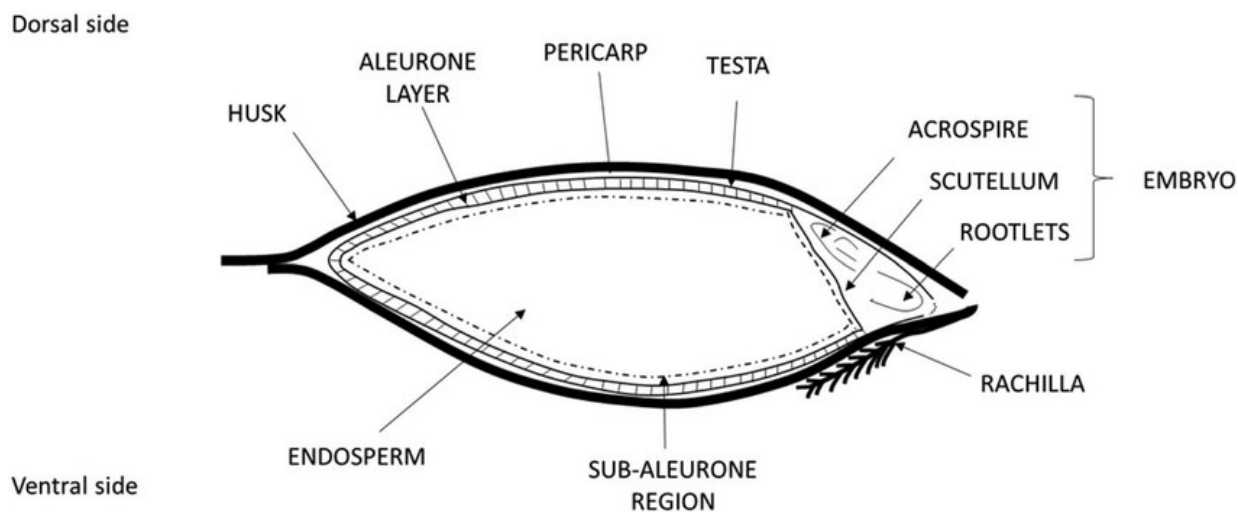


Figure 4. Representation of the barley grain structure.

© Filipowska *et al.*, 2021. Creative Commons Attribution.

BSG's carbohydrate content can be broken down to obtain various monosaccharides. Cellulose is hydrolyzed to produce β -glucose, while heteropolysaccharide hemicellulose primarily yields xylose, glucose, and arabinose.²⁵ Hemicellulose hydrolysis also produces furfural and 5-hydroxymethylfurfural. Lignin derivatizes into a variety of interesting compounds, such as acetic, caffeic, ferulic, *p*-coumaric, syringic, vanillic, and *p*-hydroxybenzoic acids.^{26, 27} While some carbohydrate derivatization occurs naturally within the grain or throughout the brewing process, further controlled processing yields greater quantities of these molecules (Figure 5).

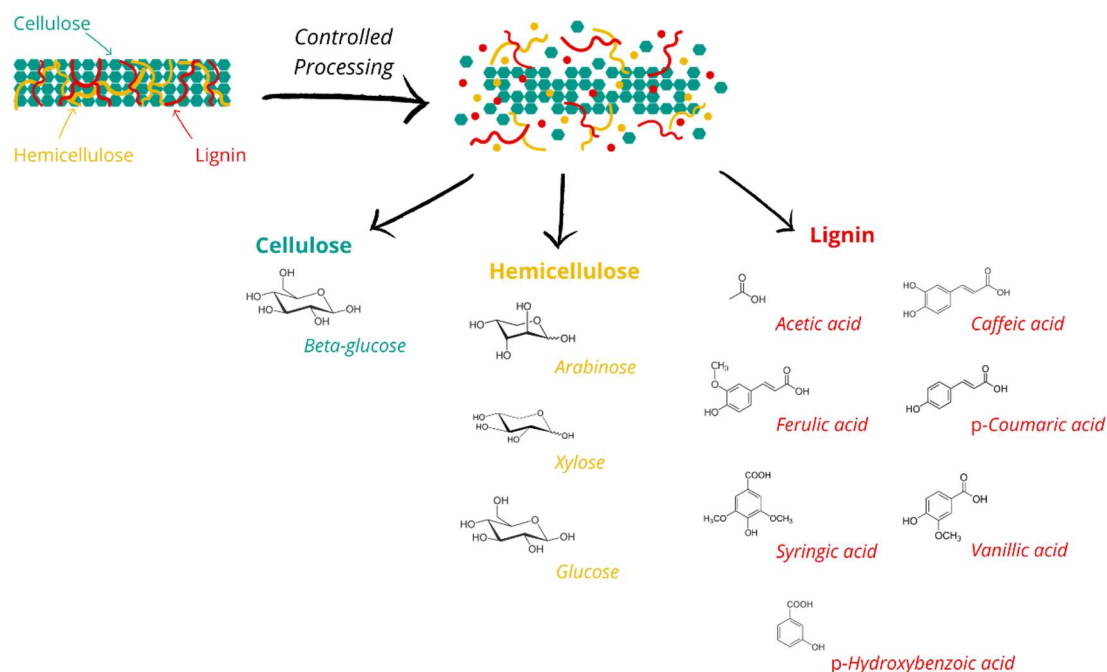


Figure 5. Schematization of some of the products resulting from the controlled processing of lignocellulosic biomass.

BSG's protein content can be broken down in terms of its constituent amino acids. The grain is a source of six essential amino acids (lysine, leucine, phenylalanine, isoleucine, threonine, and tryptophan) and all 11 non-essential amino acids. Table 2 presents the amino acid composition of BSG proteins.

Table 2. Amino acids that compose brewer's spent grain's protein content.

Non-essential	% of total protein	Essential	% of total protein
Histidine	26.27	Lysine	14.31
Glutamic acid	16.59	Leucine	6.12
Aspartic acid	4.81	Phenylalanine	4.64
Valine	4.61	Isoleucine	3.31
Arginine	4.51	Threonine	0.71
Alanine	4.12	Tryptophan	0.14
Serine	3.77		
Tyrosine	2.57		
Glycine	1.74		
Asparagine	1.47		
Glutamine	0.07		

Source: Mussatto, 2014.

BSG also contains numerous residual flavonoids (polyphenols), vitamins, and minerals that are not extracted throughout the brewing process. In biomass composition analyses, these are respectively grouped under extractives and ash (minerals). The grain is a source of B vitamins (except for vitamin B12) and choline.²² As for minerals, BSG contains sodium, magnesium, silicon, phosphorous, sulphur, potassium, calcium, iron, and zinc. Boron, aluminum, chromium, manganese, cobalt, copper, strontium, molybdenum, iodine, and barium are also present in small amounts.¹² Table 3 expresses the average quantities of these vitamins and minerals found in BSG.

Table 3. Vitamin and mineral content of brewer's spent grain.

Vitamins	Concentration (mg·kg⁻¹)	Minerals	Concentration (mg·kg⁻¹)
Thiamin (B1)	0.7	Boron	3.2
Riboflavin (B2)	1.5	Sodium	100-309.3
Niacin (B3)	44	Magnesium	1900-2400
Pantothenic acid (B5)	8.5	Aluminum	36-81.2
Pyridoxine (B6)	0.7	Silicon	1400-10,740
Biotin (B7)	0.1	Phosphorous	4600-6000
Folic acid (B9)	0.2	Sulphur	1980-2900
Choline	1800	Potassium	258.1-700
		Calcium	2200-3515
		Chromium	< 0.5-5.9
		Manganese	40.9-51.4
		Iron	100-193.4
		Cobalt	17.8
		Copper	11.4-18
		Zinc	82.1-178
		Strontium	10.4-12.7
		Molybdenum	8.6-13.6
		Iodine	11
		Barium	1.4

Source: Mussatto, 2014, and Aliyu & Bala, 2011.

1.1.4 Previously reported applications of brewer's spent grain

The current primary application of BSG is as an animal feedstock, as the grains are rich in fibre and protein.^{12, 22} While this is the quickest way to dispose of raw BSG, it has several limitations. In a local context, breweries tend to be located in urban areas while livestock farms are commonly located in rural regions.¹⁸ As raw BSG has a short shelf-life due to its high humidity and carbohydrate content, it requires rapid transport from cities to agricultural regions. Even then, other microbes naturally reside in BSG, including fungi capable of producing mycotoxins. Mycotoxins are retained by the grain during the brewing process, but BSG as a component of human food needs to be carefully monitored. Even if mycotoxin-contaminated BSG is used as animal food, these secondary metabolites may transfer to the animals' milk and eggs destined for human consumption.²⁶

Raw BSG as an animal feed is generally restricted to ruminants and must be supplemented with other feedstocks to ensure optimal nutrition and energy efficiency.²⁸ When used as feed for other animals, such as poultry, BSG must undergo protease hydrolysis.²⁹ Consequently, in Quebec, the current demand for BSG as an animal feedstock is lower than the available supply.¹⁸ Farmers may also purchase BSG to be used as a crop fertilizer or in soil remediation, due to its nitrogen and phosphorous content. BSG can be broken down in a composter beforehand, or raw BSG can be directly spread on fields.^{18, 26} These are low-value applications, with each tonne of humid spent grain being sold to farmers at an average of \$50 CAD (\$40 USD).³⁰

BSG's antioxidant activity, antiallergenic and anti-inflammatory properties, and high fiber, protein, and mineral content make it an attractive ingredient in foods destined for human consumption, such as bread, snacks, cookies, cakes, and hamburgers.²⁶ Montreal-based *Boomerang* and Rivière-du-Loup's *Malterre* are just two examples of Quebecois companies using BSG as an ingredient in bread and crackers, respectively.^{31, 32} A limitation of using BSG in these types of products, however, is that recipes often call for the grain to be dried and ground into flour before use, and even then, grain can only be used in small

amounts to avoid affecting conventional flavour and texture profiles.¹³ Humid BSG may also be converted into plant-based milk products, but the grain cannot be used in its entirety.^{33,34}

BSG is also reported as a primary feedstock in energy production via thermochemical conversion (pyrolysis, combustion), or biogas (methane) and ethanol production.³⁵ In thermochemical conversion, dry BSG has a net calorific value of 18.64 MJ·kg⁻¹. But this method also requires drying, and grain combustion emits sulfur oxide and nitrogen oxide gases, as well as particulate matter. Charcoal bricks prepared from BSG have a higher calorific value of 27 MJ·kg⁻¹ but present inferior burning properties.¹² Intermediate pyrolysis yields 29% char, 51% bio-oil, and 19% permanent gasses. While bio-oil and permanent gasses can be burned for energy, char can then be used to adsorb heavy metals and organic pollutants in wastewater.^{22,26} In a similar vein, carbonized BSG can be further processed to yield carbon quantum dots which can be used to monitor metals in water, amongst other applications.³⁶ As for biogas, anaerobic batch fermentation of BSG yields 3476 cm³ of biogas per 100 g BSG (dry weight) after 15 days. Following dilute acid hydrolysis, BSG can be fermented into ethanol by *Pichia stipitis* with 86.3% conversion efficiency. *Neurospora crassa* and *Fusarium oxysporum* are equally recognized for their conversion efficacy in this application.²² Bioethanol conversion can also be achieved by a hydrothermal, microwave-assisted, catalyzed process.³⁷

BSG is a source of several molecules of interest. Extracts may have direct uses or may be derivatized to serve other functions.²⁷ However, only specific fractions of the biomass are valorized in these applications. Sugars (glucose, xylose, arabinose) can be extracted through acid hydrolysis; lignin can be isolated through alkaline hydrolysis and precipitation with H₂SO₄. Hydroxycinnamic acids (i.e., ferulic acid) and other polyphenols may also be extracted through alkaline hydrolysis.¹² Enzymatic hydrolysis can also efficiently isolate sugars, proteins, polyphenols, or volatile fatty acids after rigorous process optimization.^{13,38} Moreover, like the methods used for ethanol production, sugars extracted from BSG can be fermented into xylitol, arabitol, and lactic acid.^{22,27} Individually these

methods do not allow to valorize the entirety of the biomass, but they may be used in cascade to reduce waste.

Other potential applications of BSG are as a substrate for microorganisms' cultivation for enzyme production (although moisture content needs to be reduced to below 10% before use) or as a carrier for cell immobilization in other fermentation processes.^{12, 39} Finally, cellulose can be fractionated from BSG, and the resulting pulp can be used to produce high-texture paper products.⁴⁰ Cellulose pulps are commonly prepared by the Kraft process (which relies on sodium sulfate for pulping),⁴¹ but other steps (acid hydrolysis, soda pulping, and hydrogen peroxide and sodium hydroxide bleaching) can yield similar results, at least from wooden biomass.⁴² Cellulose nanocrystals (CNCs) and nanofibers (CNFs) can be further derived from these pulps.^{43, 44} Furthermore, BSG-derived fibers can be used in the production of composite materials. The fibers incorporated in polymer materials facilitate their biodegradation yet decrease their mechanical strength.²⁶

1.1.5 Complete valorization of brewer's spent grain

Conventionally, BSG has been used in low-value applications (i.e., as animal feed or compost), or fractionated, only valorizing a select few high-value molecules found within.¹² Even in the case of cascade valorization, where a series of chemical or enzymatic treatments are explored to extract a wider variety of these valuable molecules, BSG may not necessarily be used in its entirety. Furthermore, cascade valorization is commonly energy-intensive and requires multiple steps.⁴⁵ This may discourage companies from adapting conventional petrochemical processes to lignocellulosic biomass.

Like most biomass, BSG's inconsistent and complex molecular structure challenges its use in industrial applications.⁴⁵ Its chemical composition fluctuates from one batch to another, as evidenced in Table 1 (section 1.1.3). Brewing conditions directly influence

BSG's composition, meaning the latter is nearly just as varied as the types of beer savoured around the world.¹³

BSG emerges from the brewing kettle as a hot and humid grain mixture, similar in appearance to a more golden-toned porridge (Figure 6). Once cooled, the grain retains between 77 and 85% humidity,^{22, 23} which primes the biomass for rapid microbiological deterioration.¹⁸ To extend its shelf life, the grain can be dried but this is an energy-intensive process. Even then, other microbes naturally reside in BSG, including fungi capable of producing harmful mycotoxins.²⁶



Figure 6. Macro photograph of brewer's spent grain.

Besides inconsistent molecular composition, high humidity, and the propensity for microbial degradation and contamination, the molecular structure of the grain itself is a challenge to BSG's use as an industrial feedstock.⁴⁵ Like all lignocellulosic biomass, BSG is primarily composed of cellulose, hemicellulose, and lignin. Linear cellulose fibers are

arranged in ordered crystalline bundles through intermolecular hydrogen bonds. These fibers are encased by mechanically resistant lignin and hemicellulose, covalently cross-linked to provide even greater strength.⁴⁶ Multiple fibers bundle together to form microfibrils, which in turn bundle together to form fibrils, which consequently form the cell wall (Figure 7).

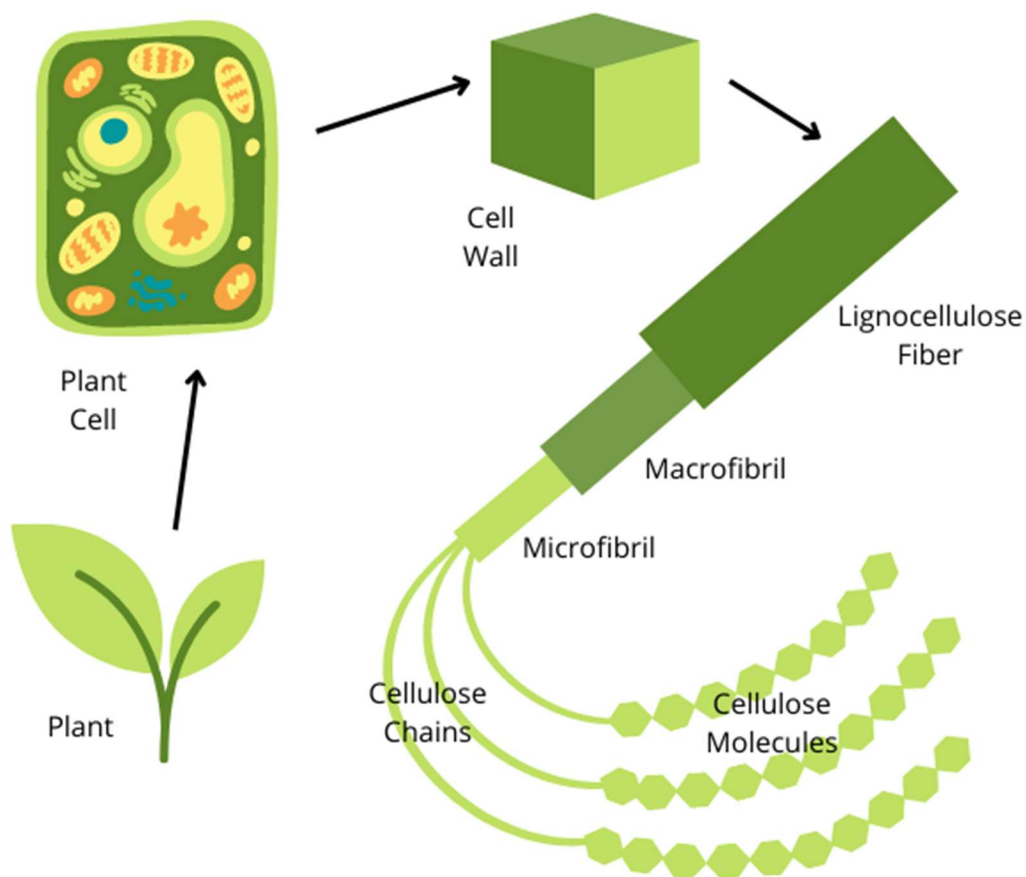


Figure 7. Schematization of plant cellulose in biomass.

To access valuable molecules encapsulated within the matrix, cellulose, hemicellulose, and lignin often need to be separated through enzymatic, acid, or alkaline pretreatment.^{38, 47} Alkaline pretreatment is commonly synonymous with delignification,

which improves the ready biodegradability and porosity of the resulting pulp yet isolates lignin as an undervalued by-product.³⁹ Pretreatment steps also allow to hydrolyze hemicellulose and cellulose more efficiently into their monomeric sugars.²⁷ Novel applications for BSG should strive to reduce the ecological impacts of biological or thermochemical pretreatment. Alternatively, finding ways to circumvent this step further minimises process costs and the number of necessary steps, increasing the method's likelihood to be adopted by industries. Moreover, BSG may potentially be valorized in its entirety.

1.2 NATURAL POLYMERS

Natural polymers, as the name would suggest, naturally occur in living organisms. By definition, DNA is a polymer of nucleotides, proteins are complex structures of polymeric polypeptides with amino acid monomers, and carbohydrates (polysaccharides) are constructed from simple sugar monomers.⁴⁸ Conventional plastics imitate these natural bonding mechanisms, using fossil-fuel-derived monomers to construct a wide variety of durable polymeric materials.⁴⁹

Researchers are increasingly turning towards natural polymers to fulfill the same functions as conventional plastics while addressing some of the drawbacks associated with these materials (mainly biodegradability). Next-generation bioplastics can be obtained through direct processing of naturally occurring polymers (i.e., cellulose, starch, alginate) or chemically synthesized from sugar derivatives (i.e., polylactic acid synthesized from lactic acid).^{50, 51} In particular, polysaccharide-based plastics are a significant area of interest due to their abundance in renewable biomass raw materials. Agriculture-based plants rich in polysaccharides, lignocellulosic plants not suitable for human or animal consumption, algae, organic or food waste, or microbiota can be readily exploited for their natural polymer content.^{52, 53} Polysaccharides can be extracted from these matrices, then chemically altered to produce a wide variety of plastics with comparable mechanical

properties to conventional petrochemical plastics. Brewer's spent grain is an example of biomass that can be valorized for its natural polymer content using these strategies.¹²

Although polysaccharide-based plastics are relatively new, natural polymers have served for millennia in the production of paper products, textiles, and composite materials. Plain paper products are readily biodegradable yet mechanically weak, with low resistances to environmental factors, chemicals, hydrolysis, and microorganisms.⁴¹ Textiles are produced from natural polymers after they have undergone chemical treatments to increase their crystallinity, average degree of polymerization (fiber length), or moisture content.⁵⁴ Like paper, these factors confer greater mechanical properties to the material and make it more resistant to biodegradability.⁴¹ Plastics take chemical treatments for increased performance a step further: depending on the polymers used, the product may still be readily biodegradable in the environment but will also present more interesting mechanical and chemical characteristics.⁴⁹ In the case of composite materials, natural fibers are reinforced with conventional plastics or impregnated with chemical additives which may restrict the product's biodegradability. In this sense, many paper products are composite materials (i.e., glassine or waxed papers).⁴¹

Natural polymer-based materials and biodegradability are not mutually exclusive. The same is true of the materials' manufacturing techniques. Some conventional plastics are manufactured in more energy-efficient ways than their biobased counterparts or use fewer toxic additives or solvents.⁵⁵ Similarly, different types of materials are better suited to different applications. A material's unique characteristics, durability, recyclability, and predicted end-life conditions influence its overall sustainability. In general, natural polymer-based materials have less of an environmental impact than conventional plastics, but there is room for improvement that further research can address.^{49, 56}

1.3 EXFOLIATING MICROBEADS IN PERSONAL HYGIENE PRODUCTS

1.3.1 Plastic pollution and microbeads

It is becoming increasingly clear that the Earth is facing a global garbage problem. Even the most remote environments are contaminated with the synthetic materials we rely upon. Plastics, pesticides, and household chemicals are some of the most common culprits, detected in mountain soils in Switzerland and Arctic ice core samples, suspended throughout the atmosphere, and sluicing down drainpipes near and far to meet the global ocean.⁵⁷

Synthetic plastics have exploded in popularity over recent decades. In 1950, less than 2 million tonnes of virgin plastics had been manufactured.^{58, 59} By 2017, researchers estimate that this number had reached a cumulative grand total of 8 300 million tonnes. In 2015, 6 300 million tonnes of this cumulative grand total had already been discarded, 9% of which had been recycled, 12% incinerated, and 79% accumulated in landfills or the environment.⁶⁰ According to different projections, by 2050 a grand total of 12,000 million tonnes of discarded plastics will be in landfills or the environment. Furthermore, yearly plastic production is expected to reach 1900 million tonnes by 2050.^{58, 59, 60} The durability of synthetic plastics contributes to their ubiquitous nature yet proves to be a double-edged sword when it comes to managing discarded materials.

Microplastics, particles with a diameter between 100 nm and 5 mm, are especially difficult to manage due to their small size. Like larger plastics, they are expected to persist in the environment for hundreds of years, until their eventual breakdown. Microplastics may be mistakenly ingested, and have been detected within various organisms, including in human tissues.^{57, 61} Their large surface areas also increase their sorptive capacities of metals and hydrophobic organic pollutants, furthering their environmental risk.⁶² These particles may also leach constituent contaminants, such as additives and residual monomers.⁶³ Microplastics originate in the environment as primary microplastics, which are produced at

small dimensions, or as secondary microplastics, which result from the breakdown of larger plastic pollution.

Primary microplastics account for a global market worth an estimated \$3.5 billion (CAD) in 2020.⁶⁴ Like petrochemical macroplastics, these microplastics are sourced from non-renewable resources, produced by energy-intensive manufacturing processes, and pose significant environmental problems when it comes to their disposal.⁶⁵ Microplastics' dimensions limit their recyclability and ability to be collected from the environment. Consequently, mitigation strategies need to target their conception. The eco-design of primary microplastics calls for products that will harmlessly break down in the environment, made from bio-based and biodegradable polymers rather than conventional petrochemicals.⁶⁶ In particular, biodegradability needs to account for structure-property relationships and complex natural environments.⁵⁶

1.3.2 Nature and fate of microbeads in personal hygiene products

Microbeads in personal hygiene products have one of two applications: hard microbeads can be used for skin exfoliation, whereas softer varieties can be loaded with bioactive compounds that are released when pressure is applied. In either case, microbeads can help unclog pores, prevent acne and signs of aging, help topical skincare products penetrate deeper, even skin tone, boost circulation and lymphatic drainage, increase cell turnover, and stimulate collagen synthesis.^{67, 68}

Besides these many benefits for the consumer, microbeads are prized by the cosmetics industry for their high marketability and their ease of incorporation into products, such as a bar of soap or body wash. Conventional plastic microbeads, derived from petrochemicals, were the industry standard for many years. Synthetic plastics are inexpensive to produce and can be shaped to produce small, uniform, spherical microbeads.

These primary microbeads can easily be made larger for use in shower gels (mean diameter of 419 μm) or smaller for use in facial cleansers (mean diameter of 197 μm).⁶²

Hard synthetic plastics, such as polyethylene (PE), provide gentle exfoliation.^{69, 70} Other softer plastics, such as acrylate copolymer and polypropylene (PP), can be readily shaped into the “bursting” microbead variety. However, synthetic plastics do not biodegrade. Personal hygiene products are designed to be washed down the drain during use, and wastewater treatment facilities are unable to remove the totality of these beads during water filtration and purification. From personal hygiene products alone, approximately 1500 tonnes of hard microplastic beads escape wastewater treatment and are released into the environment every year. This amounts to a total accumulation of up to 300,000 tonnes of microbeads since 1970.⁶²

Besides accumulating in the environment, plastic microbeads lead to increasingly visible pollution, bioaccumulation within marine organisms, and bioamplification by transfer to superior trophic levels (Figure 8). They may also form aggregates or transport organic pollutants and heavy metals.⁷¹ These observations have led many Western countries, including Canada (in 2018), to ban hard plastics from being used in personal hygiene products in recent years.^{72, 73} Although soft or liquid conventional plastics are generally ignored by legal bans, cosmetics companies are voluntarily phasing them out to keep up with an increasingly eco-conscious consumer base.

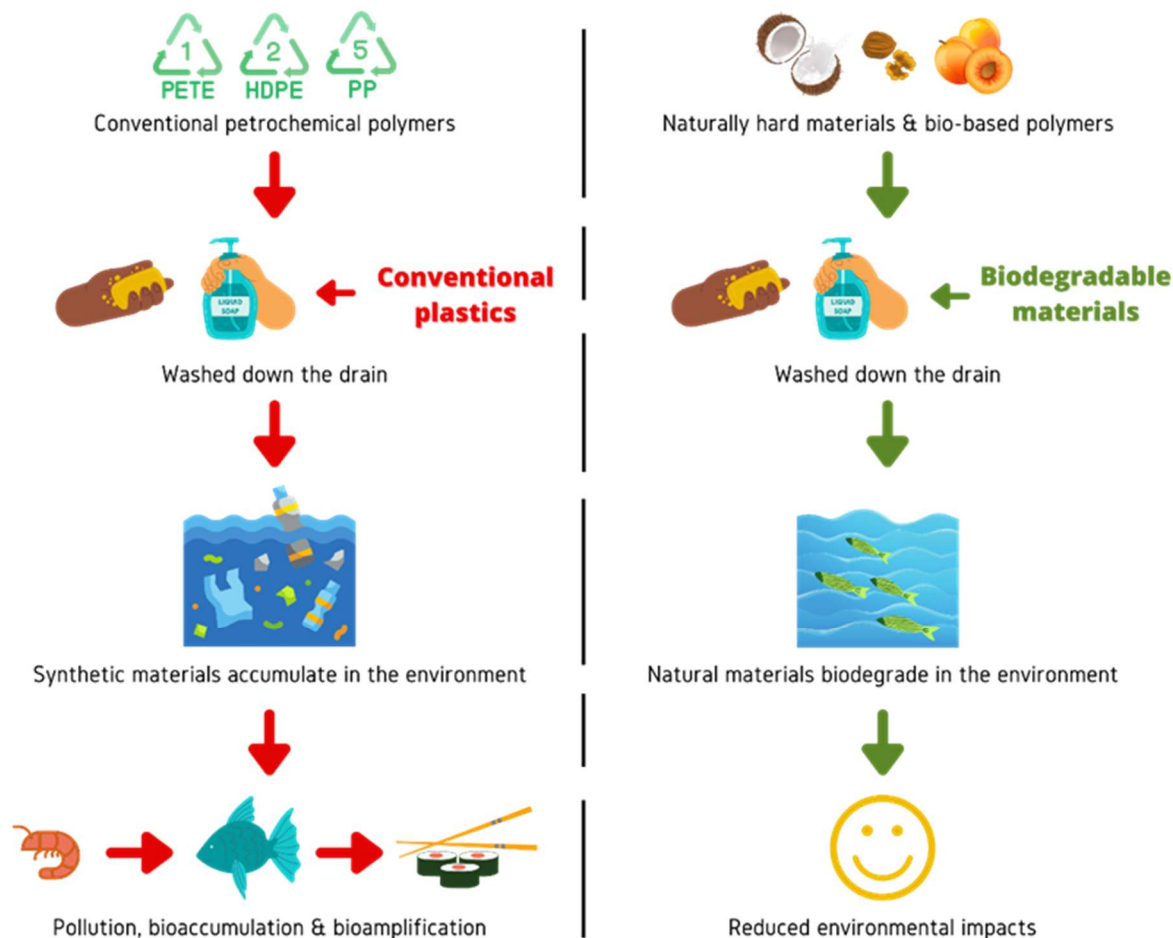


Figure 8. Typical life cycle of conventional plastic microbeads versus biodegradable alternatives when used in personal care products.

1.3.3 Current alternatives for microbeads in personal hygiene products

Natural abrasive materials, including stone fruit pits and minerals, are an alternative to exfoliating hard plastic microbeads that do not contribute to environmental pollution. However, these materials need to be ground down to meet the dimensions required of skin-exfoliating particles, resulting in sharp, irregular shapes.^{67, 74} Dermatologists do not recommend these products for use on sensitive skin, as these are the most abrasive type of scrub and people tend to apply excessive pressure when using physical exfoliants.^{67, 68}

Their abrasiveness and hardness also prevent these materials from being suitable alternatives to “bursting” microbeads.

Next-generation biopolymers offer better control over the beads’ morphologies. Biopolymers are obtained from biomass, reducing dependence on fossil fuel feedstocks. They may be chemically synthesized from sugar derivatives (i.e., lactic acid to polylactic acid) or obtained through direct processing of naturally occurring polymers (i.e., cellulose).^{50, 65} Respectively, we can refer to these two sub-categories as chemically synthesized biopolymers and naturally occurring biopolymers.

Chemically synthesized biopolymers, including polylactic acid (PLA) and polycaprolactone (PCL), are highly customizable, performing just as well as their exfoliating and “bursting” petrochemical counterparts.^{51, 75, 76} Although these biopolymers are often heralded as biodegradable, studies have shown that their breakdown is slow and condition-specific. PLA microbeads, for example, may have even greater environmental consequences than their synthetic analogues.⁷⁷ Bio-based synthetic polymers also tend to depend on either expensive ionic liquids or organic solvents in their production processes.^{51, 65, 75}

Naturally occurring biopolymers can also be shaped into uniform, spherical microbeads suitable for use on sensitive skin. The main drawbacks of these materials are that they may require expensive or petrochemical-based processing conditions,^{64, 78, 79, 80, 81, 82} that their starting materials are commonly coveted by other industries,^{83, 84} and that their mechanical properties tend to be weaker than other proposed alternatives.^{50, 51} Microbeads made from chitosan obtained from crustacean waste were recently proposed as a promising option for hard, exfoliating microbeads; chitosan beads are inexpensive and non-cytotoxic, fully biodegradable, and gently exfoliate sensitive skin.⁸⁵ Their animal-based nature is their only significant drawback, as the cosmetics industry is increasingly turning towards vegan formulations. Cellulose microbeads have all the same advantages as chitosan beads, on top of being plant-based, biocompatible, and cytocompatible.^{50, 86} However, their relative softness makes this material a better candidate for beads of the “bursting” variety. Further

research is required to develop exfoliating microbeads that satisfy the industry's demands and are environmentally sustainable.

1.3.4 Microbeads in personal hygiene products – required characteristics

Exfoliating microbeads in personal hygiene products are ideally spherical with no sharp, irregular edges. When incorporated in products to be used on the face, their mean diameter should be around 200 μm ; when incorporated in products to be used on the body, beads can be about twice as large.⁶² The size distribution within a product should be fairly homogenous.⁸⁵

Beads should be easily incorporated into a variety of solid and liquid soaps. They should stay stable in these matrices and maintain the hardness and high specific surface area associated with increased product performance.^{62, 85} However, they must be biodegradable when rinsed off into the environment.^{72, 73} Porosity is a plus, as more porous particles can facilitate better pollutant sorption from the skin, as is bead opacity.⁶⁴

For companies to choose a certain type of exfoliating particle in their products, they must be inexpensive, easy to produce, and marketable. Moreover, the industry is increasingly trending towards “clean” personal hygiene products, with criteria ranging from sustainably produced, derived from natural ingredients, or cruelty-free/vegan. Although “clean” lacks a precise definition, the global market value for products labelled as such was placed at \$43.64 billion (CAD) in 2018 and is expected to reach \$38.3 billion (CAD) by 2027.⁸⁷

1.4 OBJECTIVES

1.4.1 Objective 1

The first objective of this research is to develop an efficient method for the production of exfoliating microbeads from BSG.

Plastic microbeads in personal hygiene products have historically been a contributor to the global plastics pollution problem, leading many countries to ban their use, including Canada in 2018.^{72, 73} Biodegradable alternatives such as chitin-based microbeads provide similar characteristics to conventional plastic microbeads but cannot be considered vegan or cruelty-free.^{64, 85} This criterion is increasingly important in the personal hygiene products/cosmetics industry, encouraging researchers to evaluate plant-based and hypoallergenic alternatives.

Cellulose microbeads are one such option, but generally lack the hardness required for exfoliating particles in personal hygiene products. Extracting and purifying cellulose from biomass also commonly involves energy-intensive and expensive processes.⁸⁸ Besides, lignin has previously been added to such beads, providing them with superior mechanical performance and antibacterial properties.⁸⁹ Yet, again, this lignin had previously been extracted from biomass and purified.

Sourcing cellulose and lignin directly from BSG reduce environmental and economic impacts of the beads' production, all while appreciating this undervalued biomass for its important natural polymer content. This application can open the door to developing further high-value materials from lignocellulosic residues.

1.4.2 Objective 2

The secondary objective of this research is to valorize whole, raw BSG that has not previously been dried.

BSG is notoriously difficult to valorize in its entirety, even in cascade valorization applications.⁴⁵ As far as we know, Lorente *et al.* (2019) describes the sole method for complete solubilization of BSG through catalyzed hydrothermal liquefaction for the production of biofuels. However, biomass hydrothermal liquefaction involves initial biomass depolymerization, subsequent biomass monomer decomposition, and recombination of the resulting reactive species to yield bio-oil, bio-gas, char, and coke.³⁷ These methods and the resulting products are inappropriate for the manufacture of fibrous or polymeric materials.

However, this research also sought to develop novel techniques for BSG's complete valorization. At first, our goal was that the process developed for the production of microbeads (Objective 1) would involve the complete valorization of BSG (Objective 2). Unfortunately, in the course of this research, it quickly became clear that the combination of these two objectives would only lead to poor-quality microbeads.

Alternatively, efforts towards the complete valorization of BSG were directed towards the production of another relevant cellulose-based material: biodegradable BSG-based microparticles that were equally evaluated for their capacity to replace petrochemical-based exfoliating microbeads.

1.4.3 Objective 3

The third objective directing this research is to develop procedures that are as environmentally friendly and safe as possible. In other words, we wanted to explore new ways of valorizing BSG that could lead to added value products (Objectives 1 and 2), while

respecting the principles guiding Green Chemistry* (Objective 3). More specifically, we sought to develop processes that were as energy efficient as possible, keeping temperatures as close to ambient conditions as the method would allow. We also explored pretreatment, solubilization, and regeneration systems with low environmental impacts: dilute strong acids and aqueous NaOH solutions. While the project inherently had an eco-friendly aspect through the valorization of brewer's spent grain (Objectives 1 and 2), a waste product, we also sought to avoid producing other co-products. Keeping with this theme, design for degradation is at the core of this project, with Objective 1 being to design a novel option for biodegradable exfoliating microbeads for use in personal hygiene products.

1.5 METHODOLOGY AND PRECEDENTS

1.5.1 General

A review of the literature reveals that fibrous, polymeric materials can be obtained from lignocellulosic biomass according to three general steps: pretreatment, solubilization, and formation and solidification of the desired final product. Within the context of this research, these main steps were extended to the processing of BSG into lignocellulosic beads and particles.

Pretreatment methods have a dual mechanism that facilitates the subsequent dissolution of the biomass. Firstly, the lignocellulosic matrix of the biomass is broken apart, separating each of the components from one another. Secondly, polymeric components are hydrolyzed, reducing their degree of polymerization. As there is consequently less inter- and intramolecular bonding within the biomass, its solubilization is

* Green Chemistry is a framework for greener chemical processes and products defined by Paul Anastas and John Warner in 1998. The 12 guiding principles are : prevent waste, design for atom economy, create less hazardous chemical syntheses, design safer chemicals, use safer solvents and auxiliaries, design for energy efficiency, use renewable feedstocks, reduce derivatives, use catalysis, design for degradation, employ real-time analysis for pollution prevention, and use inherently safer chemistry for accident prevention.⁹⁰

facilitated for thermodynamic reasons. The efficiency of these mechanisms generally depends on the intensity of the chosen conditions. Pretreatment methods may also have a third mechanism of action if followed by filtration. When pretreated biomass is filtered, components that may hinder solubilization can be removed.³⁹ With this first step, we assume that BSG will behave like other lignocellulosic feedstocks.

When biomass is dissolved, the interactions between the solvent and the biomass's various components become more favourable than, for example, cellulose-cellulose interactions.⁹¹ When this occurs for all components of a complex lignocellulosic matrix, a molecularly complex yet homogenous solution can be obtained. Regarding solubilization, we hypothesize that pretreated BSG can be dissolved using cellulose's known solubilization systems, which is the primary component of interest in BSG in our intended application.

Finally, formation and solidification as a simultaneously occurring process led to the desired final product. With formation, the BSG solution is shaped into the intended shape. In the context of the current work, this final shape becomes microbeads (uniform and spherical) or particles (irregular, non-spherical) according to the chosen formation technique. Solidification is the mechanism exploited to ensure that these BSG microbeads or particles preserve their shape. Here, we assume that traditional microbead or particle formation and solidification techniques will apply to our BSG solutions.

1.5.2 Pretreatment methods

Lignocellulosic biomass commonly undergoes pretreatment for delignification, to reduce carbohydrates' degree of polymerization (DP), or to facilitate the extraction of coveted molecules. In the latter instance, pretreatment can serve as an extraction technique itself or can be followed by supercritical extraction, ultrasound-assisted extraction, ultrafiltration, electric-field-based technologies, or more traditionally, solvent extraction

(i.e., methanol, ethanol, acetone, hexane, or ethyl acetate).³⁹ Recurrent pretreatment methods are enzymatic, hydrolytic, alkaline, acidic, or solvent-based. A pretreatment method (or methods, as several techniques can be applied in succession) is chosen as a function of the biomass's desired application, all while minimizing energy consumption and cost. The present research investigated promising pretreatment methods to facilitate the complete solubilization of BSG.

Enzymatic pretreatment relies on oxidative and hydrolytic enzymes to disrupt cell walls.³⁹ Notably, proteases and carbohydrases have been used to separate proteins and polysaccharides from BSG, respectively.^{29, 47} If the intended result is to produce a high purity cellulose pulp, further pretreatment according to other methods is required.⁴⁷ This low-energy process is typically limited to small-scale operations, as the high cost of enzymes can be prohibitive in industrial processes.³⁹

Hydrolytic pretreatment, otherwise known as autohydrolysis, is used to extract hemicellulose. Under high pressures, a mixture of water and biomass is raised to an optimal temperature. At these conditions, acetyl and formyl groups (amongst other functional groups from hemicelluloses) release acids that have a catalytic effect on the process.⁹² When the temperature is too high, hemicellulose recovery decreases, and greater quantities of undesirable derivatives are formed.³⁹ This method only uses water, making it eco-friendly, inexpensive, and simple, but it is restricted to only a few applications.

Alkaline hydrolysis, or soda pulping, is another low-cost and eco-friendly method to separate hemicellulose from lignocellulosic biomass. Unlike autohydrolysis, high pH also facilitates delignification and protein removal, further enriching the residual biomass in cellulose.^{39, 43} With BSG, low concentrations of sodium hydroxide (i.e., 0.1 M) can be sufficient to separate proteins, provided the solution is heated, while delignification requires higher concentrations (i.e., 4.4 M) but can be realized at room temperature.⁴³ When heat is applied, delignification can be realized at lower soda concentrations and in less time, demonstrating the relationship between pH, temperature, and time in biomass fractionation.^{27, 44, 93}

By removing hemicellulose, proteins, and lignin, alkaline hydrolysis allows greater access to coveted phenolic phytochemicals, such as ferulic and *p*-coumaric acids.³⁹ Alternatively, when high-quality cellulose pulps are the desired product, alkaline hydrolysis is followed by bleaching, removing any residual impurities through chemical oxidation. Pretreated BSG can be boiled in solutions of sodium chlorite, followed by soaking at room temperature in aqueous sodium bisulphite.⁴³ Otherwise, dilute solutions of sodium hydroxide and hydrogen peroxide can achieve the same results at higher temperatures.²⁵ Resulting cellulose pulps have increased biodegradability and porosity (due to lignin's absence). They can be used as such or converted to cellulose nanofibers (CNFs) or nanocrystals (CNCs) through further processing.^{43, 44}

Acid hydrolysis achieves similar results to alkaline hydrolysis, all while remaining inexpensive and environmentally friendly.³⁹ This type of pretreatment involves boiling BSG in aqueous acidic solutions for relatively short periods.^{27, 35, 44, 93} The acid solution can be reused for several pretreatment cycles, provided the pH is readjusted with fresh acid.⁹³ Dilute acid hydrolysis, where strong acids are used at low concentrations, is preferred over methods that rely on high concentrations of weak acids (i.e., formic or acetic acid).⁹³ Sulfuric acid yields the best results in terms of hemicellulose degradation, but other strong inorganic acids (hydrochloric, phosphoric, nitric) may be optimal in other circumstances. For example, when optimal sugar yield is less important, a nitric acid-based hydrolysate can be neutralized with ammonia and dried, yielding a viscous fertilizer.⁹³ This provides an application for black liquor, the lignin-rich residue produced during the acid or alkaline hydrolysis of biomass.^{27, 44, 94}

Typically, the liquid hydrolysate recovered after acid hydrolysis contains the target compounds, and the solid pulp is discarded as waste. In alkaline hydrolysis the opposite is true: the hydrolysate is commonly disposed of as an unwanted by-product and the solid pulp is the desired fraction. Acid hydrolysis promotes the depolymerization of hemicellulose chains, and the resulting monomers dissolve into the liquid fraction. The sugar-rich hydrolysate is then recovered, neutralized, and fermented to produce valuable

sugar alcohols (i.e., xylitol), bioethanol, or volatile fatty acids.^{27, 35, 38, 39} Acid hydrolysis can also help reduce cellulose's DP, facilitating its solubilisation. However, if cellulose fibers are to eventually be regenerated to form a solid material, the polymer must not undergo complete hydrolysis.⁹⁵

At optimal conditions, acid hydrolysis offers better control over hydrolysate sugar yield and the formation of undesirable lignin degradation products (LDPs) when compared to alkaline pretreatment. Although LDPs such as furfural, 5-hydroxymethylfurfural (5-HMF), and acetic acid are useful in their own right, they inhibit enzymatic saccharification and the activities of fermentative microorganisms.³⁹ No matter the intended application of the biomass, the relationship between pH, temperature, and time needs to be evaluated to achieve optimal yields.^{27, 35, 93}

Solvent-based pretreatment is a less common option due to increased costs and environmental impacts. However, BSG can be boiled in organic solvents, notably ethanol, to facilitate carbohydrate extraction by partial hemicellulose hydrolysis and delignification. To increase this method's efficacy, ethanol can be acidified with dilute acid, or the pretreatment can be microwave-assisted.^{39, 96}

1.5.3 Solubilization systems

Cellulose, which represents 16-25% of the solid fraction of BSG,¹² has been extensively investigated for its potential to replace conventional plastic materials, including microbeads.^{88, 89} It can be easily chemically modified, blended with other natural polymers, or incorporated into composite materials, allowing to produce a wide variety of derivatives with specific, controllable properties.⁸⁶ When used to produce microbeads, hydrophilicity and hydrophobicity, charge, the nature of surface-grafted functional groups, porosity, pore structure, and particle size can be easily controlled.^{86, 97} In nature or when regenerated from a solution, cellulose chains have different degrees of order and organisation, amorphous

and crystalline sections, and varying DPs.⁹¹ The heterogeneity of cellulose fibers and their complex inter- and intramolecular hydrogen bonding network contribute to cellulose's resistance to solubilization.⁸⁶ Like most natural polymers, cellulose does not present melt processability, and may only be dissolved and regenerated in a select few solvent/anti-solvent systems.⁹¹

Cellulose is a homopolymer of D-glucose (anhydroglucose units, AGUs), joined by β -1,4 linkages (Figure 9). Linear cellulose chains self-arrange in the form of crystalline and non-crystalline microfibrils, and microfibrils bundle together to form fibrils. In plants, these fibrils are interwoven with lignin and hemicellulose (see Figure 7, section 1.1.5), whereas bacterial cellulose is of high purity.⁴⁶ When cellulose is sourced from biomass such as BSG, pretreatment methods disentangle these polysaccharides.³⁹ As discussed in the previous section (1.5.2), hemicellulose and lignin are dissolved into hydrolysate, as well as the lipids and proteins that form plant cells, amongst other molecules. After pretreatment, the solid fraction that remains is enriched in cellulose. Certain pretreatment methods, such as dilute acid hydrolysis, also reduce cellulose's DP, subsequently improving its solubilisation for thermodynamic reasons.^{39, 91, 93}

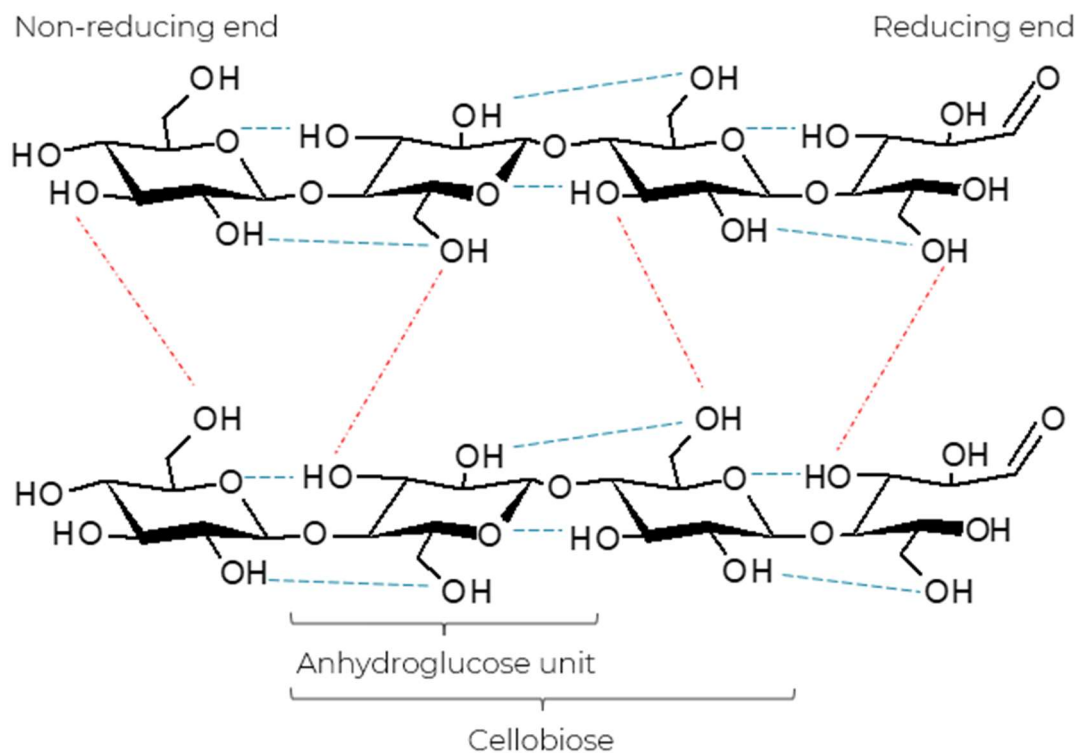


Figure 9. Molecular structure of cellulose.

There are three general routes for cellulose dissolution and shaping into materials, relying on non-derivatizing solvents, derivatizing solvents, or soluble cellulose derivatives. With non-derivatizing solvents cellulose is directly dissolved, then the dissolved cellulose is directly shaped. Conversely, derivatizing solvents chemically convert cellulose, leading to a dissolved cellulose derivative. This derivative is shaped using further chemical conversion. Finally, previously derivatized and isolated cellulose derivatives may undergo direct dissolution followed by direct shaping.⁸⁶ With cellulose-based microbeads, it is not necessary to obtain a cellulose derivative. Native cellulose (cellulose I), where chains are intermolecularly linked by hydrogen bonding on the third and sixth carbons of each D-glucose monomer (Figures 9 and 10), has the physical and chemical characteristics required for the intended application. This study consequently focuses on non-derivatizing solvent systems.

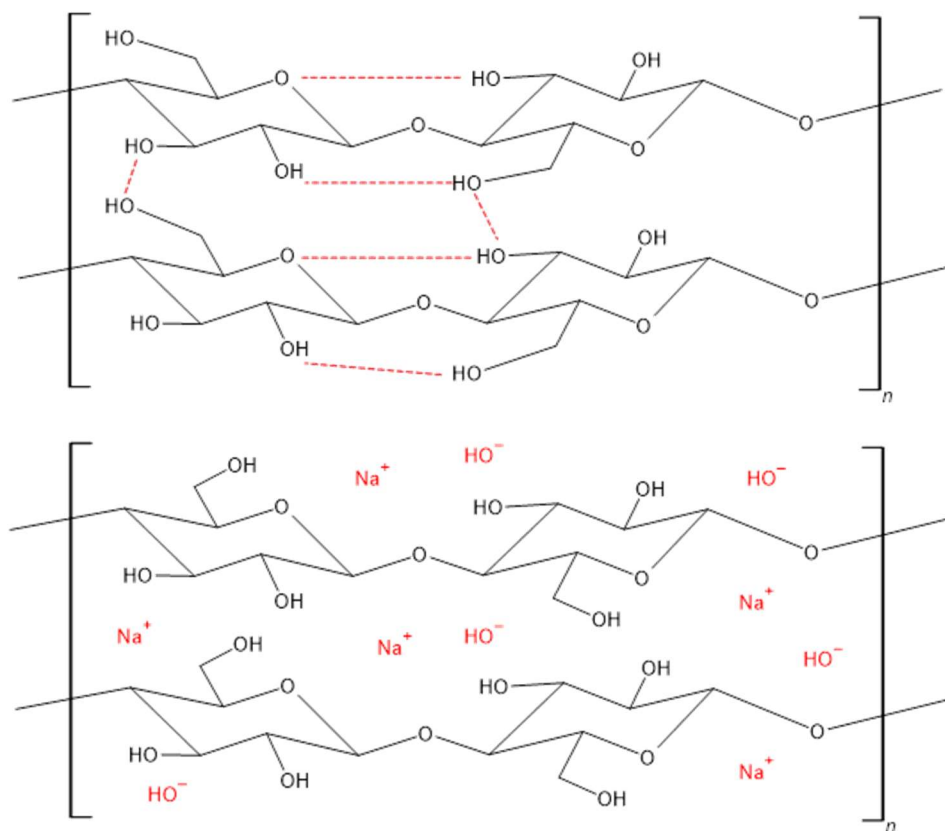


Figure 10. Schematic representation of cellulose's solubilization in aqueous NaOH. Cellulose I (above) is complexed by Na⁺ and OH⁻ ions in solution (Na-Cell, below).

Since the 1950s, various non-derivatizing methods have been investigated to produce cellulose microbeads.^{86, 98, 99, 100} Heavy metal-based solutions such as cuprammonium hydroxide are restricted due to their toxicity to humans and the environment. Solutions of *N,N*-dimethylacetamide (DMA) and LiCl, or *N*-oxide monohydrate (NMMO) are other options, but draw concerns over recyclability and thermal instability, respectively.^{86, 101} Otherwise, reusable ionic liquids (i.e., 1-ethyl-3-methylimidazolium acetate) or cold aqueous solutions of NaOH, NaOH-urea, or NaOH-urea-ZnO can be considered environmentally friendly.^{80, 81, 86, 88, 97, 99, 102} Of these, hybrid cellulose-lignin beads have been prepared from aqueous NaOH-urea.⁸⁹ However, these hybrid beads are made from previously isolated and purified cellulose and lignin. They deviate from the desired

spherical shape with increasing lignin content. Another study successfully produced cellulose-lignin films from aqueous NaOH, which we assume would equally extend to microbeads.⁸¹

With the objective of completely solubilizing BSG – cellulose, lignin, and all – to create hybrid natural polymer microbeads, aqueous solutions of NaOH seem the most promising. These systems have the particularity of only being effective at cold temperatures (-5 °C to +1 °C) and for a narrow range of NaOH concentrations (7 to 10 wt%). The limited intersection of temperature and NaOH concentration where cellulose is soluble is dubbed the “Q-state,” after the German word for swelling, *quellung* (Figure 11).^{91, 101, 103} Outside of this range, NaOH concentration and temperature can be controlled to modify the crystallinity of native cellulose fibers, resulting in a different allomorph (i.e., cellulose I becomes cellulose II during mercerization, at conditions designated by Na-Cell II, Figure 11).¹⁰⁴ Within this range, cellulose chains can be dissolved (Figure 10). The most widely held theory is that under these conditions, sodium and hydroxide ions possess the necessary hydrodynamic diameter to penetrate cellulose chains, causing them to swell, and subsequently disrupting their hydrogen bonding network.^{91, 104} When cellulose is dissolved by aqueous NaOH, there is a stable number of four NaOH molecules associated with each AGU. This roughly corresponds to a maximum solubility of 7 to 8 wt% cellulose in 7 to 8 wt% aqueous NaOH solutions, with cellulose’s DP influencing the exact stoichiometry.⁹¹ Researchers theorize that an unstable equilibrium exists between NaOH hydrates bound to cellulose chains. Even slightly higher temperatures cause cellulose-cellulose interactions to become favourable over cellulose-NaOH interactions. Cellulose coils shrink and the solution’s intrinsic viscosity decreases in a phenomenon known as gelation, preventing efficient shaping and regeneration.⁹¹

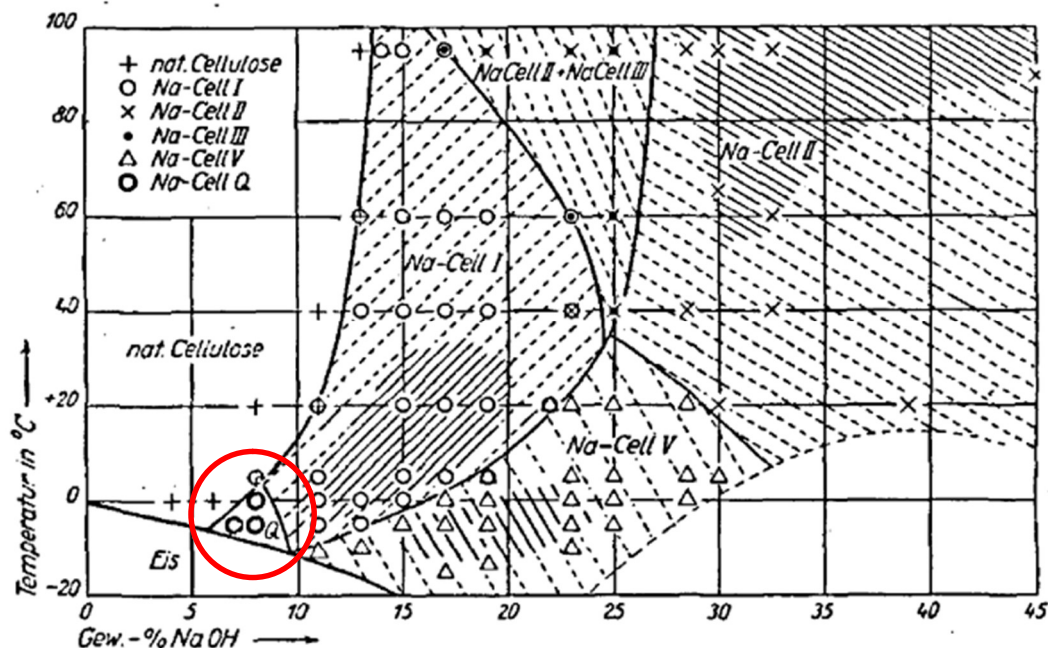


Figure 11. Phase diagram for aqueous NaOH-cellulose systems with encircled “Q-state”.

© Sobue et al., 1939.

Cellulose solubility in aqueous NaOH can be improved with the presence of additives, such as urea, thiourea, and metal oxides, which have the added benefit of being inexpensive and environmentally friendly.⁸⁶ Urea and thiourea do not modify the necessary NaOH-AGU ratio but form inclusion complexes that prevent cellulose chain aggregation/gelation. Through hydrogen bonds, hydrated NaOH bonds with cellulose molecules. Then, hydrated urea or thiourea bonds to these NaOH hydrates at the surface of the cellulose-NaOH complex.^{91, 104, 105} Starting at 2 wt% urea or thiourea these effects are observed.¹⁰⁵ Solubility is not improved by using both urea and thiourea.⁹¹

Zinc oxide and beryllium oxide also have positive effects on cellulose solubilization in aqueous NaOH by impeding gelation. At 0.5 wt%, these metal oxides improve solubility, with beryllium oxide demonstrating 70% of zinc oxide’s performance. Greater concentrations of ZnO or BeO simply precipitate with no effect on solubility.⁹¹ The exact

mechanism of metal oxides in a cellulose-NaOH-water solution is unknown, but there are several theories. Under strong alkaline conditions, zinc oxide and beryllium oxide form zincate ($\text{Zn}(\text{OH})_4^{2-}$) and tetrahydroxoberyllate ($\text{Be}(\text{OH})_4^{2-}$), respectively. These molecules may bond with cellulose fibers directly, modify cellulose's charge, or their surface hydrolyzation may bind free water, causing cellulose's stabilization.⁹⁵ Other research proposes that, like urea or thiourea, these metal oxides serve as a physical barrier to intermolecular hydrogen bonding amongst cellulose chains by forming a cellulose-NaOH-metal complex.^{91, 95} Zinc oxide also helps increase the material's porosity, at least in the case of cellulose-based microbeads.⁸⁸ It is likely that the particles are washed away during solidification, leaving behind a highly porous structure.

Dissolved cellulose's intermolecular hydrogen bonding network can be re-established with an appropriate anti-solvent. When introduced into a coagulating medium, the cellulose solution experiences a very high interfacial concentration effect, causing the regeneration of the exterior layer's hydrogen bonding network. Although this mechanism forms a very dense outer skin, the solvent/anti-solvent exchange can take place at weak points in the skin's interface. The rate of this counter-diffusion controls the kinetics of a cellulose-based material's complete regeneration.¹⁰¹ For a 7 wt% NaOH solubilization system, the most effective anti-solvents are a 1-2 M solution of a strong acid or a 10 wt% saline solution.^{89, 97, 106} Generally, maintaining this ratio if NaOH concentration is modified ensures cellulose's regeneration, although higher acid concentrations have reportedly led to more porous materials.⁹⁷

As for the other components of BSG that we aim to dissolve and regenerate, less is known about their specific dissolution and regeneration mechanisms. As a component in paper products, hemicellulose serves as an inter-fibre binding agent, reducing surface roughness, and improving overall strength, opacity, and brightness.¹⁰⁷ It's noted that these properties diminish when hemicellulose is pre-extracted from biomass, then added to products in a later step.¹⁰⁷ Hemicellulose's abundant end groups are more accessible to water molecules compared to cellulose, which may facilitate pulps' solubilization.¹⁰⁷ These

molecules are rarely crystalline or fibrous but are instead described as the “flesh” that help fill out cellulose fibres. Hemicelluloses are much more soluble and labile than cellulose and are compatible with alkali-based treatment systems.¹⁰⁸

Lignin has historically been an undesirable component in fibrous materials. Its brown colour has restricted its inclusion in the pulp and paper industry to corrugated cardboard, where at around 10.43 wt% of the material’s composition it confers desirable mechanical strength and resistance to degradation.¹⁰⁹ However, that’s not to say that lignin is non-biodegradable: on land, white-rot fungi possess the necessary enzymes to break down the lignin in native biomass, while the marine environment contains a diverse set of bacteria that can use lignin as a carbon source.¹¹⁰ Moreover, lignin’s biodegradability can be enhanced when it is subjected to acid-, alkaline-, or enzyme-based pretreatment,^{111, 112, 113} or physical grinding, milling, or steam explosion.^{114, 115}

1.5.4 Microbead production

Polymer microbeads are formed according to a two-step process: the bead is formed according to the required dimensions, then the structure is solidified. Microbeads can be formed by dropping/extrusion, emulsification techniques, coacervation, or through the use of custom molds. Solidification mechanisms include anti-solvent polymer regeneration, solvent evaporation, or crosslinking, which can be chemical (ionic or covalent), photo-induced, or thermal. Particle formation and solidification can be realized simultaneously, as is the case with spraying techniques. These commonly used techniques are chosen as a function of the polymers and additives used, as well as the desired physical and chemical characteristics of the microbeads. Certain methods can also be combined to facilitate suspension polymerization reactions.

Dropping or extrusion techniques are based on extruding the polymer solution through a small opening, such as the tip of a syringe. The polymer solution forms spherical

droplets when the combined forces of gravity and applied pressure exceed the surface tension of the solution and the capillary forces at the outlet.⁸⁶ The process can be continuous, leading to high production volumes, which is useful for industrial applications.¹¹⁶ In its simplest iteration, the technique produces relatively large beads, often several millimetres in size, whose smallest dimensions reach 100 μm .^{116, 117} However, beads of smaller dimensions and greater production volumes can be achieved by making small changes to the production setup. Gericke, Trygg, and Fardim describe these techniques (2013),⁸⁶ which are represented in the image below (Figure 12). In spinning drop atomization (rotary atomization), the polymer solution is extruded at high forces through a rotating cylindrical vessel with small outlets, achieving beads in the range of 500 μm . Spinning disc atomization also allows to produce beads at these smaller dimensions, by constantly spreading a thin film of the polymer solution onto a disc rotating at high speeds. Tiny polymer droplets are ejected from the edge of the disc due to centrifugal forces. Finally, jet cutting involves extruding the polymer solution through a small opening under high pressure, consequently generating a constant stream that is cut into droplets by a rotating blade. When this setup extrudes directly into another solution with no drop height, the technique is referred to as underwater pelletizing.

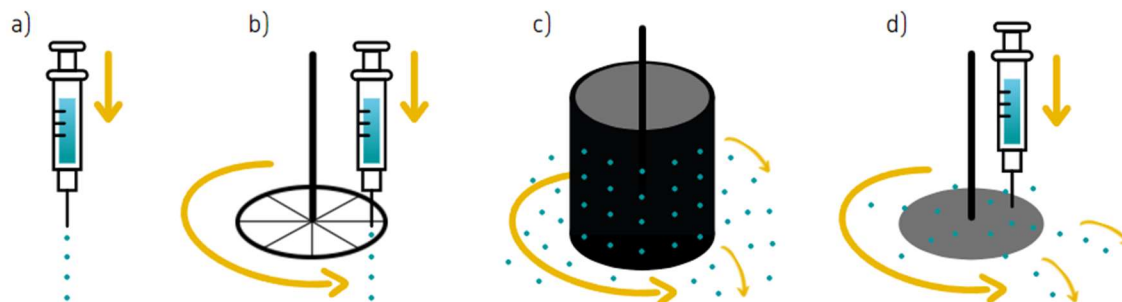


Figure 12. Representation of variants of the dropping/extrusion technique: a) simple, b) jet cutting, c) spinning drop atomization, and d) spinning disc atomization.

Dropping is commonly coupled with anti-solvent or crosslinking solidification methods, as the beads can easily be extruded into a solution of this nature. To ensure that beads do not fuse together and to equilibrate concentration gradients, solidification solutions are commonly kept under agitation. The solidification solution is chosen as a function of the polymers used in the formation of the bead. Besides this, drop height needs to be optimized when the beads are not directly extruded into the solidification medium. The shape of the beads depends on the force at which the polymer droplets hit the solution's surface: if beads are extruded from too great a height, too much pressure is applied during extrusion, or the solidification solution is too viscous, beads may flatten into discs.⁸⁸

Emulsification methods are based on the principle of creating an emulsion between a minimum of two immiscible fluids, either manually or by using a specialized porous membrane (Figure 13) or fluidic device (Figure 14). Through traditional membrane emulsification a dispersed phase is pressed through a membrane into a circulating continuous phase; in coarse/pre-mix membrane emulsification an existing emulsion is pressed through a membrane into a circulating continuous phase to obtain droplets of even smaller dimensions (Figure 13). The desired polymer is dispersed in the disperse phase, consisting of an appropriate solvent-cosolvent solution. The continuous phase is immiscible with the disperse phase and contains a surfactant to stabilize the emulsion, which may negatively impact microbeads' properties.^{86, 118} Novel methods consequently seek to eliminate the need for surfactants.¹¹⁹ Currently, multiphase emulsions between three or more phases are restricted to small-scale production volumes and require multiple surfactants to stabilize each interface.^{120, 121}

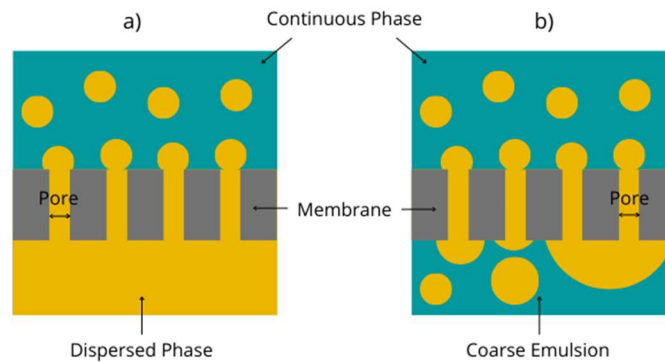


Figure 13. Representation of membrane emulsification techniques: a) traditional membrane emulsification and b) coarse membrane emulsification.

The polymer droplets dispersed in the continuous phase can be solidified and extracted using an anti-solvent or chemical crosslinking agent,⁸⁰ through the evaporation of a volatile solvent,^{75, 79} or the realization of a suspension polymerization reaction.^{119, 122} As emulsion methods allow to create dispersions of fine droplets, microbead size ranges from 10 to several hundred μm . Specific bead size and morphology can be controlled by the mixing speed, type, nature and concentration of surfactant, the ratio between different phases, and the viscosities of the solutions.⁸⁶

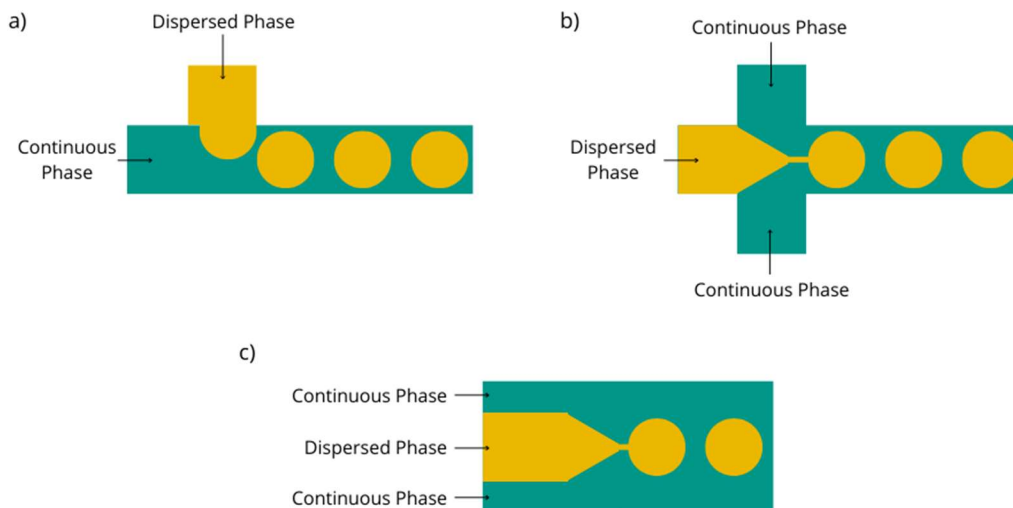


Figure 14. Schematization of common fluidic device configurations: a) T-junction, b) flow-focusing, and c) co-flow.

Coacervation is a relatively straightforward technique for the production of microcapsules, where substances are encapsulated within the bead as opposed to being dispersed throughout (matrix particles).¹¹⁶ Simple coacervates use one type of polymer and allow to encapsulate hydrophobic compounds but have relatively weak mechanical properties. These coacervates primarily result from an oil-in-water emulsion introduced drop by drop into an ionic coagulating medium, so that the organic phase carrying the encapsulated substance becomes trapped within a polymer shell. The microcapsules are then further solidified using a crosslinking agent.^{121, 123} Complex coacervates (Figure 15) are formed from the electrostatic interactions between two polymers with opposite charges, most commonly alginate in an alkaline solution and gelatin in an acidic solution.¹²⁴ The substance to be encapsulated is dispersed in the polyanionic alginate solution, both polymer solutions are vigorously mixed, and pH, temperature, or salinity is modified to induce the formation of ionic bonds.^{123, 124} Allowing the resulting beads to then soak in a crosslinking solution confers greater mechanical strength to the beads' shells through the formation of covalent bonds.^{116, 124} These microbeads are heat- and water-resistant and have dimensions in the range of 0.1 to 500 μm , and often require post-treatment by spray- or freeze-drying

to obtain better mechanical properties.¹¹⁶ Both techniques are appropriate for the encapsulation of reactive, insoluble, volatile, or sensitive (oxygen, light, humidity) substances,¹²⁵ and can be used with either petrochemical or natural polymers, so long as the polymer can be solidified through crosslinking.¹²¹

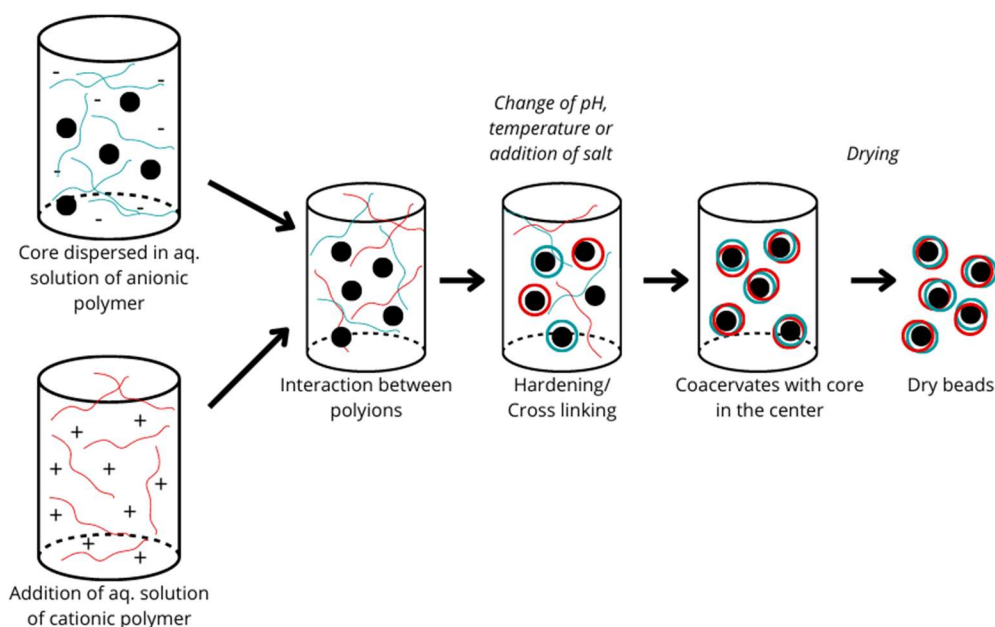


Figure 15. Representation of microbead production through complex coacervation.

Custom molds are arguably the least complicated way to produce microbeads but are generally restricted to smaller batch sizes and larger beads. To increase production volumes, larger molds can be used, then the beads can subsequently be cut to the required dimensions. This generally sacrifices bead sphericity and the homogeneity of beads' size distribution, so that the final product can more appropriately be referred to as particles. Beads can be solidified by crosslinking, anti-solvent polymer regeneration, or solvent evaporation. When chemical crosslinking or anti-solvent polymer regeneration is used, the molds should ideally be soaked in the appropriate solution. Otherwise, solvent evaporation can be used as an initial step, then the beads can be transferred to the desired solidification medium for further hardening.

Spraying, otherwise known as electrospraying or electrohydrodynamic atomization, produces large batches of very small microbeads (to the order of the micrometer or nanometer).^{121, 126} It is a rapid, continuous, and simple process that combines droplet formation and solidification in a one-step mechanism, all while maintaining control over bead size distribution and morphology.^{116, 117, 126} Sprayers use vibrating conductive nozzles to atomize polymer solutions. A high-voltage electric field generated at the nozzle charges the polymeric solution as it passes through. This charge generates an electrostatic force, specifically a Coulomb force, in the droplet, which overcomes the cohesive force of the polymeric solution. The surface tension is surpassed, the charge is released, and the droplet breaks apart into a large number of much smaller droplets.¹²¹ The ever-present Coulomb repulsive force prevents the beads from coalescing during flight.¹²⁶

A few variations of this technique exist, according to the conditions of the drying chamber into which the beads are sprayed.¹¹⁷ In spray-drying, a volatile solvent is evaporated almost instantly under high temperatures, inducing solidification. In spray-cooling or spray-freezing, restricted to thermoplastic synthetic polymers, solidification occurs at low temperatures.¹²⁷ Spraying techniques can be used to prepare microcapsules or matrix particles, so long as specialized instruments known as automatic encapsulators are used.^{86, 116}

Many polymers can be solidified by placing them in a solution in which they are no longer soluble. This solidification technique is known as anti-solvent polymer regeneration. While solvents rupture chemical bonds, allowing to extract a natural polymer from its matrix, separate polymer chains from one another, or reduce a polymer chain's DP, anti-solvents regenerate bonds and the solid polymer network. Although synthetic polymers do not need to be extracted from biomass, they often need to be solubilized and regenerated to attain a product's desired dimensions. Anti-solvent polymer regeneration is an easy and inexpensive method to solidify polymers with known solvent/anti-solvent systems (i.e., cellulose).^{89, 97}

Polymer solidification by crosslinking involves the formation of an ionic or covalent bond to join two or more polymer chains (Figure 16). The number of crosslinking bonds is directly proportional to the hardness of the beads: more bonding represents more rigid polymer chains.¹²⁸ Crosslinking can be chemically, thermally, or photo-induced, depending on the nature of the polymer, additives present, and the intended applications of the resulting product.

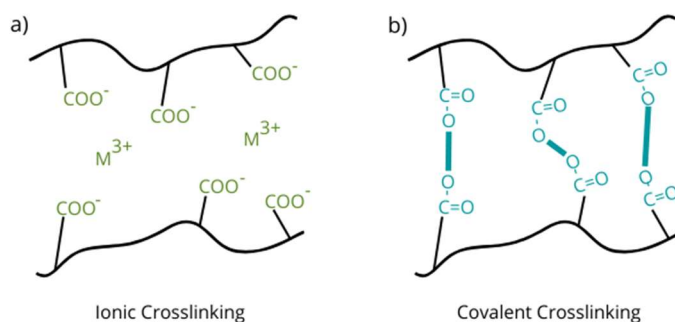


Figure 16. Representation of a) ionic and b) covalent crosslinking. This example demonstrates crosslinking bond formation across deprotonated carboxyl groups.

Ionic crosslinking (ionotropic or ionic gelation) is commonly exploited in the preparation of polymer microbeads, recognized for its simplicity, rapidity, low cost, and success in creating functionalized microbeads.⁸³ It can be used in the creation of natural or synthetic microbeads, and matrix beads or microcapsules, depending on the bead formation technique used in conjunction.^{97, 116, 128, 129} The method relies on an ionic crosslinking solidification reaction induced when a polyelectrolyte spontaneously forms an ionotropic gel when exposed to a multivalent ion. In the case of exterior ionic crosslinking, the multivalent ion rapidly gels and stabilizes the exterior layer of the polymer droplet, then diffuses into the bead to solidify the interior layers (Figure 17). Internal gelation mechanisms incorporate the crosslinking agent directly into the polymer matrix and are much less effective.¹¹⁷ Covalent crosslinking relies on the same principle, instead using aldehyde solutions (i.e., glutaraldehyde or formaldehyde) to form covalent bonds.¹²² This is a less common choice.

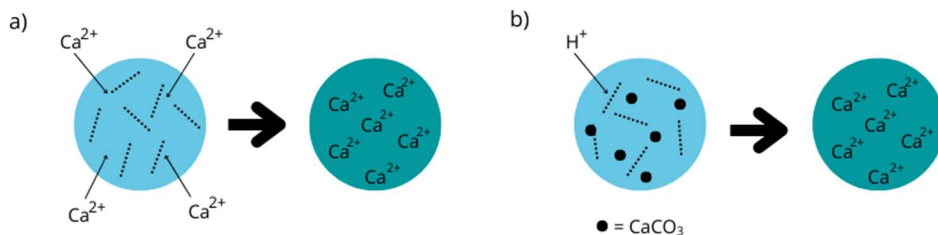


Figure 17. Schematization of the mechanisms of a) external gelation and b) internal gelation (with CaCO_3 as the gelation agent).

Crosslinking can also be triggered by light or heat.¹²⁸ Photo-induced crosslinking depends on the addition of a photoinitiator which is activated by light of a specific wavelength. Photoinitiators generally possess benzoyl structural groups which can absorb photons and produce free radicals.¹³⁰ The free radicals polymerize, then form covalent bonds to crosslink monomer chains, ensuring the formation of spherical microbeads with good mechanical properties and high porosity.^{128, 130} Thermal crosslinking applies to thermoresponsive polymers, which crosslink and solidify when critical solution temperatures are reached. As thermoresponsive polymers have ionic or secondary forces, solidification can be reversed by changing the temperature, which is an interesting property for certain applications.¹²⁸

When solvent evaporation is used as a solidification technique, the nature of the solvent affects the morphology of the resulting microbeads. Solvents with relatively low boiling points evaporate more quickly, meaning polymer chains have less time to contract and rearrange themselves, leading to porous or hollow microbeads of larger dimensions. With a less volatile solvent, polymer chains experience a greater degree of contraction during the evaporation process, leading to smaller, smoother microbeads.¹²⁶ Controlling the temperature of the solidification environment allows further control over bead morphology.⁶⁵ Solvent evaporation is best adapted to synthetic polymers that do not possess melt-processability.¹²⁶

1.5.5 Characterization methods adapted to microbeads and microparticles

1.5.5.1 General

As polymer microbeads or microparticles can be used in a wide variety of specific applications, these materials need to be properly characterized. In the case of the present research, where BSG microbeads or microparticles are envisioned as physical exfoliants in personal hygiene products, they must present similar or improved characteristics compared to currently available physical exfoliants. They must have smooth surfaces and porous interiors, be stable when incorporated into personal hygiene products, demonstrate good cleansing efficiency, be sufficiently hard, and be composed of biodegradable materials. These parameters can be characterized according to several well-known techniques, including digital imaging, microscopy, nanoindentation, energy-dispersive X-ray spectroscopy (EDS or EDX), and infrared spectroscopy (FTIR). Conversely, customized characterization protocols that rely on several techniques can better assess the materials' behaviour in other regards, notably pertaining to cleansing efficiency and stability. While many techniques can be used to characterize microbeads and microparticles, only those used throughout this project are discussed in this section.

1.5.5.2 Digital imaging

Digital imaging consists of taking digital photographs of samples and analyzing them with an image processing program to learn valuable information about a single specimen or population. ImageJ software, an open-source image processing program developed by the National Institute of Health (USA), can be used to measure a sample's size and compute shape descriptors (such as minor and major axes and circularity).^{97, 116, 131} Although microbeads tend to be slightly elliptical, if assuming perfect sphericity the volumes of the beads can be calculated using the measured length of the minor axis.¹³¹ The same can be said of square microparticles, if assuming perfect cubicity.

Herein, we also use digital imaging techniques to gain insight into sample porosity, stability, and cleansing efficiencies. When investigating porosity, we use digital imaging to compare the size of wet versus dry samples. This ratio indicates material swelling properties, which in turn serves as an indicator of porosity in cellulosic materials. When investigating stability, we use digital imaging to describe the size of samples before and after aging. When combined with qualitative observations and gravimetric analysis, this provides insight into the material's degradation over time. Finally, with cleansing efficiency, we use digital imaging techniques to analyze images of a written-on surface before and after washing. This provides insight into how efficiently a given soap can remove a model contaminant from a model surface.

1.5.5.3 Scanning electron microscopy

Scanning electron microscopy (SEM) was used throughout this project to assess the morphology of the final products. This technique produces nanometer-scale images of samples by scanning them with a focused beam of electrons.¹³² These electrons interact with the atoms in the sample and emit secondary electrons, which can be used to interpret information about the samples' surface topography and composition.¹³³ The result is a high-resolution image showing the detailed surface morphology of the sample.

Samples must be dried before SEM can be used to assess them. Some micromaterials have very delicate structures, requiring stepwise solvent exchange followed by critical point drying to preserve their morphology (evaporation can result in hornification and lyophilization can cause the collapse of the porous structure).⁸⁶ Other samples can be dried by liquid-nitrogen-enabled freeze-drying,^{89, 134} *n*-butanol drying,⁸⁰ air-drying in ambient conditions,¹³⁵ or oven-drying.¹³⁶ To examine the interior morphology of the materials, microbeads or particles can be cut using a razor blade, ruptured with a mortar and pestle, or sliced using a microtome.^{75, 80, 88, 89, 137}

Prior to analysis, dried polymer-based materials also need to be sputtered with gold, platinum, carbon, or a gold-palladium alloy under an argon atmosphere in a vacuum.^{88, 97, 132, 138} This prevents the charging of poorly conductive or non-conductive samples that would otherwise occur through the accumulation of static electron fields during electron scanning. Sputter-coating also increases the number of secondary electrons that can be detected, thus increasing the signal-to-noise ratio, and improving the quality of the resulting image.¹³⁹ Metal-based sputter coating logically increases the efficiency of SEM analysis by increasing the thermal and electric conduction of the sample,¹⁴⁰ but carbon has proved equally efficient when analyzing lignocellulose-based materials.^{89, 97} As a final step, before materials can be analyzed, the voltage of the incident electron beam is set, ranging from 1 to 30 kV.^{88, 141, 142, 143}

Besides being used to characterize the surface morphology of individual samples, SEM can be coupled with digital imaging techniques to analyse the shape, size, and size distribution of several samples. These same techniques can be used to investigate the shape, size, and size distribution of a material's porous structure.^{86, 132, 141, 144} Besides this, SEM is commonly coupled with energy dispersive X-ray spectroscopy (EDS or EDX), which determines the elemental composition of a sample.^{136, 145}

1.5.5.4 Indentation

Indentation techniques have a long history of use to determine the mechanical properties of samples. With these techniques, a hard tip whose properties are known is pressed into a sample at an increasing load. Once the loading has reached a user-defined maximum, it may be held constant for a period before removal.¹⁴⁶ The area of the residual indentation in the sample is measured by light microscopy, which then allows to determine the hardness of the sample using Equation 1:

Equation 1. Sample hardness (H) determined by indentation techniques

$$H = \frac{P_{max}}{A_r}$$

Where H is the sample hardness, P_{max} is the maximum load, and A_r is the residual indentation area as a function of h_{max} , the penetration depth.

Indentation studies also allow to calculate the indentation modulus (M) of the sample, according to Equation 2:

Equation 2. Sample indentation modulus (M) determined by indentation techniques

$$M = \frac{S \cdot \sqrt{\pi}}{2 \cdot \sqrt{A_r}}$$

Where M is the sample indentation modulus, S is the unloading slope, and A_r is the residual indentation area as a function of h_{max} , the penetration depth.

Microindentation is a type of indentation-based hardness test applied to small samples, where the indentation area is only a few square micrometers in size. Nanoindentation is another variant where the indentation is in the nanometer range. To reduce the error associated with these small-scale analyses, a Berkovich tip with a three-sided pyramid geometry is used. Moreover, as the tip penetrates the sample's surface, the instrument records a load-displacement curve. This can be used to determine other properties of the sample, including elastic modulus, strength, residual stresses, and fracture properties.¹⁴⁷ A challenge to micro- and nanoindentation analysis of polymer-based materials is their relative roughness. An additional factor to consider is the likelihood of the probe becoming dirtied by dust broken off from relatively soft samples. Because of this, instrumentation needs to be carefully calibrated for use with rough or soft samples.¹⁴⁶

1.5.5.5 Energy-dispersive X-ray spectroscopy

Energy-dispersive X-ray spectroscopy (EDS or EDX) uses X-rays to irradiate samples to determine their elemental or chemical composition. When bombarded with X-rays, atoms become excited and emit electrons in a characteristic manner, which allows to identify their nature. EDS is a destructive technique, meaning the sample cannot be recuperated afterwards. However, it has the advantage of providing the elemental composition for an entire sample or elemental dispersion throughout a sample. EDS is commonly used in compliment to SEM.^{136, 145, 148}

1.5.5.6 Infrared spectroscopy

Infrared (IR) spectroscopy, or vibrational spectroscopy, is likely the most used technique for the characterization of the chemical structures of polymer materials. This technique involves measuring the interaction between a spectrum of infrared radiation (longer wavelength and lower frequency than visible light) with a sample through absorption, emission, or reflection, where different heteronuclear functional groups interact characteristically based on a change in their dipole moment.¹⁴⁹ Consequently, IR spectroscopy has a low sensitivity for non-polar functional groups.¹⁵⁰ Results are plotted in a spectrum of radiation transmittance or absorbance as a function of the wavelength or frequency of radiation. Fourier-transform infrared spectroscopy (FTIR) is the most popular variant of the technique, allowing to simultaneously collect high-resolution spectral data over a wide spectral range, converting raw data through Fourier transformation into a spectrum that can be analyzed and interpreted.

FTIR, especially, can be used to identify the chemical composition of a sample and to reveal chemical modifications within a structure by detecting the possible formation or destruction of polymer groups.^{63, 119, 135, 151} Consequently, this technique can be used to monitor degradation, ongoing chemical reactions, microbial attacks, the encapsulation of

another substance, or a material's purity.^{64, 116, 136, 152} However, it is important to note that hybrid materials or samples containing multiple additives make be particularly difficult to characterize using FTIR, as the presence of many functional groups can make identifying spectral subtleties difficult.¹⁵¹

With FTIR, samples are ground into a powder, which is then mixed with an excess of potassium bromide (KBr) or Nujol (a chemically inert paraffin oil) prior to analysis.^{140, 153} An FTIR equipped with an attenuated total reflectance device (ATR) allows to skip this step, as this device facilitates the direct characterization of very absorbent, thick, or irregular samples at a high resolution of 2 cm^{-1} .¹⁴⁵ This method is particularly useful when characterizing natural polymers and is consequently used throughout the present research. With ATR-FTIR, an ATR crystal in contact with the sample leads to the formation of an evanescent wave; IR radiation enters the crystal and reflects within at each point of contact with the sample (Figure 18). This mechanism limits the radiation path length into the sample, avoiding the problem of signal attenuation.¹⁵⁴

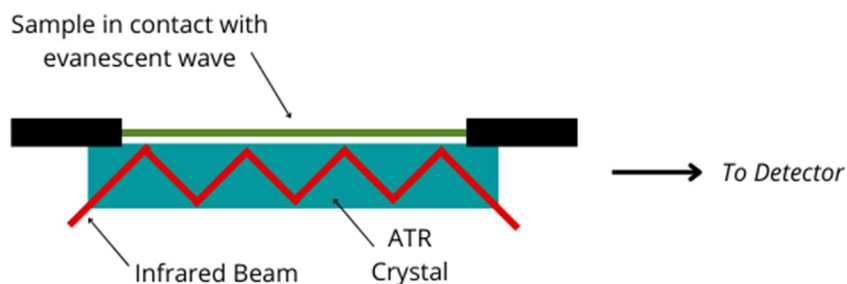


Figure 18. Representation of the mechanism of an ATR device used in FTIR spectroscopy.

1.6 ORGANIZATION OF THE CHAPTERS

The present research is mostly presented in the form of two academic articles which will be submitted for publication following the evaluation of this manuscript. Each article occupies a unique chapter in the present manuscript. The first article is included in Chapter 2, and the second article is included in Chapter 3. There are two distinct chapters as the

research led to two distinct sets of results, although they are linked by being defined by the same original objectives.

Chapter 2 is titled *Biodegradable Spherical Microbeads from Brewer's Spent Grain for Sustainable Personal Hygiene Productions*. This article discusses a fractionating dilute acid hydrolysis pretreatment method for BSG that allows to dissolve the remaining cellulose-enriched fraction in a cold aqueous NaOH-ZnO system. Spherical microbeads are subsequently shaped according to the dropping/extrusion method and solidified by anti-solvent polymer regeneration in an acid bath. Characterization proves that these beads present the properties required for exfoliating microbeads in personal hygiene products. This chapter also references, as a compliment to the research described within, the results of a lab and pilot scale-up of the method (see Chapter 4.1), as well as a techno-economic assessment demonstrating its financial feasibility (Chapter 4.2). This information will not be included in the article that we will submit for publication.

Chapter 3, titled *Complete Solubilization of Brewer's Spent Grain for the Production of Exfoliating Particles*, describes a second method for producing biodegradable BSG-based microparticles. This dilute acid hydrolysis pretreatment described herein allows to solubilize the entirety of the hydrolysate and solids using a cold aqueous NaOH-ZnO system. Microparticles can be shaped by pouring the resulting BSG-NaOH-ZnO solution into custom molds. Dried particles can be neutralized in an acid bath, or directly incorporated into personal hygiene products. Both varieties are characterized, demonstrating their potential as exfoliating particles in personal hygiene products. As is the case for Chapter 2, this chapter references a techno-economic assessment demonstrating its financial feasibility (Chapter 4.2).

The work presented in these articles relies on similar methodologies but has different outcomes. The protocol outlined in Chapter 2 yields spherical, uniform microbeads with morphologies that are closely in keeping with industry standards. However, these results are only achieved after BSG fractionation, resulting in the loss of approximately 50% of the biomass to the hydrolysate. Conversely, Chapter 3 highlights a novel method for the

complete solubilization of BSG that facilitates its regeneration to form fibrous polymeric materials. To the best of my knowledge, this method is the first of its kind and could pave the way for the development of a wide variety of biodegradable materials from BSG. However, the microparticles produced according to this method are not as spherical as those produced with the method described in Chapter 2, as the BSG-NaOH-ZnO solution proves incompatible with the dropping/extrusion shaping method.

Chapter 4, which is not a manuscript destined for publication, serves to prove the industrial feasibility of the methods described in Chapters 2 and 3. This chapter presents the experimental work surrounding lab- and pilot-scale-up of the BSG-based microbead production process (section 4.1), as described in Chapter 2. This work serves to add further validation to the protocols presented in Chapters 2 and 3, aiding in the eventual commercialization process of the resulting materials. Section 4.2 then goes on to describe a technoeconomic assessment of both methods, presented alongside that of a similar protocol for the production of purified cellulose microbeads. The cost and quantity of raw materials required in the production of BSG-based microbeads or particles, as well as cellulose-based microbeads, are presented, with values normalized for 1 kg of the final product. We also estimate costs associated with the equipment required for a proper scale-up of the process.

CHAPTER 2

BIODEGRADABLE SPHERICAL MICROBEADS FROM BREWER'S SPENT GRAIN FOR SUSTAINABLE PERSONAL HYGIENE PRODUCTS

2.1 FRENCH ABSTRACT AND CONTEXT OF THE FIRST ARTICLE

2.1.1 Résumé

Microbilles sphériques biodégradables à base de drêches pour des produits d'hygiène personnelle durables

Plusieurs pays ont récemment interdit la production et l'importation de produits d'hygiène personnelle contenant des microbilles de plastique synthétiques. Ces produits se retrouvent aux égouts lors de leur utilisation et les particules de plastique sont trop petites pour être retirées des eaux usées, ce qui mène à leur accumulation dans l'environnement. Dans l'environnement marin, les plastiques synthétiques peuvent sorber et transporter des polluants inorganiques et organiques et nuire à la santé de plusieurs espèces, notamment via leur bioaccumulation dans certains organismes. Afin de pallier ces importants désavantages, plusieurs recherches actuelles visent à développer des alternatives biosourcées qui offrent des propriétés mécaniques comparables à leurs homologues en plastique synthétique. La drêche de brasserie, le principal résidu de l'industrie brassicole, constitue à cet effet une matière première prometteuse. Les travaux reportés dans cet article démontrent une nouvelle voie de valorisation de ce coproduit via le développement de microbilles exfoliantes biodégradables, non-toxiques et végétaliennes. Après prétraitement par hydrolyse acide, la biomasse lignocellulosique est solubilisée par une solution aqueuse de NaOH et ZnO. Les microbilles sont ensuite formées et solidifiées par leur extrusion, goutte à goutte, dans une solution HCl qui sert d'anti-solvant. Les microbilles résultantes ont un diamètre moyen de 1.25 mm, une distribution granulométrique homogène et une dureté de 199.05 MPa. Les billes s'avèrent stables dans des savons liquides et solides pendant au moins trois mois et démontrent une capacité de nettoyage supérieure par rapport aux particules exfoliantes naturelles commercialement disponibles. Les microbilles à base de drêche s'avèrent ainsi une option prometteuse pour une utilisation en tant qu'agent exfoliant physique dans divers produits d'hygiène personnelle.

Mots-clés : *drêche de brasserie, cellulose, microbilles, biodégradable*

2.1.2 Contexte du projet

Cet article, intitulé « *Biodegradable Spherical Microbeads from Brewer's Spent Grain for Sustainable Personal Hygiene Products* », sera soumis pour publication dans un journal scientifique à l'automne 2022. Le principal journal visé pour l'évaluation par les pairs et la publication est *Green Chemistry* de la maison d'édition *Royal Society of Chemistry*. Sinon, nous avons identifié *Current Research in Green and Sustainable Chemistry (Elsevier)* ou *Sustainable Chemistry and Engineering (American Chemical Society)* comme d'autres options potentielles. En tant que premier auteur, j'ai contribué à l'essentiel de la recherche sur l'état de la question, au développement de la méthode et à l'exécution de la caractérisation du produit développé. Les chercheurs Vincent Banville et Charles Emond, second et troisième auteur, ont aidé à l'élaboration de l'idée originale et ont influencé le développement de la méthode et les stratégies de caractérisation. Le professeur Sébastien Cardinal, en tant que directeur du projet de recherche, a également influencé le développement de la méthode et les stratégies de caractérisation, ainsi que l'organisation de l'article de recherche. Les résultats préliminaires de ce projet ont été présentés aux conférences *Green Food Tech* de l'Institut de nutrition et des aliments fonctionnels (INAF) de l'Université Laval (virtuel, Québec) et *ComSciCon* (virtuel, Québec) en 2021. Une version abrégée de l'article final a été présentée sous forme d'affiche à la *Gordon Research Conference in Green Chemistry* à Castelldefels (Espagne) en juillet 2022. Ce chapitre est également complété par une analyse technicoéconomique et des résultats de la mise à l'échelle pilote de la méthode qui forment le Chapitre 4. Toutes les références sont regroupées dans la bibliographie générale à la fin de ce manuscrit.

2.2 CONTENT OF THE MANUSCRIPT

Biodegradable Spherical Microbeads from Brewer's Spent Grain for Sustainable Personal Hygiene Products

A. McMackin^{1,2}, V. Banville², C. Emond², S. Cardinal¹

¹ Département de biologie, chimie et géographie, Université du Québec à Rimouski (UQAR), Rimouski, Québec, Canada

² Centre de développement bioalimentaire du Québec (CDBQ), Sainte-Anne-de-la-Pocatière, Québec, Canada

Many countries have recently banned the production and importation of petrochemical plastic microbeads for use as exfoliating agents in personal care products. Products of this nature are designed to rinse off and plastic particles are too small to be retrieved during wastewater treatment, leading to their accumulation in the environment. In the marine environment, synthetic plastics sorb inorganic and organic pollutants, bioaccumulate, and negatively impact living organisms. Researchers have consequently been forced to investigate sustainable alternatives which offer comparable mechanical properties to their synthetic plastic counterparts. Brewer's spent grain (BSG), the primary residue of the brewery industry, is shown herein to be a promising starting material in the development of biodegradable, non-toxic, and vegan microbeads for use in personal hygiene products. After dilute acid hydrolysis, pretreated lignocellulosic pulp is solubilized using an aqueous system of NaOH and ZnO. Microbeads may then be formed and solidified by dropping the resulting solution into an acid bath, filtering, and drying. The conditions of each step required optimization to successfully produce spherical microbeads with a mean diameter as small as 1.25 mm, a homogenous size distribution, and a hardness of 199.05 MPa. The beads' proved stable in liquid and solid soaps over three months. The beads also demonstrate superior cleansing abilities compared to commercially available natural exfoliating particles. BSG-based microbeads are therefore a promising option for use as a physical exfoliating agent in various personal hygiene products.

Keywords: *Brewer's Spent Grain, Cellulose, Microbeads, Biodegradable*

2.2.1 Introduction

The world is shaped by plastics – to the extent that their presence has become the indicator of a new geological era.¹⁵⁵ Plastics' durability is reason for their widespread use but leads to their persistence in the environment. Microplastics, particles ranging from 1 μm to 5 mm in diameter,⁷³ are of particular concern as there is no feasible method for their retrieval from the environment.¹⁵⁶ Marine environments especially bear the consequences of plastic pollution, with 14 million tonnes of microplastics littering the ocean floor,¹⁵⁷ not to mention the countless other particles suspended in the water column. Due to their small size, microplastics may be ingested at all levels of the food chain and are known contaminants of human food and drinking water sources.^{57, 158} Microplastics also leach the chemical additives they contain and transport toxic chemicals (such as persistent organic pollutants and heavy metals), which bioaccumulate as they are ingested and transferred up the food chain.¹⁵⁹ When incorporated into marine sediments, microplastics can especially affect benthic organisms, and the extreme conditions of these zones further slow their breakdown.⁷⁷

Microplastics can be grouped into two categories, primary and secondary, according to their origin. While secondary microplastics result from the decomposition of larger plastic items, primary microplastics are produced at these sizes for use in a variety of commercial applications.¹⁶⁰ One such application is as a physical exfoliating agent in personal hygiene products, such as soaps, scrubs, and toothpastes – products designed to be washed down the drain during use.^{161, 162} Wastewater treatment facilities are able to remove the majority of these beads, but a significant fraction escapes filtration and ends up accumulating in aquatic environments.^{70, 163, 164} Consequently, plastic microbeads have recently been banned or voluntarily phased-out in many countries,¹⁶⁵ motivating researchers and industry members alike to explore sustainable alternatives.

Plastic microbeads for personal hygiene products have conventionally been made from polyethylene (PE), polyester (PES), polyvinyl chloride (PVC), polypropylene (PP),

and polystyrene (PS) as these are low-cost materials with desirable mechanical characteristics.^{69, 70} A 2021 study by the Korea Research Institute of Chemical Technology (KRICT) lists three classes of potential biodegradable alternatives: natural abrasive materials, bio-based synthetic polymers, and natural polymers.⁸⁵ Examples of each class of materials are currently used in personal hygiene products but exhibit noteworthy drawbacks. Naturally hard materials, like stone fruit pits or aluminum oxide, need to be ground down to meet the required dimensions, resulting in sharp, irregular particles.^{67, 74} Accordingly, personal hygiene products containing these abrasives are not recommended for use on sensitive skin.^{67, 68} Bio-based synthetic polymers, such as polylactic acid (PLA), can be liquified and easily shaped into uniform, spherical microbeads with good hardness.^{65, 75, 76} However, these processes commonly rely on the use of expensive ionic liquids or organic solvents,^{51, 65, 75} and rates of biodegradation are so slow and condition-specific that these microbeads may have even greater environmental consequences than their petrochemical-based analogues.⁷⁷ Natural polymers can also be suspended in solutions that can be readily shaped and solidified into microbeads but may also require expensive or toxic processing conditions.^{64, 78, 79, 80, 81, 82} Moreover, their starting materials are commonly coveted by other industries,^{83, 84} and their mechanical properties tend to be weaker than other proposed alternatives.^{50, 65} Microbeads made from chitosan obtained from crustacean waste were recently proposed as a promising option: these beads are inexpensive to produce, use non-cytotoxic cross-linkers, and present the characteristics required of mechanical exfoliants.⁸⁵ However, their animal-based nature restricts their use in the cosmetics industry, which is increasingly turning towards vegan formulations for ethical reasons and to reduce the likelihood of allergic reactions.

Cellulose, the most abundant polymer in nature, has been extensively investigated as a biodegradable building block for new materials, including microbeads.^{81, 86, 88, 97, 152} Pretreated cellulose fibers can be dissolved in a limited choice of solvents, including ionic liquids and aqueous alkali solutions.^{81, 91, 166} Beads can be shaped by dropping, spraying, or membrane emulsification techniques, amongst others, and the polymeric structure is solidified by the regeneration of the polymeric structure's hydrogen bonding network.^{88, 97}

While these microbeads are desirable for many applications (notably functional foods, pharmaceutical uses, and biomedical applications),^{80, 86, 88, 97, 152} they generally lack the hardness required of exfoliating microbeads. Lignin, another abundant natural polymer, can be added to these systems to create composite lignin-cellulose microbeads, as it can be dissolved and regenerated using the same solvent/anti-solvent systems as cellulose.^{89, 167, 168} These materials have increased hardness,¹⁶⁸ as well as antioxidant and antimicrobial properties.^{76, 89, 168} Lignin also shows an affinity for adsorbing organic contaminants and metal ions.⁸⁹

Meanwhile, the global brewery industry generates an estimated 39 million tonnes of undervalued lignocellulosic biomass annually.¹³ This residue, known as brewer's spent grain (BSG), is the primary by-product of beer production, accounting for approximately 85% of total waste generated throughout the process.¹² Beer is the product of the fermentation of sugars extracted from malted grain; BSG is the insoluble fraction left behind. Having previously been seen as having little added value, the main use of BSG is as a component of animal feed, with each tonne being sold to farmers at an approximate cost of \$40 (USD).³⁰ The greatest challenges to using BSG as a starting material in more valuable industrial applications are its variable molecular composition, depending on the precise conditions used in the brewing process, the exact cereal blend used, and its high humidity. In general, the solid mass fraction of BSG contains 16-25% cellulose, 21-28% hemicellulose, 11-27% lignin, 15-24% proteins, 2-4% ash, and around 10% soluble matter.²³ Humidity commonly represents between 77 and 85% of the total weight of the biomass.^{22, 23}

Herein, we sought to develop a process to valorize BSG for the production of biodegradable exfoliating microbeads for use in personal hygiene products. Despite the variable composition and humidity of the biomass, we sought to develop a method that does not require drying or composition uniformization prior to further processing. After developing a reliable protocol for the production of BSG-based microbeads, we characterized the final product to ensure its compliance with industry requirements.

Notably, we tested the beads' mechanical properties and stability in various personal hygiene product matrices, demonstrating that BSG microbeads provide an alternative to conventional plastics and yielding a novel use for an undervalued biomass.

2.2.2 Results & Discussion

2.2.2.1 Preparation of Brewer's Spent Grain Microbeads

a) *GENERAL*

BSG-based materials are produced by following three distinct steps: pretreatment, BSG solubilization, and shaping/solidification. To determine the best conditions, we modified one system parameter at a time. These experiments were realized on BSG from the same batch; the reproducibility of the optimized method for BSG of different composition was evaluated afterwards on samples obtained from different batches. Quantities of BSG used to prepare the samples is reported on a dry solids' basis, not as a function of the total weight of humid biomass used in the sample.

b) *PRETREATMENT*

Early on in this study, preliminary attempts at the preparation of brewer's spent grain (BSG) microbeads demonstrated the necessity of BSG pretreatment by trituration. Although pretreatment adds an additional step to the overall process, it proved to be a critical first step in the solubilization of the grain and the subsequent production of BSG microbeads. Using work on the enhancement of cellulose dissolution as inspiration,⁹⁶ we evaluated BSG hydrolysis facilitated by aqueous solutions containing various concentrations of HCl.

Initial attempts clearly established that trituration noticeably improved BSG solubility. Dilute acid solution concentration varied from 0.20 M to 0.60 M, at 0.05 M increments. Acid hydrolysis was evaluated at 55, 65, 75, 85, and 95 °C. Pretreatment duration varied, with tests at 0.5-, 1-, 2-, and 3-hour periods. Clear trends were observed during our investigation. First, acid concentration used during the pretreatment was directly proportional to the capacity to dissolve BSG during the solubilization step: higher acid concentration represented a greater degree of solubilization, indicating that other acids may be used for pretreatment (such as HNO₃) provided pH remains the same. The same can be said of temperature, with higher temperatures yielding better solubilization and lower yields. The duration of the pretreatment played a less important role in grain fractionation and subsequent solubilization. This relationship between pH, temperature, and time in the dilute acid hydrolysis of BSG is explored by several publications,^{27, 35, 44, 93} and their findings are in keeping with our observations. More detailed results (% of BSG recovery and solubility of BSG after pretreatment) of our various pretreatment assays can be found in the Supporting Information.

Tests demonstrated that the mildest pretreatment conditions allowing for complete grain solubilization were 0.45 M HCl (initial pH of BSG-dilute acid samples = 0.5; final pH = 1.2) for 2 hours at 75 °C. An increase in pH is to be expected, as the acid is partially consumed by the process.⁹³ BSG could equally be completely dissolved in the NaOH-ZnO system when pretreatment involved greater acid concentrations, longer time periods (up to 3 hours), or higher temperatures, but a greater quantity of the BSG was dissolved and disposed of with the filtrate, reducing pulp yield. Accordingly, the aforementioned optimized conditions offer the best compromise between the recovery yield after pretreatment and achieving ensuing grain solubilization. At these conditions, pulp yield was 52.5% after the overall pretreatment process (filtering and rinsing pretreated BSG to a neutral pH). Despite attempts to recuperate solids from the filtrates by centrifugation and filtration, yields were not significantly improved. This may be due to a high proportion of colloids in the filtrate, which consequently could inhibit microbead formation. HPLC

analysis of the hydrolysate confirmed that lignin degradation products, amongst other molecules, were removed from the BSG during pretreatment (see Supporting Information).

c) *DISSOLUTION OF BREWER'S SPENT GRAIN IN AN AQUEOUS NaOH-ZnO SYSTEM*

We chose to evaluate BSG's solubility in a non-derivatizing, environmentally-friendly aqueous NaOH system known for its capacity to readily dissolve purified cellulose. This system's long-known compatibility with purified cellulose at specific cellulose and NaOH concentrations (7-8 wt% each) and low temperatures (around 5 to -10 °C) provided a starting point for our work with pretreated BSG.¹⁰³ We also identified ZnO as a potential additive to prevent the spontaneous gelation of the BSG solutions, which can also help confer porosity to the final beads that may otherwise be hindered by the presence of residual lignin.^{88, 89} All tests of BSG solubility were evaluated at 24, 48, and 72 hours.

A first series of samples (5 to 10 wt% BSG, 5 M NaOH, 1 wt% ZnO) were evaluated at 5 °C. A second series of samples of the same composition were evaluated at 0 °C and showed improved solubility. At -5 °C, BSG solubility decreased. Given those results, temperature was varied at 1 °C increments between -5 and 0 °C, which revealed complete BSG solubilization between -2 and -1 °C. To ensure that this is genuinely the optimum temperature range, select samples were placed in a bath to evaluate solubilization temperatures of -10 and -15 °C. At -10 °C, solubilization was visibly worse; at -15 °C, samples froze, effectively preventing solubilization.

NaOH concentration was subsequently optimized. All samples were prepared with 5 to 10 wt% BSG and 1 wt% ZnO and dissolved at -2 °C. A first set was prepared with 10 M NaOH, which demonstrated reduced BSG dissolution. Samples were prepared with 15 M NaOH and results were markedly worse; samples prepared with 2.5 M NaOH instead were visibly more homogenous. Concentrations of 1, 1.5, 2, and 3 M NaOH were consequently evaluated. The best results were obtained at 2 and 2.5 M NaOH. The optimal temperature

and NaOH concentration determined for BSG are consistent with those of purified cellulose dissolved in NaOH-water systems. The phase diagram for cellulose solubilization in aqueous NaOH systems indicates that cellulose may not necessarily regenerate as a different allomorph under these conditions,^{91, 103, 104} in contrast with the experimental findings of Luo (2010)¹⁶⁹ and Mohamed (2015),⁸⁸ which reported at least a certain degree of regeneration as the stronger cellulose II allomorph.

As a next step, ZnO concentration was optimized. Full sets of samples were prepared with either 0.5, 1, or 1.5 wt% ZnO. Surprisingly, a minimum of 1 wt% ZnO was deemed necessary for the complete solubilization of up to 9 wt% BSG. With pure cellulose, zinc oxide's reported role is in preventing the solution's spontaneous gelation and is not thought to directly intervene in solubilization mechanisms. Moreover, above 0.5 wt%, the additive reportedly has no further desirable effects and precipitates,^{91, 95} contrasting our observations.

While conducting this optimization work, we realized that, even when using our highest concentration of BSG (9 wt%) at which we could achieve complete solubilisation, solid matter in the sample was not sufficient to regenerate solid microbeads in the latter stages of our overall process. To compensate, after 9 wt% BSG had been completely dissolved in 2-2.5M NaOH with 1 wt% ZnO at -2 to -1 °C over 24 hours, various quantities of different types of purified cellulose were dissolved in the sample. Purified cellulose was not added from the beginning, as it impeded BSG solubility and increased solubilization time.

The degree of polymerization of the purified cellulose used directly influenced the quantity necessary to achieve the same results, as well as the further required time period to solubilize the cellulose. Longer cellulose chains, with greater DP, required more time to dissolve, but a lesser quantity was necessary to successfully regenerate the microbeads. This is consistent with previously reported thermodynamic and rheometric data on cellulose fiber solubilization.^{91, 170} We observed that Celova® 500 (Weidmann Fiber Technologies) or α -cellulose fibers (Sigma-Aldrich) allowed the best balance between time and fiber DP:

2 wt% and an additional 24 hours were all that were necessary to obtain solid, resistant microbeads at the end of the process.

d) SHAPING AND SOLIDIFICATION OF BREWER'S SPENT GRAIN MICROBEADS

A 1 mL syringe was used to withdraw and extrude samples, one drop at a time, into a coagulation bath. The solid beads could then be recuperated by filtration over a Büchner funnel. The humid microbeads obtained were oven-dried to yield our final product.

The solution that allowed to best regenerate the beads was 1 M HCl, followed by HCl solutions of greater concentration. Solutions of HNO₃, no matter the concentration, provided poor results. Beads yellowed, indicating the oxidating effect of HNO₃. Saline solutions of 10% NaCl solidified the beads but results were inconsistent. Greater concentrations of the saline solution impeded bead solidification. These observations echo previously reported observations for the solidification of pure cellulose and hybrid cellulose-lignin microbeads.^{89, 97, 106} At 1 M HCl, the acid can be used to regenerate beads six times before negative effects are observed. After this, the acid can be repurposed for dilute acid hydrolysis pretreatment by adjusting the pH, with no negative effects on the process.

The size of the needle used for dropping the BSG solution in the coagulation bath directly influenced the size of the resulting beads, with smaller needle diameter yielding smaller beads (Figure 19). However, the two parameters are imperfectly correlated (i.e., by reducing needle ID by half, bead diameter only reduces by approximately 5%). Bead dimension results as a function of needle size are presented in section 2.2.2.2.c). Microbead shaping was achieved using needles with ID \geq 260 μ m. Needles with smaller ID were assessed but couldn't be used for dropping due to the high viscosity of the BSG solution (approximately 6000 cP).

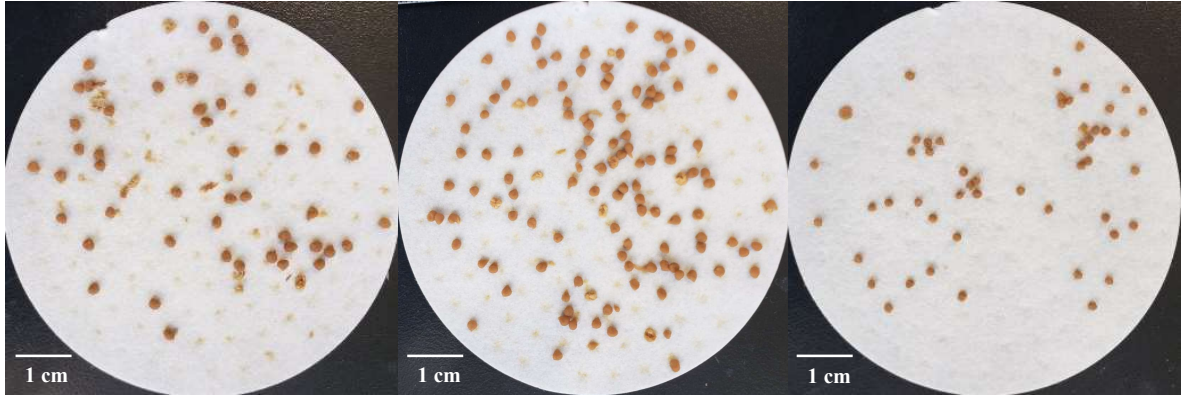


Figure 19. Humid microbeads prepared from BSG solutions using various needle sizes: 21 G (left), 22 G (center), and 26 G (right).

Optimal drop height was between 1 and 2 cm. At greater heights, the beads flattened upon impact; lesser heights did not allow sufficient droplet breakup but showed promise for extending the dropping technique to jet-cutting to achieve even smaller bead dimensions.⁸⁶ The same size beaker and the same volume of solution was used for each test, so that variations in surface tension could be directly attributed to the inherent nature of the solutions or the temperature.

Ambient temperatures yielded the best results. At greater temperatures, the beads dissolved into the coagulating solution; at lower temperatures, the beads seemed to solidify but did not hold up to filtration. Longer time periods provided the best solidification of beads. Periods of regeneration shorter than 12 hours provided beads of reduced mechanical properties.

2.2.2.2 Characterization

a) BREWER'S SPENT GRAIN COMPOSITION

The composition of multiple batches of brewer's spent grain provided by local breweries and used throughout this project were analysed by a unique combination of NREL, ASTM, and TAPPI protocols⁹² as well as the Kjeldahl method for protein quantification.¹⁷¹ Results show little variability in terms of the composition of the biomass (Figure 20). Results are normalized and expressed in terms of percent composition, where the total of the fractions for each sample adds up to 100. Complete biomass composition data can be found in the Supporting Information.

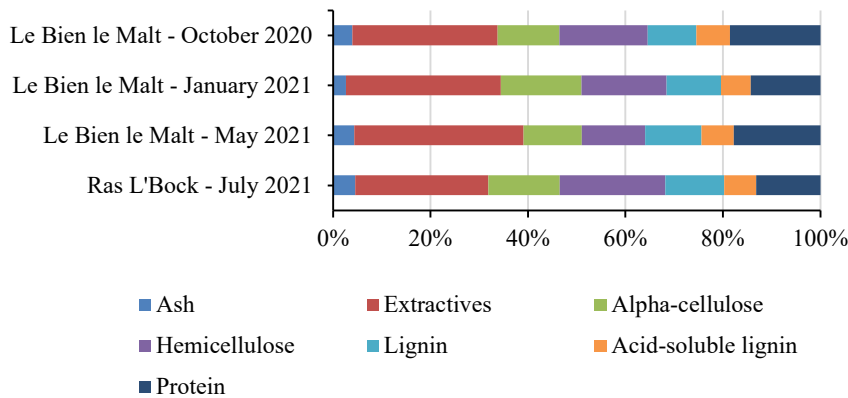


Figure 20. Percent composition of the samples of raw BSG used throughout this project.

Extractives (i.e., volatile organic compounds, monomeric sugars, degradation products) represent the largest component of each sample at an average of 30.9%. Previous studies on the composition of BSG present these as a much less significant fraction of the biomass, accounting for around 10% of samples.²³ Higher extractives content thus diminishes the weights of the fractions of all other components. Yet: ash, protein, and total lignin content fall within the expected ranges, and cellulose and hemicellulose content are respectively 2.9% and 4.2% lower than anticipated.

As cellulose is the main component of interest in BSG for the intended application, proving the method's suitability for relatively low cellulose content can be interpreted as a positive. Previous studies place cellulose content in BSG at a minimum of 2.9% higher,²³ up to 12.1% higher.¹⁷² When working with BSG of higher cellulose content, we hypothesize that BSG solubilization and regeneration would be a more straightforward process, and less quantities of purified cellulose would be required as an additive. Further work could explore this question.

Discrepancies between our results and those found in the literature, notably pertaining to extractives content, are likely due to differences in analytical protocols. Values obtained in the literature are the result of one or two-cycle Soxhlet extractions,^{12, 22} while values obtained here are the result of a four-cycle Soxhlet extraction (hexane, toluene-ethanol, ethanol, water) which provides more comprehensive extractive quantification.⁹² If extractives were quantified according to the same method, it can be assumed that each constituent fraction of our BSG samples would fall into the ranges reported in the literature. Humidity content is consistent with the literature: the average humidity of our samples (77%) is the lower bracket of the previously reported range (77-85%).^{22, 23}

b) *BREWER'S SPENT GRAIN COMPOSITION AFTER PRETREATMENT*

The molecular composition of BSG changes following pretreatment (dilute acid hydrolysis, filtration, rinsing). Figure 21 shows how the composition of raw biomass (Le Bien le Malt October 2020) changes following this process (complete data can be found in the Supporting Information). Regarding our desired application, we can affirm that pretreatment effectively fractionated the biomass, as it enriches the sample in alpha-cellulose and lignin by dissolving extractives, acid-soluble lignin, and protein. Higher acid concentration (lower pH) leads to lower yields in pretreated pulp, although this pulp is increasingly enriched in alpha-cellulose and more readily dissolved in aqueous NaOH-ZnO.

This supports previous works that suggest protein needs to be extracted from lignocellulosic biomass before carbohydrate content can be dissolved,⁴³ as well as the aforementioned theory that higher cellulose content BSG may be more readily dissolved and regenerated. The mechanism is likely synergistic: by extracting protein and enriching the sample in cellulose and lignin – for which the NaOH system has already proven to be compatible – BSG can be effectively solubilized after pretreatment using a lower acid concentration.⁸⁹

Pretreated BSG (0.45 M HCl, 2h, 75 °C) contain 67.38% cellulose, hemicellulose, and lignin. As 9 wt% pretreated grain can be dissolved alongside 2 wt% cellulose, this brings the total content in cellulose, hemicellulose, and lignin to just above 8 wt%. Typically, cellulose solubilization is restricted to a maximum of 8 wt% solids for 2-2.5 M NaOH with ZnO as an additive.⁹¹ Hybrid cellulose-lignin beads, produced by Gabov *et al.* (2016)⁸⁹ do not surpass 5 wt% cellulose and below 3.4 wt% lignin for similar solubilization conditions. Our findings demonstrate that we are able to dissolve a greater quantity of total solids (9 wt% BSG and 2 wt% cellulose) but similar amounts of cellulose, hemicellulose, and lignin. This indicates that protein and extractives do not impede fiber solubilization but can be used to boost the total amount of solids in the solution (and the solids from BSG in the microbeads).

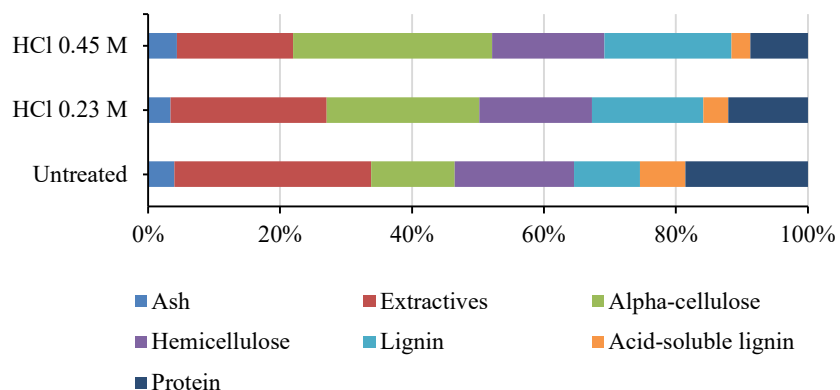


Figure 21. Percent composition of BSG after dilute acid hydrolysis pretreatment.

c) *WEIGHT, SIZE, AND SHAPE OF DRIED BEADS*

Bead weight, size, and shape were directly influenced by the interior diameter of the needle used in their production. For a 21 G needle (ID = 514 μm), the microbeads ($n = 91$) had an average Feret's diameter of 1.31 ± 0.20 mm, weight of 1.25 ± 0.12 mg, and roundness of 0.70 ± 0.11 . A 26 G needle (ID = 260 μm) provided the closest possible dimensions to current industry standards while using the dropping/extrusion method (shower gels, mean diameter of 419 μm ; facial cleansers, mean diameter of 197 μm).⁶² The beads ($n = 90$) had a Feret's diameter of 1.25 ± 0.20 mm, weight of 0.94 ± 0.12 mg, and roundness of 0.86 ± 0.10 . The automation of the dropping technique through jet cutting is likely to reduce bead size, resulting in a similar microbead Feret's diameter to that of the ID of the extruding needle.⁸⁶ We see this by measuring the diameter of dried BSG-filaments continuously extruded into the acid bath with a 26 G needle, which is approximately 0.34 mm.

d) *SWELLING OF BEADS IN WATER*

We compared the total area occupied by a sample of 20 microbeads before and after their soaking in room temperature water for 24 hours. These changes were measured by comparing before and after images using ImageJ software. Assuming perfect bead sphericity, this can be used as an indicator of changes in total bead volume. Wet beads were 16.94% bigger than dried beads, indicating the permeability of their outer layer and their porous interior structure. This is consistent with information regarding hybrid cellulose-lignin microbeads from purified natural polymers, which exhibit 15-20% swelling for similar wt% cellulose and lignin.⁸⁹

e) SEM-EDS

Scanning electron microscopy (SEM) revealed the microbeads' exterior and interior morphologies (Figures 22 and 23). At 200 X magnification, beads maintain the sphericity observed with the naked eye. Average roundness is 0.61 ($n = 3$). Beads' surfaces are relatively smooth, and fibers are densely intertwined with no visible pores. Cross-section images reveal a less dense interior structure with a greater number of visible pores. Images of individual cellulose fibers, obtained at 20,000 X magnification, reveal relatively smooth cellulose fibrils. This may be due to the "filling" effect of hemicellulose, which has been shown to reduce surface roughness in paper products.¹⁰⁷

Energy-dispersive spectroscopy (EDS) provided insight into the elemental composition of the microbeads. Semi-quantitative analysis ($n = 3$) revealed an average of 54.22 wt% C, 39.61 wt% O, 1.88 wt% N, and 1.32 wt% Si at the microbeads' surface layer. The interior layers of the beads did not significantly differ, with mainly 54.20 wt% C, 40.71 wt% O, 1.45 wt% N, and 1.48 wt% Si. Trace amounts of Al, Cl, Cu, and Zn are detected throughout the beads, which may be attributed to the elemental composition of BSG,¹² or residual HCl. In the case of Zn, it is most likely that these trace amounts are due to residual ZnO trapped within the beads. However, this indicates efficient solvent/anti-solvent diffusion between the microbeads and the solidification bath, as Zn would otherwise be present in much higher amounts. This is consistent with the findings of Mohamed *et al.* (2015),⁸⁸ who produced microbeads from an aqueous cellulose-NaOH-ZnO solution using the dropping/extrusion technique and found that acid-regenerated beads did not contain ZnO. Sodium is not detected, indicating that the beads were completely neutralized in the acid bath and thoroughly rinsed, further proving efficient anti-solvent polymer regeneration.

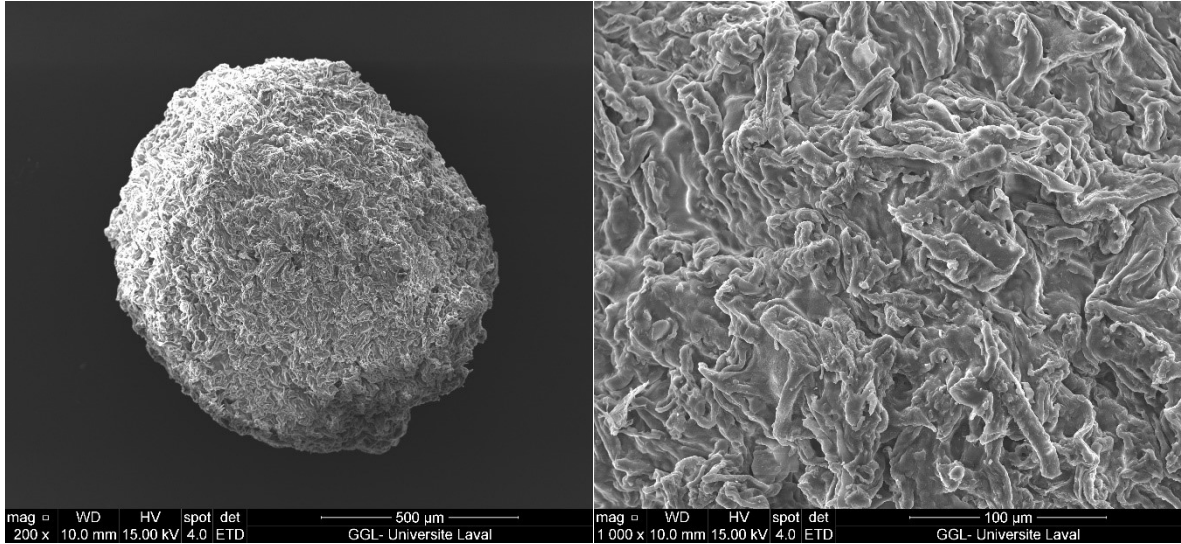


Figure 22. SEM images of a BSG microbead at 200 X magnification (left) and 1000 X magnification (right).

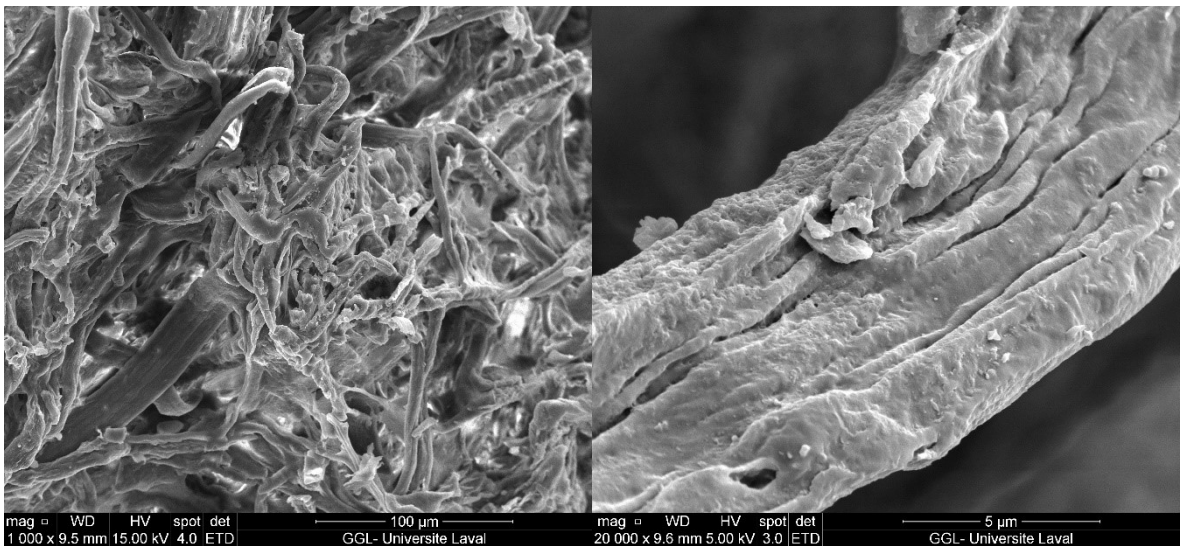


Figure 23. SEM imaging of the interior of a BSG microbead at 1000 X magnification (left) and an individual cellulose fibril at 20,000 X magnification (right).

f) ATR-FTIR

Spectroscopic analysis of dried BSG microbeads provided insight into their composition compared to the added purified cellulose powder and raw BSG used in their production (Figure 24). The broad peak around 3250-3350 cm^{-1} for both starting materials and the final beads corresponds to the stretching vibrations of O-H and N-H groups.¹⁷³ For purified cellulose and the microbeads, this peak is centered at a higher wavelength, likely due to the greater influence of the O-H bonds. A sharper peak around 2850-2950 cm^{-1} can be attributed to C-H bonds, which is most intense for BSG due to the biomass's greater molecular complexity.¹⁷⁴ Another intense band is observed around 1620-1660 cm^{-1} , especially for BSG. As peaks in this area are most often associated with aromatic skeletal vibrations (C=C) and the carbonyl stretch (C=O) of ketone and carboxylic acid groups, it is unsurprising that peaks are most intense for raw BSG, then for microbeads, and relatively weak for purified cellulose.^{174, 175} In the range of 1100 to 1500 cm^{-1} , a greater number of peaks for BSG and microbeads' spectra further demonstrate their greater molecular complexity over purified cellulose, with N-H and C-N deformations.³⁶ In all three spectra, an intense peak is observed around 1030 cm^{-1} which can be associated with the C-O-C pyranose ring vibration known to be integral to the samples.¹⁷⁶ As for the peak around 898 cm^{-1} , this represents the β -glycosidic linkages of cellulose,¹⁷⁶ hence its relative weakness in raw BSG. A final peak around 665 cm^{-1} is associated with C-OH out of plane bending, present in all samples.^{88, 176}

Generally, when comparing microbeads' spectra with those of their precursors, we can see that beads are not solely composed of cellulose. Instead, peaks mirror those found in the spectra of purified cellulose and raw BSG, showing that the final product does indeed result from the solubilization and regeneration of both, with slight shifts indicative of this solubilization-regeneration process yet the maintenance of cellulose I throughout.¹⁷⁷

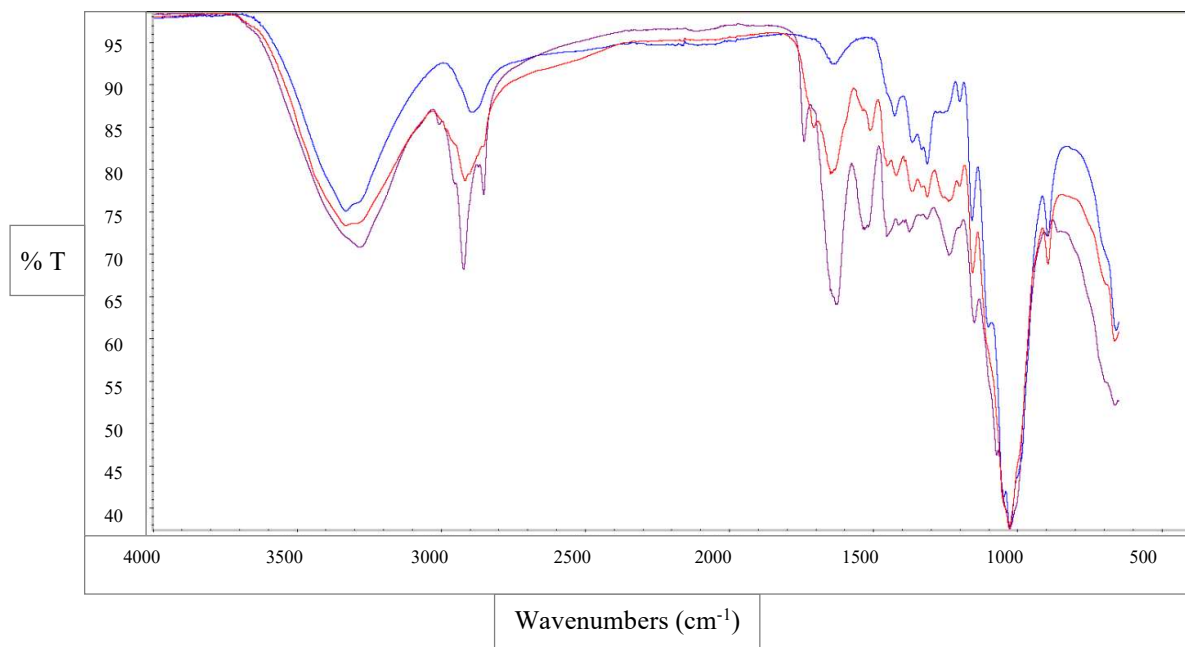


Figure 24. FTIR spectra for raw BSG (purple), purified cellulose (blue), and BSG-based microbeads (red).

g) STABILITY IN MATRICES RELEVANT TO PERSONAL HYGIENE PRODUCTS

The microbeads' stability was evaluated over a month in various matrixes: water, a set of two commercial shower gels, and a commercial body cream ($n = 3$). BSG-based microbeads proved to be incompatible with the body cream matrix (complete disintegration in this matrix) and could not be separated from the cream for further characterization. In both body washes and water, beads demonstrated very good stabilities. Figure 25 demonstrates the beads' stabilities in terms of mass yield (%), and Figure 26 represents stability in terms of total area yield (%) as a representation of the beads' sizes.

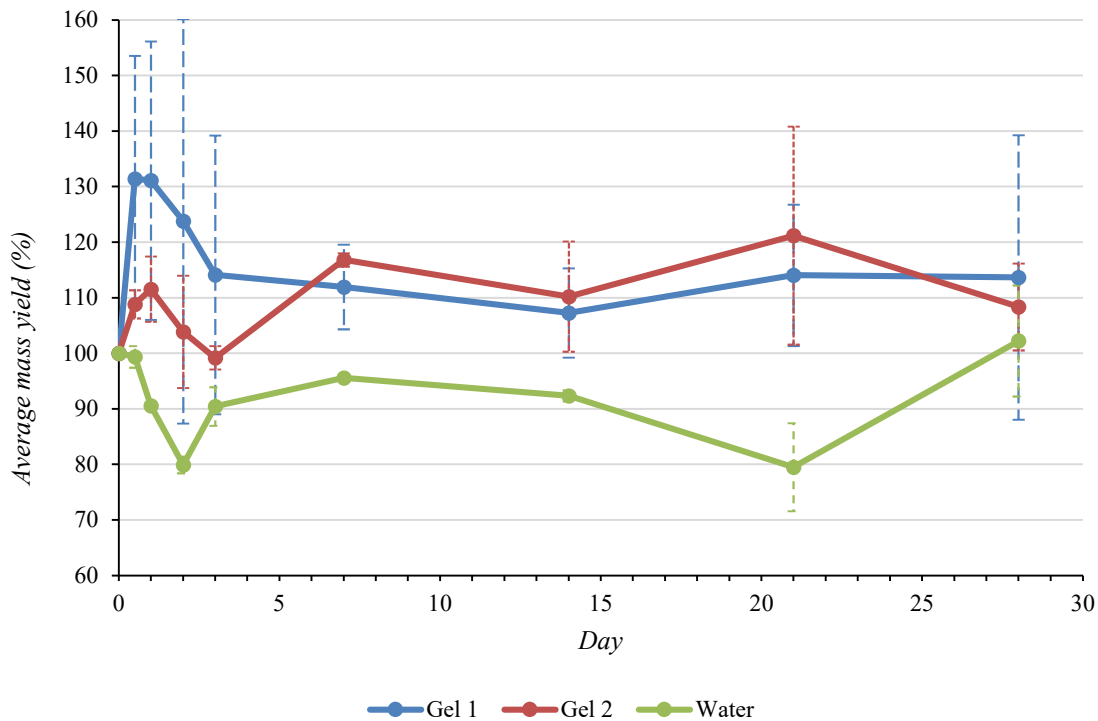


Figure 25. Average mass yield of dried BSG microbeads after soaking in shower gels or water for a specified time period ($n = 3$).

Beads incorporated in shower gel samples had average mass yields above 100% (except for gel 2, day 3, at 99.2%). This may be due to the beads' absorption of surfactants from the shower gels, or other molecules able to penetrate the beads' fibrous structure. In gel 1, average bead mass yield was highest over the first few days, then seemed to stabilize around 110% with high deviation between samples. In gel 2, average bead mass yield slowly and inconsistently rose over the 28 days, seemingly stabilizing around 110% as well. Beads incorporated into water presented their lowest mass yield after 21 days (79.5%) and their highest mass yield after 28 days (102.2%), while demonstrating the least variability amongst replicates. This final mass yield may be due to unevaporated water, trapped within the beads, or to the formation of an imperceptible biofilm. In general, bead mass yield hovers around 90% in water.

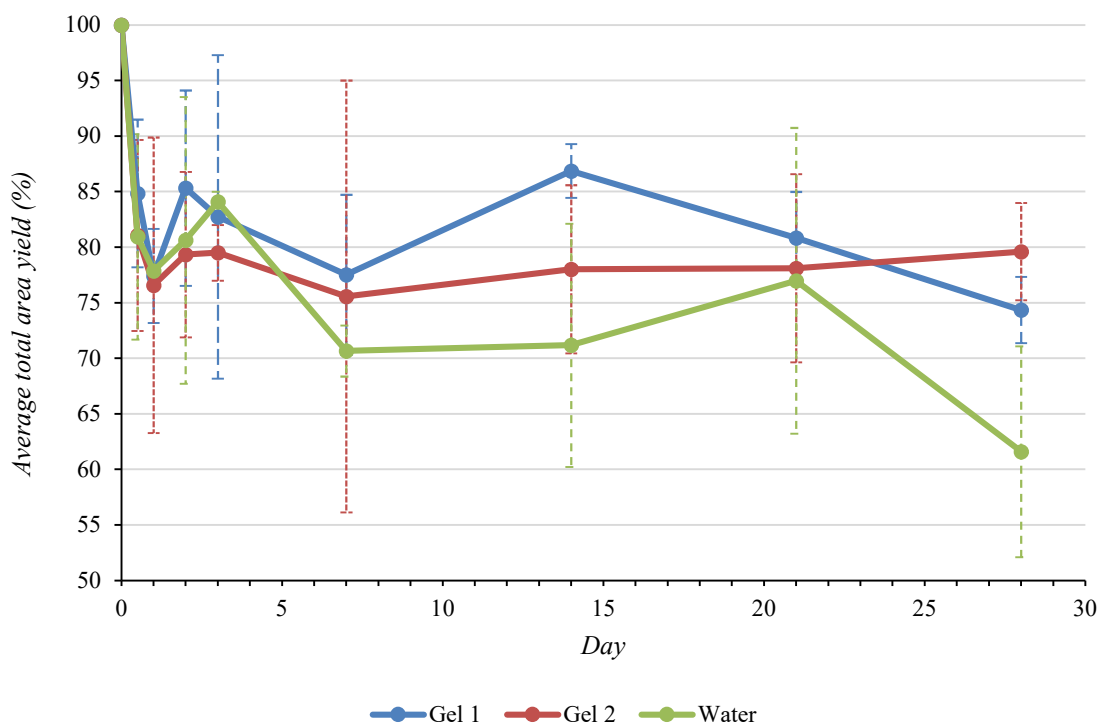


Figure 26. Average total area yield (%) of BSG microbeads after soaking in shower gels or water for a specified time period ($n = 3$).

The average total area yield (%) of the dried beads after soaking in shower gels or water steadily decreased over time with relatively high variation between replicates. For gel 1 and water, the lowest area yield values were for the final measurement (day 28), at 74.4% and 61.6%, respectively. For gel 2, the lowest value was for day 7, at 75.7%. Total area yields seemingly stabilized around 78% after day one.

Total area yields do not follow the same patterns as mass yields. Bead size likely decreased due to slight lignin-leaching, as the matrixes became slightly discoloured over time (brownish), which we observed visually. This may account for the loss of mass from beads soaked in water, which is otherwise compensated by the absorption of other compounds by beads soaked in the shower gels. Alternatively, the microbeads' fibrous structure may increasingly contract after a second wetting-drying cycle, as is the case with

cellulose pulps sourced from wood.¹⁷⁸ Lignin-leaching, absorption of other molecules, or increasing contraction aside, beads maintained their hardness throughout the 28 days, according to manual observations.

A further set of stability samples prepared with 1 g of dried beads dispersed throughout 40 g of both sample body washes, water, or a solid glycerine soap base, provided greater insight into the beads' stabilities. The pH (FiveEasy Plus Benchtop FP20, Mettler-Toledo, USA) and viscosity (DV1 digital viscometer, Brookfield AMTEK, USA) of each liquid matrix did not change following the three months. As for solid soaps, the samples maintained the same visual appearance throughout the entire aging period. Finally, beads kept at ambient conditions for 12 months maintained their characteristics throughout.

h) CLEANSING EFFICIENCY

Solid soaps containing roughly 3 wt% of natural exfoliating particles (ground walnut or coconut shells) were compared to soaps containing BSG microbeads (average diameter of 1.25 mm or 1.31 mm) and a control (plain soap) in terms of their cleansing efficiency for removing an eyeliner pencil mark on real skin and plastic “fake” skin after a standard number of washes (10 washes, $n = 3$). Figure 27 shows that all soaps containing exfoliating particles performed better than the control, validating that physical exfoliants help remove dirt from skin and encourage epidermal desquamation.^{67, 68} A series of photos offering a more visual demonstration of the efficiency of our samples can be found in the Supporting Information. Exfoliating soaps were more effective on natural skin than on plastic “fake” skin, although replicates demonstrated a greater degree of error. The smallest BSG microbeads (1.25 mm diameter) demonstrated the best performance, likely due to the larger specific surface area of smaller beads.^{62, 85} Qualitatively, real skin was less irritated (less redness) by using BSG microbead-containing soaps as opposed to the other natural exfoliants. This indicates that BSG microbead-containing soaps may gently exfoliate the

epidermis, preventing acne progression and leading to smoother-appearing skin, all while reducing the potential for cutaneous irritation associated with more abrasive physical exfoliants.^{67, 68}

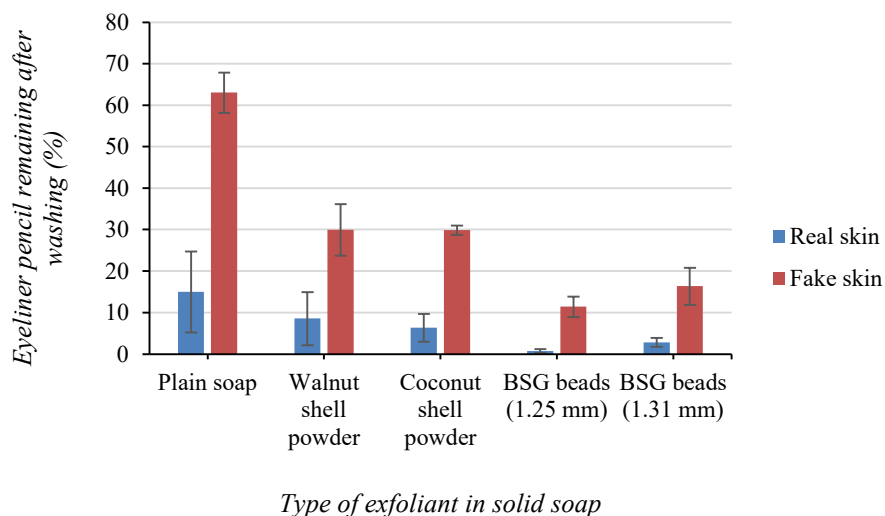


Figure 27. Cleansing efficiency of solid soap, with or without physical exfoliating particles ($n = 3$).

Soaps were equally evaluated for the number of washes it took to completely remove an eyeliner pencil mark from plastic “fake” skin (Figure 28) ($n = 5$). In this case, the smallest BSG-microbeads still demonstrate the greatest cleansing efficiency with an average of six washes to completely remove the crayon. Larger BSG-microbeads have a comparable cleansing efficiency to the other commercially available natural exfoliants (10.6 washes compared to 10.8 and 9.8 washes for walnut and coconut, respectively). When coupled with the data from the previous cleansing efficiency testing, this represents that soaps containing larger BSG-beads may be more effective than commercial exfoliants over the first five washes, but that they converge to similar efficacy after nine to ten washes. All soaps containing physical exfoliants demonstrate superior cleansing capacities than the control, which required an average of 38.8 washes.

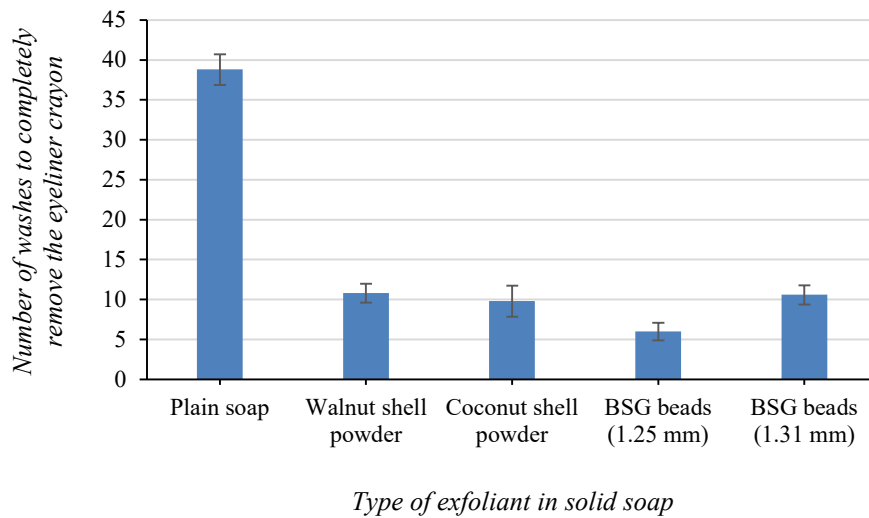


Figure 28. Cleansing efficiency of solid soap, with or without physical exfoliating particles ($n = 5$).

i) SAMPLE HARDNESS

Sample hardness was determined by microindentation testing using a UNHT ultra-high-resolution nano-indenter (Anton Parr, Austria) equipped with a Berkovich tip operated in Continuous Multi-Cycle (CMC) mode. The average maximum penetration depth was 2767.96 ± 274.39 nm ($n = 15$). From this, the average indentation modulus (M) and hardness (H) values were found to be 5.64 ± 1.04 GPa and 199.05 ± 43.80 MPa, respectively ($n = 15$). The coefficient of variation (CoV) for M and H values is about 18.4% and 21.0%, respectively, at the maximum penetration depths (h_{max}) of CMC tests. Average value and CoV seem to converge at a constant value after 10 tests, representing that the uncertainty cannot be reduced by further testing. Instead, uncertainty is a consequence of the material microstructure. Complete CMC results can be found in the Supporting Information.

Average bead hardness is the key piece of information resulting from microindentation testing. It is important to ensure that microbeads in personal hygiene

products are hard enough to remove contaminants from the skin without damaging human tissues. As stated above, bead hardness is around 199 MPa. This value is in keeping with the hardness required of exfoliating microbeads for personal hygiene products. Synthetic polymers are generally between 22 (low-density polyethylene) and 245 MPa (polyacrylic acid) with the exact hardness as a function of the specific polymer.¹⁷⁹ Chitin-based microbeads, proposed as an alternative to conventional plastics in personal hygiene products, presented hardnesses of depending on the sample's degree of acetylation.⁸⁵ The same publication found chitosan to be ineffective with a hardness value of 83 MPa. On the other hand, apricot pit hardness is around 244 MPa,¹⁸⁰ various natural nutshells (i.e., coconut and walnut shells) cover a range of 290 to 570 MPa,^{181, 182} and sodium tetraborate crystals present a hardness of 417 MPa.¹⁸⁰ The greater hardness of these materials, in addition to their jagged, irregular particle shape, represents a greater likelihood of damaging the skin.

2.2.3 Conclusion

Brewer's spent grain (BSG) was shown herein to be a promising starting material in the development of exfoliating microbeads. After dilute acid hydrolysis (0.45 M HCl, 2 h, 75 °C), pretreated BSG could be dissolved up to 9 wt% (solids basis) in 2-2.5 M NaOH with 1 wt% ZnO as an additive. Solubilization of the BSG occurred at -2 to -1 °C over 24 hours, with an additional 24 hours to dissolve 2 wt% α -cellulose powder. Spherical beads were produced by extruding the BSG solution through a syringe (26 G) into a 1 M HCl bath. Filtered, dried microbeads had an average diameter of 1.25 mm, which we expect could be reduced by adopting the automated jet-cutting technique for microbead production instead of manual dropping/extrusion. BSG-microbeads exhibit porous internal structures, confirmed by their swelling in water and SEM imaging. Beads do not contain residual NaOH and only trace amounts of ZnO, and FTIR demonstrates that cellulose maintains its native structure, indicating the biodegradability of the material. Measuring matrix viscosity

and pH confirms what is visually and manually observed : the beads are stable in commercial cleansers, water, and solid soaps for at least three months, and under ambient, dry conditions for at least one year. Moreover, the BSG-microbeads exhibit improved cleansing abilities when compared to commercially available natural exfoliating particles, and a sought-after average hardness of 199 MPa. BSG-microbeads are consequently a promising option for exfoliating particles in personal hygiene products and provide a high-value application for a significant residual biomass.

2.2.4 Experimental Section

2.2.4.1 Materials

a) *BREWER'S SPENT GRAIN*

Brewer's spent grain (BSG) was obtained from two local Quebec microbreweries throughout this project: Le Bien le Malt (Rimouski, QC, Canada), and Ras L'Bock (La Pocatière, QC, Canada). Samples had an average humidity of 77% as determined gravimetrically. The exact cereal composition of these samples was never specified, but the main component was always malted barley. We worked with four batches of BSG obtained from different brews to account for the effects brewing conditions may have on BSG's composition.

b) *OTHER MATERIALS*

Purified cellulose was obtained from a variety of sources. Celova® Cellulose Powder samples (C500, C1000, C2000) were provided by Weidmann Fiber Technology (Switzerland). Microcrystalline cellulose was purchased from Alfa Aesar (USA). Cellulose

fibers (medium) and α -cellulose fiber (99.5%) were purchased from Sigma-Aldrich (USA). See Supporting Information for product specifications about cellulose fiber length. Non-nano zinc oxide (-200 mesh powder, 99.9%) and sodium hydroxide pellets (98%) were obtained from Alfa Aesar (USA). Hydrochloric acid (ACS grade, 36.5-38%) and nitric acid (ACS grade, 68-70%) were purchased from VWR (USA).

2.2.4.2 Preparation of Brewer's Spent Grain Microbeads with Optimized Conditions

Humid BSG was pretreated by dilute acid hydrolysis with HCl. Accordingly, 77% humidity BSG was combined with dilute acid at a 1 : 4 mass ratio and heated at 75 °C for 2 hours. After pretreatment, BSG was isolated from the liquid hydrolysate by filtering over a 1 mm sieve. Pretreated grain was rinsed with distilled water until it had a neutral pH using the same 1 mm sieve, then dissolved (upon agitation with a magnetic stir-bar) using an aqueous solution of 2 M NaOH and 1 wt% ZnO, alongside 2 wt% medium-DP cellulose fibers. A recirculating chilling bath was used to maintain the samples at -2 °C over 48 hours. From the resulting BSG solution, shaping of the beads and the regeneration of the polymeric structure was completed using the dropping/extrusion technique. The BSG-NaOH-ZnO solution was introduced, drop by drop, into a tenfold (*v/v*) acidic regenerating solution, at a drop height of 2 cm. The BSG solution was extruded through syringes equipped with needles of various sizes with the smallest compatible needle size being 26 G. As for the acid bath, 1 M HCl at ambient temperature yielded the best results. Following a minimum regeneration period of 12 h, the supernatant was poured away. Beads were filtered from the remaining solution and dried at in an oven at 50 °C. Once dry, beads were stored in a closed vessel for later characterization.

2.2.4.3 Characterization

a) *BREWER'S SPENT GRAIN COMPOSITION*

The molecular composition of BSG samples – both as a raw material (section 2.2.2.2.a) and after the various tested pretreatment methods (section 2.2.2.2.b) - was determined according to a unique combination of NREL, ASTM, and TAPPI protocols.⁹² Details of the specific protocols used can be found in Damay *et al.* 2018, sections 2.5.1 to 2.5.6. Each sample consisted of 100 g of dry BSG and was analysed for ash, extractables, alpha-cellulose, hemicellulose, lignin, acid-soluble lignin, and proteins. Briefly: extract content is determined after four successive Soxhlet extractions with hexane, ethanol/toluene (2 : 1, v/v), ethanol, and water, and ash content is determined by heating at 575 °C. Holocellulose is isolated by depolymerizing and solubilizing lignin using acetic acid and sodium chlorite, then filtering on a fritted glass funnel. Alpha-cellulose is then isolated from holocellulose by treatment with sodium hydroxide and acetic acid, followed by filtration. Hemicellulose accounts for the remaining fraction, assuming holocellulose is solely composed of alpha-cellulose and hemicellulose. Lignin and acid-soluble lignin were quantified by hydrolysis with concentrated sulfuric acid, which allowed to separate the fractions from the biomass. Finally, proteins were quantified using the Kjeldahl method.¹⁷¹

b) *WEIGHT, SIZE, AND SHAPE OF DRIED BEADS*

The weight of the beads was determined using a micro-balance. Size and shape were determined by taking pictures of beads on a clean, high-contrast surface. The images were then analyzed using ImageJ software (NIH, USA). The size was represented as Feret's diameter, while the shape was represented in terms of roundness (Equation 3) where a perfect circle, represented by \bigcirc , has a value of 1.000. The measurements of 90 beads were taken and averaged.

Equation 3. Circularity of particles

$$\text{○} = \left(4 \times \frac{[Area]}{\pi \times [Major\ axis]^2} \right)$$

Where ○ is the calculated circularity of the sample, *Area* is the surface area of the samples in mm², and *Major axis* is the length of the line segment going through the farthest points on an ellipse in mm.

c) SWELLING OF BEADS IN WATER

The swelling behaviour of air-dried BSG beads was determined by noting the changes in bead dimensions after soaking in distilled water at room temperature for 24 hours. Dried beads were photographed on a high-contrast, smooth background, and images were analyzed with ImageJ software (NIH, USA). They were then placed in room temperature distilled water. After the soaking period of 24 hours, the particles were filtered from the water. Immediately after, the swollen size of the beads was determined by photographing them on a high-contrast, smooth background, and analyzing the images with ImageJ software. The swelling degree, expressed in %-units, was calculated as a function of the total surface area occupied by beads, assuming perfect sphericity.

d) SEM-EDS

The morphology of the regenerated, dried BSG microbeads was examined using a scanning electron microscope (SEM), model Inspect F50 by the FEI Company (USA). An energy-dispersive (EDS) detector (Octane Super-A, Edax Ametek, USA) was used to semi-quantitatively determine sample composition. Whole beads and their cross-sections (obtained by slicing beads with a razor blade) were coated with silver and palladium using a sputter coater. Three beads and cross-sections were imaged at 200 X and 1000 X at an

optimum accelerating voltage of 15 kV, and their elemental composition was detected at a resolution of 131.7 eV. One cross-section sample was imaged at 20,000 X to better visualize individual cellulose fibers.

e) ATR-FTIR

Dried beads and purified cellulose samples were analyzed by ATR-FTIR using a Nicolet iS50 instrument (Thermo Scientific, USA). A total of 64 scans were realized for each sample at a resolution of 4 cm⁻¹. OMNIC spectra software (Thermo Scientific, USA) was used to normalize the spectra and investigate peaks.

f) STABILITY IN MATRICES RELEVANT TO PERSONAL HYGIENE PRODUCTS

To measure beads stability in model commercial personal hygiene products, 40 mg of beads were mixed in either 1 g of distilled water, one of two shower gels (Super Leaves™ Orange Leaves and Oatmeal Sensitive Extra Gentle, ATTITUDE™, Canada), or a body cream (Super Leaves™ Orange Leaves, ATTITUDE™, Canada). Herein, the shower gels are simply referred to as gel 1 and gel 2, respectively, and the body cream is described as such. Samples were prepared in triplicate for each testing period and aged in ambient conditions. After 0.5, 1, 2, 3, 7, 14, 21, and 28 days, the microbeads were removed from the matrices, gently rinsed with distilled water, and dried in a vacuum oven at 50 °C for 24 h to remove any residual humidity. Body cream samples were additionally rinsed with ethanol, due to the matrix's relative hydrophobicity. Dried beads were weighed, and stability was calculated by comparing the mass of the beads before and after soaking in the sample matrixes using Equation 4, below:

Equation 4. Stability (S_W) of microbeads, determined gravimetrically

$$Stability_W (\%) = \frac{W_n}{W_0} \times 100$$

Where W_n is the weight in grams of the dried beads after n days and W_0 is the initial weight in grams of the same beads.

Stability was further characterized by analyzing beads' dimensions using ImageJ, according to the same methods described previously, before and after soaking in the sample matrices. In this case, stability is determined as follows (Equation 5):

Equation 5. Stability (S_A) of microbeads, determined by surface area

$$Stability_A (\%) = \frac{A_n}{A_0} \times 100$$

Where A_n is the total area in mm^2 of the dried beads after n days and A_0 is the initial total area in mm^2 of the same beads.

A further set of stability samples was prepared with 1 g of dried beads dispersed throughout 40 g of both sample body washes, water, or a solid glycerine soap base. Samples were aged in ambient conditions for three months. The pH and viscosity of each liquid matrix were taken before bead incorporation and following the 3-month aging period. The pH of samples was measured using a digital pH-meter (FiveEasy Plus Benchtop FP20, Mettler-Toledo, USA) and the viscosity of samples was measured using a rotational viscometer (DV1 digital viscometer, Brookfield AMTEK, USA). Dried beads were also kept at ambient conditions for one year. Qualitative observations were noted throughout the experiment.

g) *CLEANSING EFFICIENCY*

The protocol for determining cleansing efficiency was adapted from Ju *et al.* (2021)⁸⁵ and modified for enhanced reproducibility. Approximately 0.3 g of beads or commercial natural exfoliant (ground walnut or coconut shells) were incorporated into 9 g of solid glycerine soap base. Squares of soap with and without beads were mounted on a stick attached to a swivel, which was in turn attached to a fixed surface. The word “SOAP” was written on the interior of an individual’s arm with a waterproof black eyeliner pencil, as this is a flat surface of sensitive skin with little hair. The written-on skin was gently wetted and washed by the soap at a pressure defined by the swivel/stick system for 10 seconds (passed over 10 times by the soap). Pictures were taken of the written-on skin before and after washing with the soaps and processed with ImageJ software (black-and-white contrast processing) to determine just how efficiently the makeup was removed, with cleansing efficiency defined by Equation 6 (See Supporting Information). Skin was monitored for signs of irritation. Additionally, the same experiment was performed with plastic “fake skin” as the written-on surface (ReelSkin silicone light tone sheet, UK). Both experiments were done in triplicate.

Cleansing efficiency was equally measured in terms of the total number of swivels required to completely remove the word “SOAP” written with waterproof black eyeliner from the plastic “fake skin.” The experiment was done in five replicates.

Equation 6. Cleansing efficiency of soaps

$$\text{Cleansing efficiency (\%)} = \frac{A_f}{A_i} \times 100$$

Where A_i is the total area in mm^2 of the crayon immediately following drawing on the skin and A_f is the total area in mm^2 of the remaining crayon after washing.

h) *SAMPLE HARDNESS*

Prior to microindentation testing to determine the microbeads' hardness, samples were immobilized in epoxy resin discs. These discs were cured at 30% relative humidity and room temperature for a week. Discs were then sanded down and polished to expose the interiors of the microbeads. Microindentation testing to determine sample hardness was performed with an UNHT ultra-high-resolution nano-indenter (Anton Parr, Austria) equipped with real force and displacement sensors. This instrument virtually eliminates the effect of thermal drift and compliance due to its unique and patented active surface referencing system and is consequently perfectly suited for long-term measurements of small-scale samples. The instrument was equipped with a Berkovich tip (at an indentation angle of 65.03°) and analysis was run according to the Continuous Multi-Cycle Method (CMC). We ran 10 cycles with an acquisition rate of 30.0 Hz and a linear maximum loading increment. The first load was 1.00 mN, the maximum load was 30.00 mN, the time to maximum load was 2.0 seconds, the time to unload was 2.0 seconds, and we unloaded to 30.00%. We included a 1.0 second pause between cycles. Prior to analysis, the instrumentation was calibrated with the samples to eliminate indentation offset, and preliminary CMC testing was carried out to determine the penetration depth at which the results can be considered homogenous (unaffected by possible heterogeneity of the samples' microstructure). We performed a total of 15 CMC tests measuring the area of residual indentation in the sample by light microscopy (A_r) and the maximum load (P_{max}) as a function of the penetration depth (h_{max}), as well as the unloading slope (S). From these parameters, we can use Equations 1 and 2 to measure the sample hardness (H) and indentation modulus (M), respectively:

Equation 7. Sample hardness (H) determined by indentation techniques

$$H = \frac{P_{max}}{A_r}$$

Where H is the sample hardness, P_{max} is the maximum load, and A_r is the residual indentation area as a function of h_{max} , the penetration depth. Then, to measure indentation modulus (M):

Equation 8. Sample indentation modulus (M) determined by indentation techniques

$$M = \frac{S \cdot \sqrt{\pi}}{2 \cdot \sqrt{A_r}}$$

Where M is the sample indentation modulus, S is the unloading slope, and A_r is the residual indentation area as a function of h_{max} , the penetration depth.

2.2.5 Acknowledgements

This work was supported by funding from MITACS, Canada. Special thanks to the Bien le Malt (Rimouski) and Ras L’Bock (La Pocatière) microbreweries for supplying brewer’s spent grain at no cost, Weidman Fiber Technologies (Switzerland) for donating cellulose samples to the project, as well as ATTITUDE™ (Montreal) for providing advice regarding stability testing and the required matrixes at no charge. We would also like to acknowledge the contributions of the Laboratoire des technologies de la biomasse (Université de Sherbrooke), Prof. Thierry Ghislain, and Emy Leblanc for the analysis of biomass composition, the Laboratoire de microanalyse (Université Laval), Dr. Marc Choquette, and Suzie Côté for SEM-EDS analysis, and the Laboratoire de nano-mécanique pour les matériaux de construction (Université Laval), Dr. Luca Sorelli, and Mahdiar Dargahi for microindentation testing. Additional thanks to Dr. Charles Lavigne for the involvement of the Centre de développement bioalimentaire du Québec in this project and Dr. Élise Caron for her contributions to the early stages of the project. This research was conducted thanks to the financial support of the MITACS Accelerate program, the

Partenariat canadien pour l’agriculture, and the Fonds de recherche Nature et Technologies du Québec.

2.2.6 Supporting Information

2.2.6.1 Biomass Composition

The molecular composition of BSG samples – both as a raw material (section 2.2.2.2.a) and after the various tested pretreatment methods (section 2.2.2.2.b) - was determined according to a unique combination of NREL, ASTM, and TAPPI protocols.⁹² Each sample was analysed for ash, alpha-cellulose, hemicellulose, lignin, acid-soluble lignin, and proteins. The complete normalized data presented in Figures 20 and 21 can be found in Table 4 below.

Table 4. Complete normalized data for BSG batches and according to pretreatment conditions.

Brewery	Ras L’Bock		Le Bien le Malt			
	Batch	July 2021	May 2021	Jan. 2021	Oct. 2020	
Pretreatment				Untreated	HCl 0.23 M	HCl 0.45 M
Ash	4.58	4.37	2.65	3.99	3.38	4.35
Extractables	27.28	34.75	31.76	29.82	23.68	17.65
Alpha-cellulose	14.66	11.91	16.57	12.66	23.14	30.14
Hemicellulose	21.66	12.99	17.48	18.08	17.09	17.05
Lignin	12.11	11.58	11.12	10.00	16.86	19.23
Acid-soluble lignin	6.51	6.64	6.11	6.90	3.78	2.87
Proteins	13.21	17.77	14.31	18.55	12.07	8.72

2.2.6.2 Pretreatment Conditions, BSG Recovery, and BSG Solubility

Preliminary attempts at solubilizing BSG demonstrated the necessity of adding a pretreatment step to the protocol. Pretreatment by dilute acid hydrolysis (with HCl), which untangles the lignocellulosic matrix of the grain and reduces the fibers' DPs, was followed by a filtration step, after which only a fraction of the pretreated grain was recovered. Although greater concentrations of HCl, higher temperatures, and longer durations of the trituration pretreatment ensured more dependable BSG solubility (and allowed higher wt% of BSG in the sample, solids basis), lesser quantities of pretreated grain could be recovered. Experimental optimization required finding a balance between pretreatment intensity, BSG recovery, and maximum BSG solubility in the subsequent NaOH-ZnO solution. Select experimental data from this work is reported below (Table 5), where entry No. 4 was determined to be the best set of results:

Table 5. Select experimental data for the relationship between pretreatment conditions, BSG recovery, and BSG solubility.

Sample	[HCl] (M)	Duration (h)	Temperature (°C)	BSG Recovery (%)	Max. BSG Solubility (wt %, dry)
1	0.23	2	75	47	8
2	0.23	1	75	67	8
3	0.23	0.5	75	77	7.5
4	0.45	2	75	53	9
5	0.45	1	75	53	8.5
6	0.45	0.5	75	75	8
7	0.60	2	50	89	7
8	0.60	1	50	92	7
9	0.45	2	90	29	9
10	0.45	1	90	44	9

2.2.6.3 Grain Appearance

Grain appearance changes over the pretreatment-solubilization process. The figure below demonstrates the differences in appearance between raw BSG, BSG pretreated according to the best set of conditions (row No. 4), and the resulting solution of dissolved BSG (Figure 29).

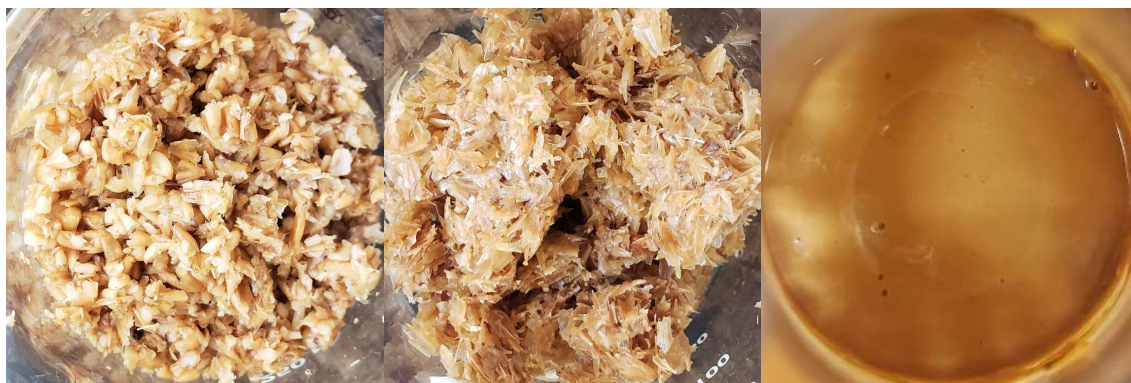


Figure 29. Appearance of BSG during microbead production: raw BSG (left), pretreated BSG (center), and dissolved BSG (right).

2.2.6.4 Analysis of Degradation Products

Acid hydrolysate, generated during BSG pretreatment, was analyzed by high-performance liquid chromatography (HPLC) using a 1200 Series instrument (Agilent Technologies, USA) equipped with a Roc C₁₈ column (5 μm , 150 mm X 4.6 mm; Restek, USA). Volume of injection was 20 μl and isocratic elution was performed using acetonitrile/water (1:8 with 0.1% trifluoroacetic acid) as eluent, and 0.8 $\text{cm}^3 \cdot \text{min}^{-1}$ flow rate at 25 $^\circ\text{C}$. Analytes were detected with UV detection at 276 nm. Prior to analysis, samples were neutralized with NaOH pellets.

Acid hydrolysate generated as a co-product of BSG pretreatment is assumed to be a cocktail of hemicellulosic sugars and degradation products, due to the similarity of the method to other studies of the dilute acid hydrolysis of BSG.^{27, 35, 39, 45} As these previously

reported methods generally seek to reduce the formation of degradation products, instead favouring high hemicellulosic sugar yields for subsequent fermentation processes, dilute acid hydrolysis takes place for shorter time periods and at higher temperatures.

Chromatographic analysis of the hydrolysate obtained as a result of the method reported herein and comparison with reported data confirmed the formation of degradation products such as acetic acid (retention time = 7.630), 5-hydroxymethylfurfural (retention time = 11.043), and furfural (retention time = 20.782), as well as other LDPs (retention times = 28.474 and 38.784) (Figure 30).^{27, 183} The presence of these compounds indicates that any hemicellulosic sugars contained in the hydrolysate may not necessarily be able to be fermented.²⁷ However, degradation products are valuable in other applications.

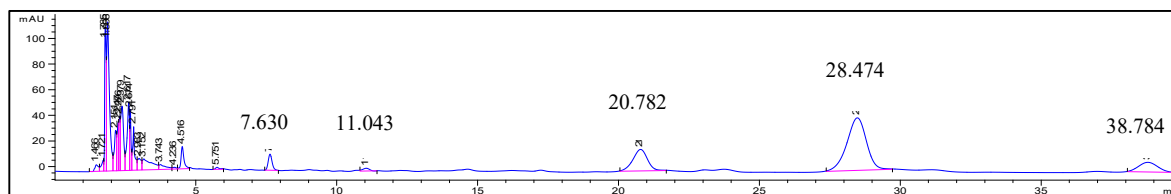


Figure 30. HPLC chromatogram of BSG hydrolysate with UV detection at 276 nm.

2.2.6.5 Cleansing Efficiency

Cleansing efficiency evaluated the capacity of soaps formulated with or without exfoliating particles for their capacity to remove a model pollutant, a black waterproof eye pencil, from real and fake skin. The word “SOAP” was written on the model surface, which was then gently wetted and washed by the soap samples. Pictures were taken of the written-on skin before and after washing with the soaps and processed with ImageJ software (black-and-white contrast processing) to determine just how efficiently the makeup was removed, with cleansing efficiency defined by Equation 6:

Equation 6. Cleansing efficiency of soaps

$$\text{Cleansing efficiency (\%)} = \frac{A_f}{A_i} \times 100$$

Where A_i is the total area in mm^2 of the crayon immediately following drawing on the skin and A_f is the total area in mm^2 of the remaining crayon after washing.

Alternatively, cleansing efficiency was measured in terms of the total number of washes required to completely remove the word from the model surface. Examples of photos used to determine cleansing efficiency are pictured below (Figures 31 and 32).



Figure 31. Eye pencil on skin before (left) and after (right) washing with a soap containing no exfoliating particles.



Figure 32. Eye pencil on skin before (left) and after (right) washing with a soap containing small BSG microbeads (1.25 mm average diameter).

2.2.6.6 Sample Hardness

The microbeads' mechanical properties are determined by microindentation testing using an UNHT ultra-high-resolution nano-indenter (Anton Parr, Austria) equipped with a Berkovich tip operated at Continuous Multi-Cycle mode (10 cycles, $n = 15$). Complete CMC results for the maximum penetration depth, indentation modulus, and indentation hardness with corresponding average and standard deviation values are presented below, in Table 6.

Table 6. Complete CMC results for the maximum penetration depth, indentation modulus, and indentation hardness of 15 CMC tests.

Test number	h_{max} (nm)	M (GPa)	H (MPa)
1	2780.44566	4.97518	192.62627
2	2271.86872	7.64557	286.14051
3	3093.11199	5.11259	149.74512
4	2516.45732	6.53253	234.08530
5	2832.86439	5.65171	181.11381
6	3249.34113	3.60691	143.25758
7	2946.71653	5.18698	167.61357
8	2949.9955	5.32457	166.31515
9	2928.42614	4.52506	175.38419
10	2972.34041	4.53446	168.97171
11	2305.02753	7.27426	283.63082
12	2771.58468	5.50905	191.95030
13	2860.58534	6.27425	173.68899
14	2521.37768	6.07839	236.96120
15	2519.22195	6.42767	234.34237
Average	2767.95766	5.64394	199.05513
STD	274.39197	1.04388	43.79792

2.2.6.7 Cellulose Fiber Length

Product specifications for the various cellulose powders provide a rough indication of their DP (Table 7). Screen analysis revealed that 15-25% and 65-75% of C2000 were retained on 1000 and 63 μm sieves respectively, indicating high DP. For C1000, 2-10% was retained on a 500 μm sieve, while the remaining 70-90% was retained on a 32 μm sieve. Samples C500 and medium cellulose fiber have similar DP, each with 5-15% retained on a 125 μm sieve and the remaining 60-75% on a 32 μm sieve. For α -cellulose powder, average DP was slightly lower, with 35% on a 200 μm sieve, 50% on a 100 μm sieve and 20% on a 32 μm sieve. Microcrystalline cellulose's average DP of 350 was provided directly from the manufacturer.

Table 7. Screen analysis of the various cellulose powders used, as provided by the manufacturers.

Sample	1000 μm (%)	500 μm (%)	200 μm (%)	100 μm (%)	63 μm (%)	32 μm (%)
C2000	15-25	-	-	-	65-75	-
C1000	-	2-10	-	-	-	70-80
C500	-	-	5-15	-	-	60-75
Cellulose fibers (medium)	-	-	5-15	-	-	60-75
α-cellulose fiber	-	-	35	50	-	20

CHAPTER 3

COMPLETE SOLUBILIZATION OF BREWER'S SPENT GRAIN FOR THE PRODUCTION OF SUSTAINABLE LIGNOCELLULOSIC MATERIALS

3.1 FRENCH ABSTRACT AND CONTEXT OF THE SECOND ARTICLE

3.1.1 Résumé

Solubilisation complète de la drêche de brasserie pour la production de matériaux lignocellulosiques durables

La drêche de brasserie est une biomasse abondante qui peut servir dans de nombreuses applications industrielles. Au cours des dernières décennies, ce composé lignocellulosique a été évalué en tant que matière première dans la production de biocarburants de deuxième génération, comme source de certaines molécules recherchées, dans l'alimentation animale ou comme ingrédient dans des aliments destinés à la consommation humaine. Ces applications sont soit à faible valeur ajoutée (i.e., aliments, agriculture) ou n'arrivent pas à valoriser l'entièreté de la drêche. D'ailleurs, la liquéfaction hydrothermale assistée par micro-ondes permet de transformer l'intégralité de la drêche en biocarburants en évitant la production d'autres résidus, mais ne permet pas la liquéfaction de la drêche pour son utilisation dans d'autres applications. Nous démontrons ici que la drêche, à la suite d'un prétraitement acide, peut être entièrement solubilisée au moyen d'un système aqueux d'hydroxyde de sodium et que la solution résultante peut être gélifiée ou régénérée dans l'acide pour donner forme à des films lignocellulosiques. Comme les microplastiques primaires dans les produits d'hygiène personnelle représentent une source notable de pollution environnementale, nous démontrons par la suite que ces films peuvent être découpés en particules qui servent d'exfoliants physiques dans des savons liquides et solides. Ces particules de drêche s'avèrent être aussi efficaces que les particules biodégradables déjà utilisées dans des produits d'hygiène personnelle. Plus important encore, la méthode décrite ici fournit une alternative aux processus préexistants de valorisation complète à haute valeur ajoutée de la drêche qui reposent sur la décomposition complète de sa structure polymérique ou qui sont associés à des émissions de composés organiques volatils potentiellement nocifs.

Mots-clés : *drêche de brasserie, cellulose, biomasse, valorisation complète*

3.1.2 Contexte du projet

Cet article, intitulé « *Complete Solubilization of Brewer's Spent Grain for the Production of Sustainable Lignocellulosic Materials* », sera soumis pour publication dans un journal scientifique à l'automne 2022. Le principal journal visé pour l'évaluation par les pairs et la publication est *Cellulose* de la maison d'édition *Springer*. Sinon, nous avons identifié *Bioresource Technology (Elsevier)* ou *Waste and Biomass Valorization (Springer)* comme d'autres options potentielles. En tant que premier auteur, j'ai contribué à l'essentiel de la recherche sur l'état de la question, au développement de la méthode et à l'exécution de la caractérisation du produit développé. Les chercheurs Vincent Banville et Charles Emond, second et troisième auteur, ont aidé à l'élaboration de l'idée originale et ont influencé le développement de la méthode et les stratégies de caractérisation. Le professeur Sébastien Cardinal, en tant que directeur du projet de recherche, a également influencé le développement de la méthode et les stratégies de caractérisation, ainsi que l'organisation de l'article de recherche. Une version abrégée de l'article a été présentée sous forme de présentation orale à la *Gordon Research Seminar in Green Chemistry* à Castelldefels (Espagne) en juillet 2022. Ce chapitre est également complété par une analyse technoéconomique qui forme le Chapitre 4 (section 4.2). Toutes les références sont regroupées dans la bibliographie générale à la fin de ce manuscrit.

3.2 CONTENT OF THE MANUSCRIPT

Complete Solubilization of Brewer's Spent Grain for the Production of Sustainable Lignocellulosic Materials

A. McMackin^{1,2}, V. Banville², C. Emond², S. Cardinal¹

¹ Département de biologie, chimie et géographie, Université du Québec à Rimouski (UQAR), Rimouski, Québec, Canada

² Centre de développement bioalimentaire du Québec (CDBQ), Sainte-Anne-de-la-Pocatière, Québec, Canada

ABSTRACT

Brewer's spent grain (BSG) is an abundant yet economically undervalued biomass that possesses the potential for use in a wide variety of industrial applications. In recent decades, this lignocellulosic biomass has been explored as a feedstock in second-generation biofuel production, as a source of valuable molecules, or as a component of animal feed or human-destined foods. These applications are either low-value (i.e., food, agriculture) or do not valorize the entirety of the grain. Alternatively, microwave-assisted hydrothermal liquefaction transforms the entirety of the grain into biofuels, generating no further waste. Herein, we demonstrate a novel process to liquify BSG that leaves its constituent polymers intact so that the resulting solution may be regenerated into fibrous materials. An aqueous sodium hydroxide-based solution dissolves acid hydrolysis-pretreated grain, and the resulting solutions can be shaped into films solidified through gelation or anti-solvent polymer regeneration. In an effort to combat primary microbead pollution from personal hygiene products, we then demonstrate that these films can be cut into small particles that serve as biodegradable physical exfoliants in liquid and solid soaps. When compared to other commercially-available biodegradable exfoliants, BSG-based particles demonstrate slightly improved cleansing efficiencies, demonstrating their potential as a sustainable alternative to petrochemical plastic microbeads. Most importantly, the method described herein for BSG solubilization provides an alternative to pre-existing one-pot BSG valorization processes, which either completely decompose its polymeric structure or are associated with potentially harmful volatile organic compound emissions.

Keywords: *Brewer's Spent Grain, Biomass, Complete Valorization*

3.2.1 Introduction

Brewer's spent grain (BSG) is the primary residue of the brewery industry, representing 85% of the total co-products generated throughout the beer brewing process.¹² For each hectoliter of beer, an average of 20 kg of humid BSG is produced,¹³ which represents a tremendous amount of residual grain when extrapolated to the 177.50 billion liters of beer consumed worldwide annually (2020).² As the global beer market continues to grow, it is becoming increasingly important to develop new applications for BSG to fill the gap between available supply and demand.

Like most agri-food wastes, BSG has a variable molecular composition. The solid fraction generally contains 16-25 % cellulose, 19-42% hemicellulose, 11-27% lignin, 15-24% proteins, 1-4% ash, and 1-6% of soluble matter.²³ This variability can prove challenging when using BSG in high added-value applications that rely on consistent yields. Moreover, BSG has very high humidity, commonly between 77 and 85% of the grain's total weight, which makes it highly susceptible to microbiological spoiling.^{22, 23} When used as a feedstock for animals, which is currently its most common application, BSG either needs to be dried or rapidly transported to farms for use.¹⁸ This may pose logistical issues or may be cost-inhibitive to brewers who sell their BSG for \$40 (USD) per humid tonne.³⁰

Besides use as a feedstock for ruminants,²⁸ BSG can be used as an ingredient in human-destined bread products.²⁶ Furthermore, BSG can be composted or spread directly on fields in its raw form, providing precious nutrients to agricultural soils.^{18, 26} It can also undergo pyrolysis to produce biochar used in soil remediation.²⁶ These applications allow to use the entirety of the BSG but are seen as having little added value. If not for legislation preventing brewer's from disposing of the grain to landfills, their motivation to find avenues of valorization for the BSG they generate would likely be little to none. Every brewery aims to keep waste disposal as inexpensive and uncomplicated as possible.¹⁸⁴

Higher-value applications are more interesting, as greater method profitability pushes industrial actors towards seeking out the biomass themselves. Recently, an increasing number of valuable applications for BSG have been brought to light, including using the residue as a source of several sought-after molecules or in the production of second-generation biofuels. Molecules of interest include hydroxycinnamic acids and other polyphenols, proteins, volatile fatty acids, or simple sugars which may be subsequently fermented into alcohols.^{12, 13, 22, 27, 38} When used in energy production, different fractions of BSG can play roles in thermochemical conversion (pyrolysis, combustion), and biogas (methane) and bioethanol production.³⁵ Individually, these methods do not allow to valorize the entirety of the biomass, but they may be used in cascade to avoid producing further by-products.⁴⁵

Once cascade valorization techniques have been optimized, BSG may be able to play an important role in the biorefineries of the future alongside other biowastes.^{45, 185} Until then, developing profitable one-pot strategies for the valorization of whole, raw BSG is the most promising avenue for maximizing its potential. Currently, few techniques for BSG valorization fall into this category. A catalyzed hydrothermal microwave-assisted method for BSG liquefaction is one such rare instance. Developed by Lorente *et al.* (2019),³⁷ this process yields three distinct fractions (gas, aqueous fraction, bio-oil) that may be used as bio-fuels or platform chemicals. Although this method is deemed “a very promising approach to achieve an environmentally-friendly and integral valorisation of brewer’s spent grain” by the study’s authors,³⁷ the process effectively completely decomposes the fibrous components of the biomass. It consequently cannot be applied in the fabrication of fibrous or natural polymer-based materials from BSG.

The natural polymers that compose BSG are widely recognized for their capacities to produce paper products, replace conventional petrochemical plastics, and/or serve in the fabrication of composite materials.^{12, 26, 186} Despite this, to this day, few studies have investigated using BSG as a source of these molecules, tending towards using more traditional biomass as a feedstock instead (i.e., wood). Even fewer studies have looked into

the potential of directly using lignocellulose in the production of more sustainable materials, instead preferring to extract and purify select components of BSG. For example, a 2021 study by A. Hejna *et al.* examined extruding whole, dried BSG through a twin-screw press and using the resulting fibrous powder in the production of composite materials.¹⁸⁶ The authors found that modified, extruded BSG exhibited greater melanoidin content than raw BSG, due to the high extrusion temperatures. Although this further improves the thermooxidative stability of conventional polymer materials, they also noted the downfalls of needing to thoroughly dry the grain beforehand and the potential health and environmental consequences due to volatile organic compound emissions during high-temperature extrusion.¹⁸⁶

Reconciling objectives surrounding green BSG valorization and final product performance, we sought to present a gentle one-pot method for the complete solubilization of raw, humid BSG. We aimed to realize this objective through dilute acid hydrolysis pretreatment, followed by solubilization in a low-temperature aqueous system of NaOH and ZnO. In theory, the relatively mild conditions of the method would suffice to completely dissolve the grain while preserving polymers' degrees of polymerization (DP) at levels allowing the production of fibrous final materials. By using the water already present in the grain to facilitate its pretreatment and subsequent solubilization, we hope to overcome challenges regarding BSG's high humidity. As for the grain's variable composition, we apply the method to various batches of BSG, obtained from different brewing conditions. Inspired by our previous work on the production of spherical porous microbeads from BSG,[†] we then aim to produce microparticles from the resulting BSG-based solutions. Finally, we hoped to validate these particles' potential to replace conventional petrochemical microbeads, used as physical exfoliating agents in personal hygiene products and associated with environmental pollution,^{161, 162} by characterizing their

[†] This sentence references the work presented in Chapter 2, which we will submit for publication before submitting the present research article. Once the first article has been published, we will be able to reference it in this work. Similarly, applicable passages of the Results & Discussion and Experimental Section of this chapter will be modified to instead reference overlapping results and methodologies presented in Chapter 2.

stabilities in a variety of cosmetics matrices. This envisioned application provided yet another eco-friendly objective to the project. Assuming we would be able to reach these goals, we predicted that this research may serve as a promising starting point in the production of other natural polymer-based materials from whole, raw BSG for a wider variety of future applications.

3.2.2 Results & Discussion

3.2.2.1 Preparation of Brewer's Spent Grain Microparticles

a) *GENERAL*

BSG-based materials are produced by following three distinct steps: pretreatment, BSG solubilization, and shaping/solidification. To determine the best conditions, we modified one system parameter at a time. These experiments were realized on BSG from the same batch; the reproducibility of the optimized method for BSG of different compositions was evaluated afterward on samples obtained from different batches. Quantities of BSG used to prepare the samples is reported on a basis of the solids, not as a function of the total weight of humid biomass used in the sample.

b) *PRETREATMENT*

Our precedent work[‡] as well as preliminary work in this project quickly proved the necessity of dilute acid pretreatment of BSG for its subsequent solubilization. Lower pH, higher temperatures, and longer pretreatment periods further break down the lignocellulosic

[‡] See page 101.

matrix of BSG and lead to greater depolymerization of the cellulosic chains.¹⁸⁷ The relationship between pH, temperature, and time in the dilute acid hydrolysis of BSG has been explored by several publications, notably for optimizing hemicellulosic sugar yield while keeping lignin degradation product formation to a minimum.^{27, 35, 44, 93} With our intended application, it was important that pretreatment was able to sufficiently detangle the lignocellulosic matrix so that BSG could be dissolved, but to ensure that polymer chains remained long enough for regeneration into fibrous materials. For these reasons, we sought to identify the least intensive pretreatment parameters that would still allow, in the next step, the complete dissolution of BSG in our chosen system. Dilute acid solution concentration varied from 0.5 M to 2.0 M, at 0.1 M increments. Acid hydrolysis was evaluated at 50 to 100 °C at 10 °C intervals. Pretreatment duration varied, with tests at 0.5-, 1-, 2-, and 3-hour periods. Experimentally, we found that the most effective pretreatment could be achieved with 0.60 M HCl (initial pH of BSG-dilute acid samples = 0.2; final pH = 0.9) for 2 hours at 90 °C. The acid is partially consumed by the process, which slightly increases the pH of the mix over the reaction period.⁹³ A minimal quantity of dilute acid was used during pretreatment, just ensuring that grain was submersed in the liquid, which worked out to be a 2 : 3 ratio (wet grain : dilute acid).

c) *DISSOLUTION OF BREWER'S SPENT GRAIN IN AN AQUEOUS NaOH-ZNO SYSTEM*

The pretreated grain was not separated from the acid hydrolysate through filtration; instead, solubilization occurred directly in the same vials. We evaluated BSG's solubility in a non-derivatizing, environmentally-friendly aqueous NaOH system known for its capacity to readily dissolve purified cellulose, that also allowed to directly neutralize unreacted HCl. This system's long-known compatibility with purified cellulose at specific cellulose and NaOH concentrations (7-8 wt% each) and low temperatures (around 5 to -10 °C) provided a starting point for our work with pretreated BSG.¹⁰³ We also identified ZnO as a potential additive to prevent the spontaneous gelation of the BSG solutions, which can also help

confer porosity to the final materials that may otherwise be hindered by the presence of lignin.^{88, 89} All tests of BSG solubility were evaluated at 24, 48, and 72 hours.

We evaluated a first series of samples at 5 °C with 1 wt% ZnO, and NaOH concentration was varied between 2 and 5 M at 0.5 M increments. Solid NaOH was used as opposed to NaOH solutions to keep water use to a minimum. However, NaOH dissolution in water is exothermic, meaning further time was required to cool samples to the required temperatures. We found that a concentration of at least 3 M of NaOH was required to begin dissolving the pretreated grain. When accounting for the NaOH required to neutralize the pretreated grain and unreacted acid, this would lower the real NaOH concentration to be within values reported for optimum cellulose solubility.^{91, 103}

From here we were able to optimize solubilization temperatures. The initial temperature of -5 °C was chosen in accordance with the cellulose-sodium hydroxide-water system's relationship with temperature reported by Sobue, Kiessig, and Hess in 1939.¹⁰³ Upon raising sample temperature at 1 °C increments to 0 °C, where grain solubility markedly decreased, we were able to validate that optimum grain solubility could be achieved at -3 °C. A further set of samples was prepared at 5 °C, which allowed to confirm that solubility did not improve at higher temperatures. For these conditions we expect cellulose to remain as cellulose I, which is validated by Ying Wang in her 2008 work on cellulose-NaOH systems.¹⁰⁴ However, Luo (2010)¹⁶⁹ and Mohamed (2015)⁸⁸ found that cellulose regenerated from aqueous alkali under similar conditions exhibited changes to its hydrogen bonding structures.

Thereafter, full sets of samples were prepared with either 0.5, 1, or 1.5 wt% ZnO. A minimum of 1 wt% ZnO was deemed necessary for the complete solubilization of up to 9 wt% BSG, while greater amounts would simply precipitate in the solution. In contrast, other work reports that ZnO precipitation begins at 0.5 wt%.^{88, 91, 95} Under these conditions, complete grain solubility could be achieved after 24 hours.

Although our experiments showed that 9 wt% BSG solutions could be used to produce films and particles as is, adding purified cellulose improved the materials' mechanical properties. Up to 2 wt% of Celova 500 or α -cellulose fibers could be dissolved in the system over a further 24 hours, which effectively created saturated cellulose-NaOH solutions. Cellulose powders of greater DP were resistant to solubilization within the system, likely for thermodynamic reasons.^{91, 170} Cellulose powders of lesser DP could be incorporated into the solution in greater quantities, but they did not positively influence the mechanical properties of the resulting materials, probably because of their shorter fiber length. Although purified cellulose represents a significant portion of the final material (approximately 20% wt.), the remaining solids are derived from BSG, improving the material's overall industrial feasibility. Other methods rely solely on the use of purified cellulose.

d) SHAPING AND SOLIDIFICATION OF BREWER'S SPENT GRAIN-BASED MATERIALS

The BSG solutions were poured into 10 cm X 10 cm molds in volumes that ensured that their wet thickness was approximately 1 mm (approximately 0,25 mm, dry).

One set of samples were set to dry at room temperature for 24 hours, which we found was sufficient to completely dry and gel the cellulosic matrix. By increasing the temperature, the length of this step could be reduced.

A second set of samples was prepared and subsequently placed in acid bath to regenerate the films' polymeric structures. The molds were submersed into the bath in a very gentle manner, so as to avoid the mixing of the two liquids. In a range of 0.5 to 4 M HCl, we found that 1 M HCl allowed to sufficiently regenerate the films, and greater concentrations of acid led to observable salt deposits that reduced the dried materials' strengths. However, we found that the HCl bath was not able to wash away the ZnO from the inferior layer of the film encased in the mold. Further research can address if this

behaviour can be solved by washing gelled, dried films in an anti-solvent acid bath. As for the other factors influencing film regeneration, we found that ambient temperatures and a regeneration period of a minimum of 12 hours yielded the best results. The regenerated films could then be gently removed from the solution and dried at ambient temperatures for about 24 hours.

Once dried, the gelled (first set of samples) or regenerated films (second set of samples) can be used as is or cut to smaller dimensions for use in other applications. We manually cut the films into square 1 mm^2 particles whose thicknesses depended on the nature of the film. Both types of particles had an approximate thickness of 0.25 mm , measured by caliper, with gelled particles being slightly thicker. Figure 33 shows gelled and regenerated particles.

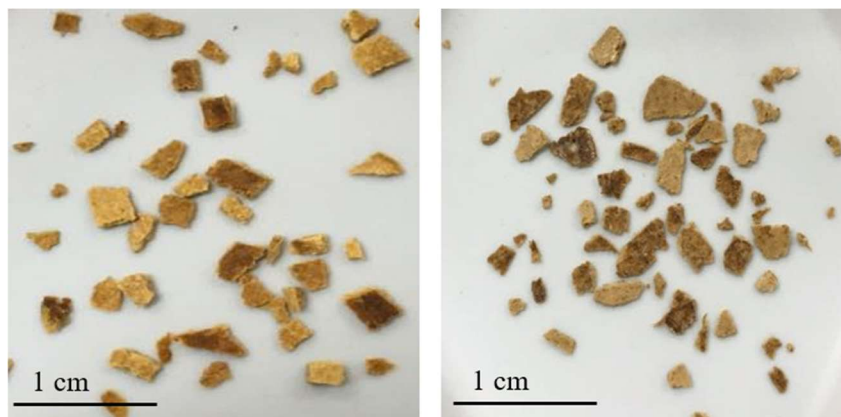


Figure 33. Dried gelled (left) and regenerated (right) particles cut from BSG films.

3.2.2.2 Characterization

a) *BREWER'S SPENT GRAIN COMPOSITION*[§]

The molecular composition of the batches of BSG used throughout our experiments was determined by a unique combination of NREL, ASTM, and TAPPI protocols.⁹² Results show little variability in terms of the composition of the biomass (Figure 34). Results are normalized and expressed in terms of percent composition, where the total of the fractions for each sample adds up to 100. Complete biomass composition data can be found in the Supporting Information (Table 8).

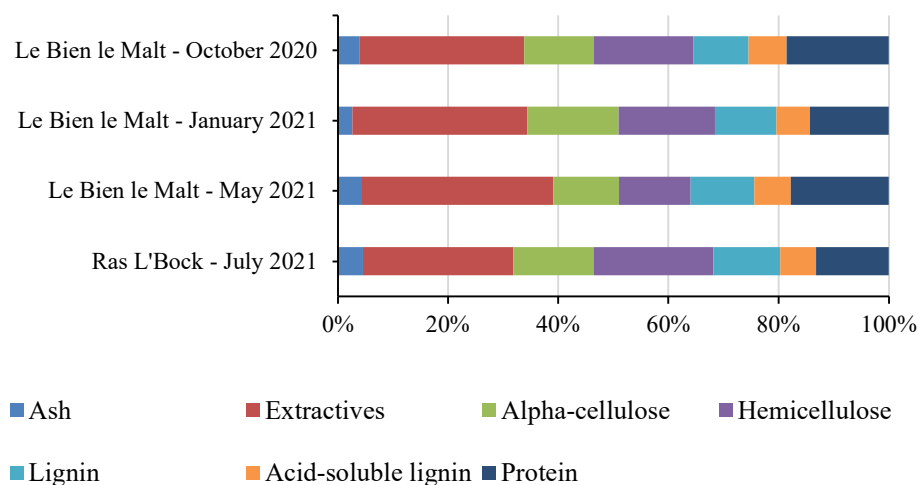


Figure 34. Percent composition of the samples of raw BSG used throughout this project.

Extractives represent the largest component of each sample at an average of 30.9%. Previous studies on the composition of BSG present these as a much less significant fraction of the biomass, accounting for around 10% of samples.²³ This discrepancy is likely due to use of a four-cycle Soxhlet extraction (hexane, toluene-ethanol, ethanol, water),⁹² as

[§] See page 101.

opposed to a one- or two-cycle Soxhlet extraction commonly reported in the literature.^{12, 22} If extractives were quantified according to the same method, it can be assumed that each constituent fraction of our BSG samples would fall into the ranges reported in the literature.

Despite this, ash, protein, and total lignin content fall within the expected ranges, and cellulose and hemicellulose content are respectively 2.9% and 4.2% lower than anticipated. As cellulose is the main component of interest in BSG in the development of lignocellulosic materials, proving the method's suitability for relatively low cellulose content can be interpreted as a positive. Previous studies place cellulose content in BSG at a minimum of 2.9% higher,²³ up to 12.1% higher.¹⁷² When working with BSG of higher cellulose content, we hypothesize that BSG solubilization and gelation or regeneration would be a more straightforward process, and less quantities of purified cellulose would be required as an additive. Meanwhile, humidity content is consistent with the literature with average humidity of our samples (77%) as the lower bracket of the previously reported range (77-85%).^{22, 23}

b) DIMENSIONS OF DRIED PARTICLES

Particles presented different measurements according to if they were solidified through gelation or regeneration. In both cases, the films were prepared so that their dry thickness was about 0.25 mm and they were subsequently approximately cut by hand into 1 mm² particles. For an application in personal hygiene products these dimensions are quite large, as the industry standard is currently around 419 μm for body soaps and 197 μm for facial cleansers.⁶² However, especially with method automation techniques, particle size can be readily adapted. The irregular shapes of the particles can also be improved upon by automating the cutting of the films into particles or by using molds custom-made to the desired dimensions of the final product. As for particle weight, gelled particles had an average weight of 3.34 ± 1.26 mg ($n = 60$), whereas regenerated particles were less dense

with an average weight of 2.77 ± 1.33 mg ($n = 60$). The relatively high standard deviation of the particles' weights can be directly attributed to their greater deviance in size, and again, can be improved upon with method automation.

c) *PARTICLE SWELLING IN WATER*

We compared the total area occupied by a sample of 20 gelled or regenerated particles before and after their soaking in water for 24 hours. These changes were measured by comparing before and after images using ImageJ software. Assuming a perfect cubic shape, this can be used as an indicator of changes in total particle volume. Wet gelled particles were 29% bigger than their dried counterparts whereas regenerated particles disintegrated in water and swelling could not be measured. As the swelling capacity of lignocellulosic materials indicates their porosity,⁸⁹ these gelled particles likely have a highly porous interior structure. This is superior to that of other hybrid cellulose-lignin materials, which exhibit 15-20% swelling for similar wt% cellulose and lignin.⁸⁹

d) *SEM-EDS*

Scanning electron microscopy (SEM) revealed the gelled and regenerated dried particles' surface morphologies (Figures 35, 36, and 37). Images show that the particles' inferior surfaces (that were in direct contact with the mold) are smoother than the superior surfaces (Figures 35 and 36). At 1000 X magnification (Figure 37), differences between the particles' fibrous structures at their inferior surfaces are more evident. Regenerated fibers are more visible yet remain encased in NaOH-ZnO, representing that the inferior surface may not be accessible by the regenerating acid bath, or at least that the solubilization medium is not entirely washed away. However, even the superior surface of the regenerated particles is smooth, indicating the "filling" effect of hemicellulose, which has been shown

to reduce surface roughness in paper products.¹⁰⁷ Alternatively, this may be due to the “two-sidedness” effect, which is a commonly observed phenomena in mechanically-produced papers where one side of the mold is a porous net (bottom, forming wire) and the other is a smooth roller (top, felt side). This configuration leads to an accumulation of the smaller particles on the inferior side of the paper and observable topographical dissymmetry in paper products.¹⁸⁸

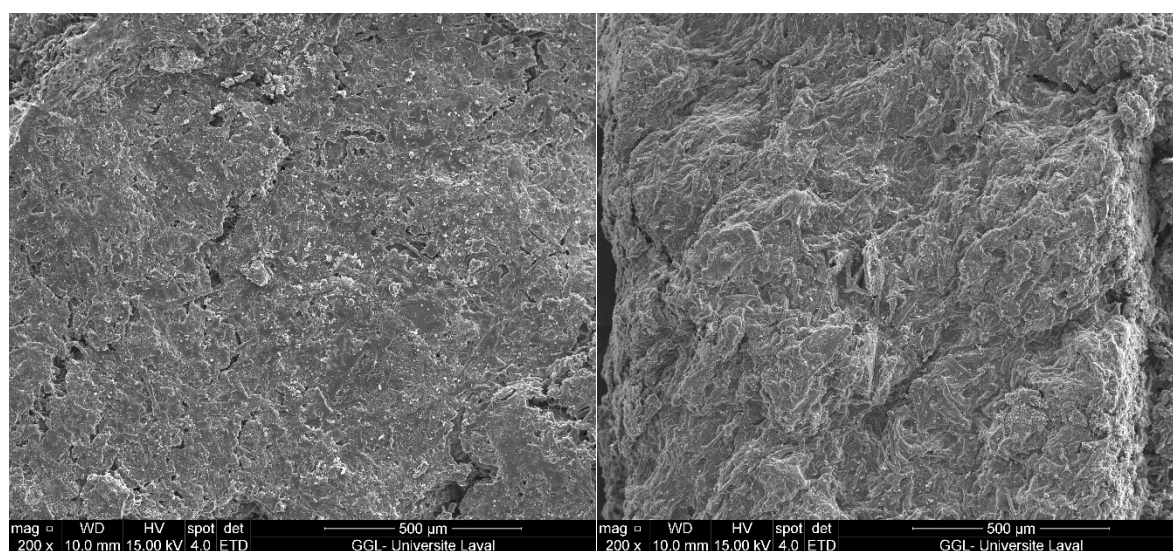


Figure 35. SEM images of dried gelled BSG particles at 200 X magnification: “smooth” side (left) and “rough” side (right).

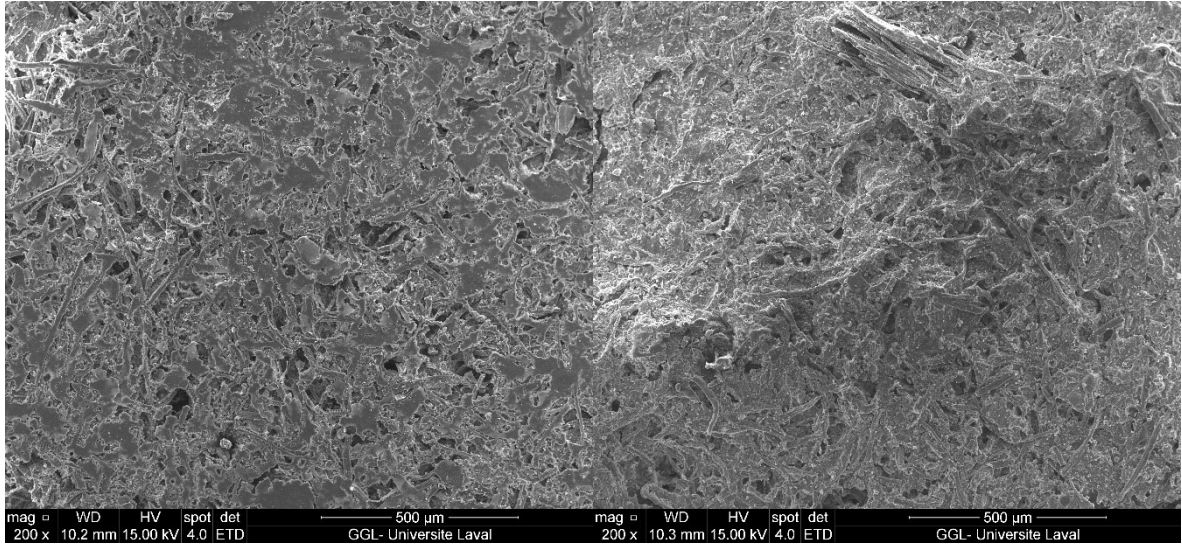


Figure 36. SEM images of dried regenerated BSG particles at 200 X magnification: "smooth" side (left) and "rough" side (right).

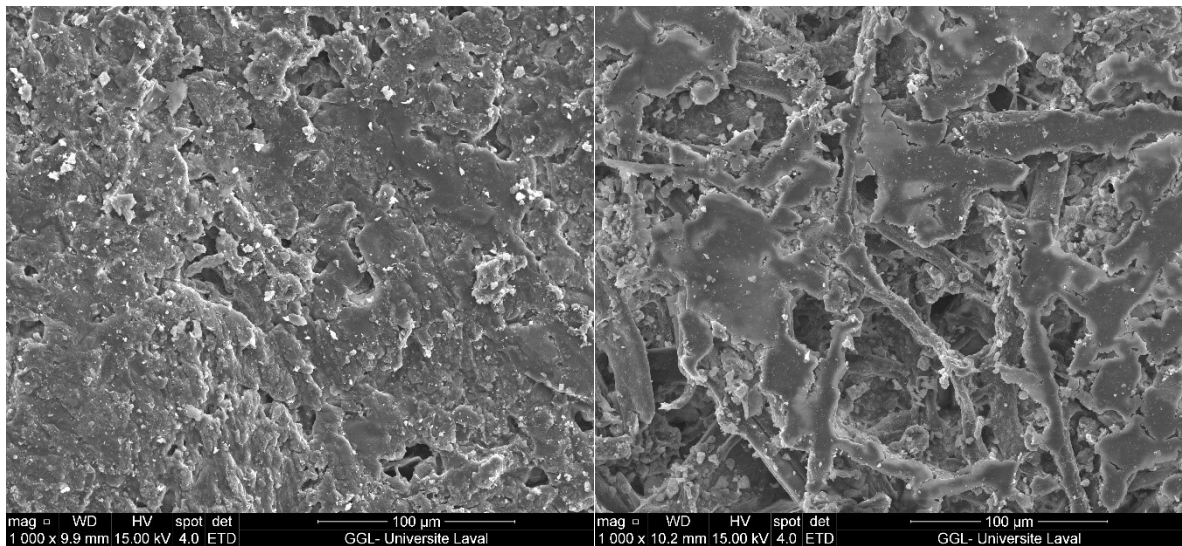


Figure 37. SEM images of dried BSG particles at 1000 X magnification: gelled (left) and regenerated (right).

Energy-dispersive spectroscopy (EDS) confirms that the solubilization medium is not entirely washed away in regenerated particles. Semi-quantitative analysis revealed that gelled particles contain 35.48 wt% C, 32.29 wt% O, 25.95 wt% Na, 3.86 wt% Zn, and 2.42 wt% Cl. Regenerated particles contain 38.81 wt% C, 29.76 wt% O, 15.2 wt% Zn, 10.03 wt% Na, 3.91 wt% Cl, 0.78 wt% P, and 0.59 wt% Si, as well as trace amounts of Cu and Ca. Gelled and regenerated particles are both mainly composed of cellulosic material, with carbon and oxygen representing their primary components. In both particles, ZnO remains in the amounts in which it was added to the solutions. It is not washed away by the acid bath in the case of regenerated particles while lignocellulosic material is, which accounts for it representing a higher fraction of the final material than in gelled particles. This also represents reduced yields in terms of complete valorization of BSG solids. Gelled particles also contain solid sodium hydroxide, which further reduces the elemental fraction representative of ZnO. Phosphorous, silicon, and trace amounts of copper and calcium may be attributed to the elemental composition of BSG.¹²

e) *ATR-FTIR*

An examination of both gelled and regenerated particles' IR spectra, as well as those of the purified cellulose powder and raw BSG used in their production, provided insight into their composition (Figure 38). The broad peak between 3250 and 3350 cm^{-1} corresponding to the stretching vibrations of O-H and N-H groups is significantly blunted for gelled particles, which may be attributed to the strong presence of NaOH within the sample.¹⁷³ A sharper peak around 2850-2950 cm^{-1} can be attributed to C-H bonds, which is most intense for BSG due to the biomass's greater molecular complexity.¹⁷⁴ Another intense band is observed around 1550-1650 cm^{-1} . Peaks in this area are most often associated with aromatic skeletal vibrations (C=C) and the carbonyl stretch (C=O) of ketone and carboxylic acid groups, explaining why the peak is weakest for purified cellulose.^{174, 175} For gelled and regenerated particles, this peak is shifted to the lower end of

this range, as a likely indicator of the method's solubilization process. In the range of 1100 to 1500 cm^{-1} , a greater number of peaks for BSG and particles' spectra further demonstrate their greater molecular complexity over purified cellulose, with N-H and C-N deformations.³⁶ For gelled and regenerated particles, prominent peaks centered at 1412.94 cm^{-1} and 1403.11 cm^{-1} , respectively, can be associated with the NaOH within the sample and consequent O-H bending.¹⁸⁹ In all four spectra, an intense peak is observed around 1020-1050 cm^{-1} which can be associated with the C-O-C pyranose ring vibration known to be integral to the cellulose within the samples.¹⁷⁶ Unsurprisingly, it is most intense for purified cellulose and weakest for gelled particles, where cellulose represents a lesser amount of the sample's composition. The same can be said of the peak around 870-890 cm^{-1} , representative of the β -glycosidic linkages of cellulose.¹⁷⁶ A final peak around 665 cm^{-1} is associated with C-OH out of plane bending, present in all samples.^{88, 176}

The overall comparison of the particles' spectra with those of their precursors demonstrates that both types of particles are not solely composed of cellulose. Instead, peaks mirror those found in the spectra of purified cellulose and raw BSG, showing that the final products do indeed result from the solubilization and regeneration of both, with slight shifts indicative of this solubilization-regeneration process yet the maintenance of cellulose I throughout.¹⁷⁷ More noticeable shifts within the spectra for gelled particles can be attributed to the presence of NaOH.¹⁸⁹

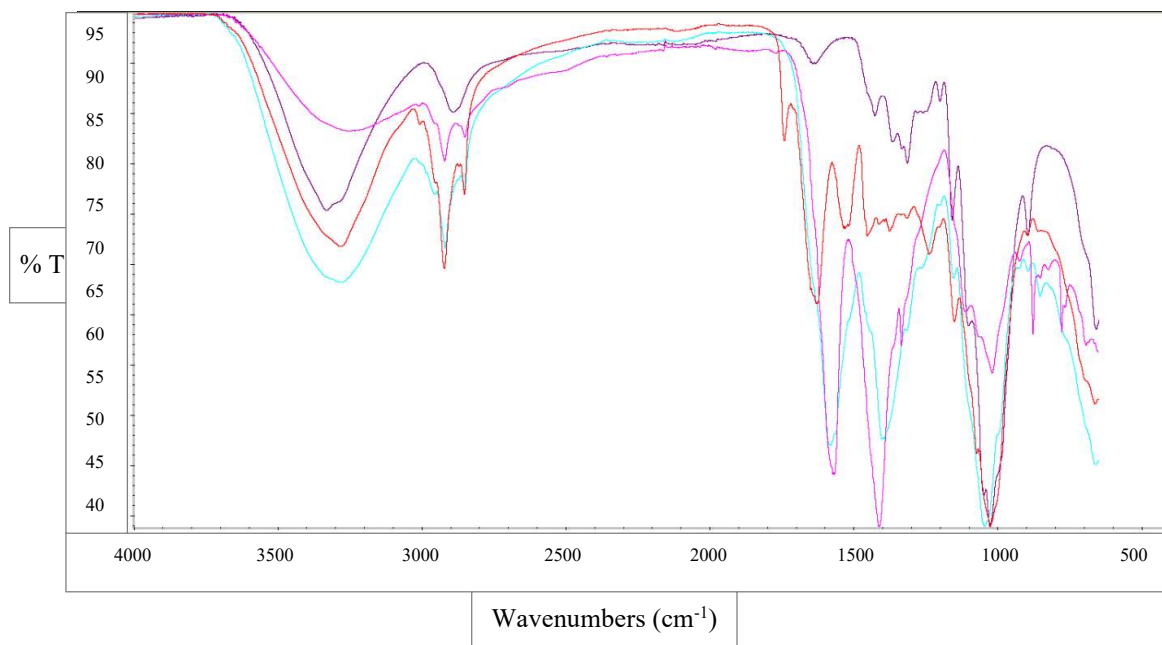


Figure 38. FTIR spectra for raw BSG (red), purified cellulose (purple), gelled BSG particles (pink), and regenerated BSG particles (turquoise).

f) STABILITY IN MATRICES RELEVANT TO PERSONAL HYGIENE PRODUCTS

The particles' stability was first evaluated over a month in various matrixes: water, a set of two commercial shower gels, and a commercial body cream ($n = 3$). Both gelled and regenerated particles proved to be incompatible with the body cream matrix and could not be separated from the cream for further characterization. In both body washes and water, gelled particles demonstrated very good stabilities. Overall, regenerated particles proved to be less compatible with liquid matrixes, experiencing rapid deterioration in water and shower gels. Figure 39 demonstrates the particles' stabilities in terms of mass yield (%), and Figure 40 represents stability in terms of total area yield (%) as a representation of the particles' sizes. Complete data on particle stability (including standard deviation values) can be found in the Supporting Information (Tables 9 and 10).

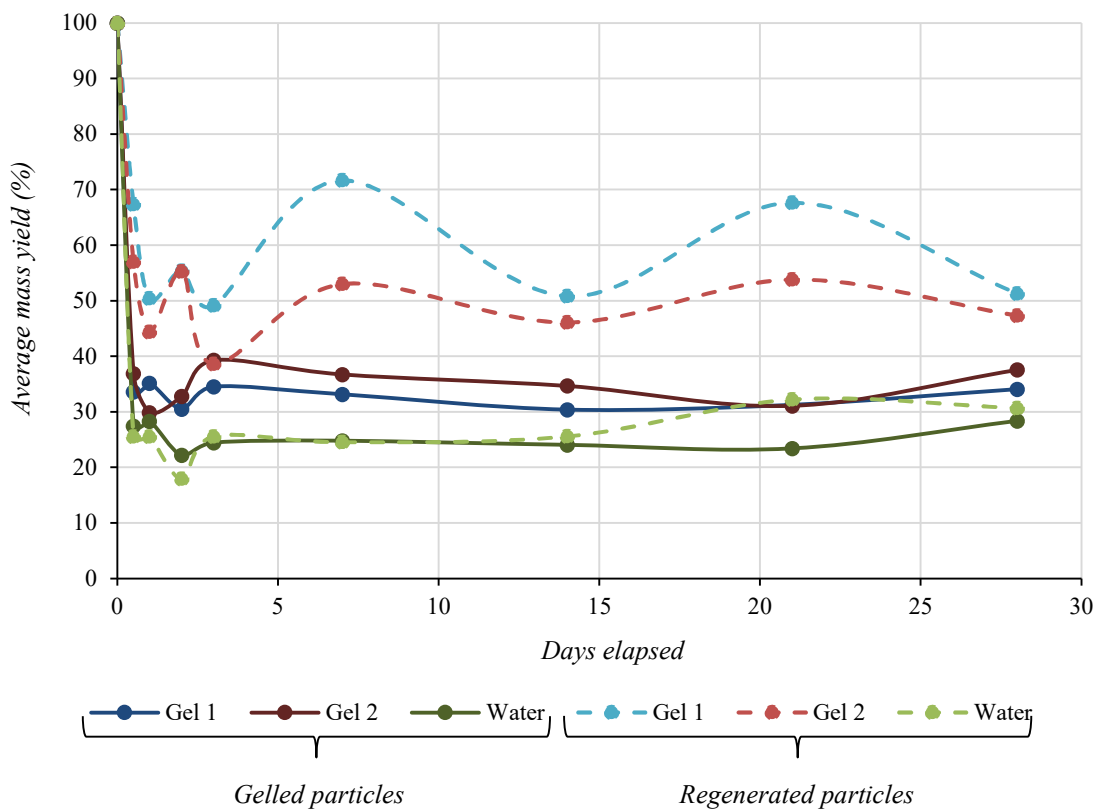


Figure 39. Average mass yield of dried gelled and regenerated BSG particles after soaking in shower gels and water for a specified time period ($n = 3$).

All mass yields of the particles decrease immediately upon their incorporation into liquid matrices and seemingly stabilize over the first week. Mass yields of gelled particles are low, between 20 and 40 %, with a maximum average mass yield of 39.3% reported on day 3 with Gel 2 (Figure 39). This can be partially attributed to the dissolution of the NaOH contained within the particles, which is further validated by an increase in the matrix pH after the introduction of gelled particles (discussed later in this section). Based on the decrease in mass and the colour change of samples, it is likely that ZnO is also washed away into the matrix and a certain degree of delignification occurs. Despite this, particles were solid enough to be easily separated from the matrix throughout the experiment.

Regenerated particles were noticeably softer after aging in the liquid matrices, especially in water where they would completely disintegrate upon being manipulated. Yet, their mass yields were consistently higher than those of their gelled counterparts (Figure 39). This can be attributed to the regeneration process, which washes away the NaOH used for grain solubilization before the grains' incorporation into the liquids. Regenerated particles do experience delignification, as demonstrated by the particles' whitening and the matrices' browning. A high degree of delignification may further facilitate the particles' breakdown in the liquid matrices.¹⁹⁰

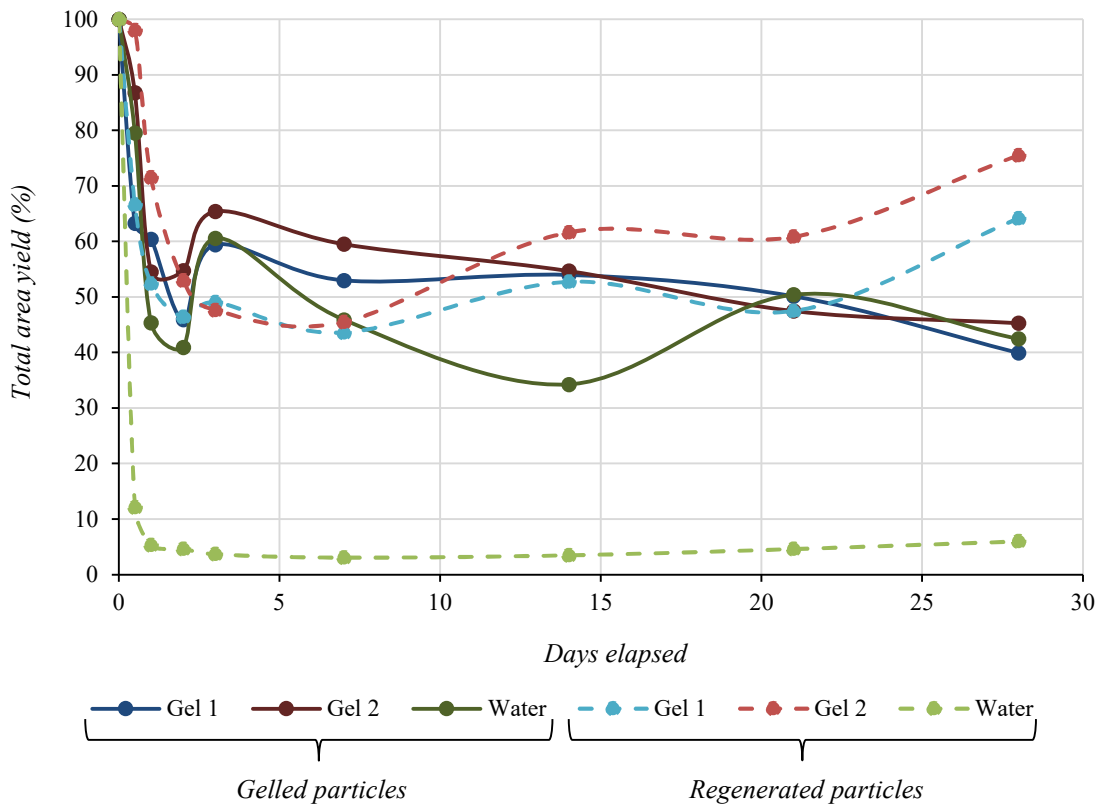


Figure 40. Average total area yield of dried gelled and regenerated BSG particles after soaking in shower gels and water for a specified time period ($n = 3$).

The total area yield (%) of the dried particles after soaking in shower gels or water decreased in all samples (Figure 40). Regenerated particles in water disintegrated within the

first 12 hours, dropping down to a mere 3-5 % yield shortly thereafter. Regenerated particles in shower gels do not exhibit any further significant degradation after the first three days, after which average total area yield increases to 64.2% and 75.5%, respectively. At this point surfactant exchange from the soaps is likely superior to delignification, whereupon particles experience swelling. Gelled particles present greater total area yields than their regenerated counterparts. Again, particles demonstrate the same stabilization trend over the first three days, reaching peaks at 59.4%, 65.4%, and 60.6% for gel 1, gel 2, and water, respectively. Total area yield then steadily decreases over time, reaching 39.9%, 45.3%, and 42.5%, respectively. Despite this, the particles do not exhibit a decrease in their macroscopic mechanical properties. A decrease in particle size may be attributed to delignification or the loss of NaOH or ZnO retained in the particles, or by the increased contraction of cellulose chains after a second wetting-drying cycle, as is reported in wood pulps.¹⁷⁸

Another set of samples was aged for three months in the same set of matrixes as well as into a solid glycerine soap base. The stability of samples aged for three months in shower gels or water revealed that the particles affect matrix pH (FiveEasy Plus Benchtop FP20, Mettler-Toledo, USA), but not matrix viscosity (DV1 digital viscometer, Brookfield AMTEK, USA). Unsurprisingly, gelled particles containing NaOH increased sample pH to the greatest degree. The pH of the shower gels increased from 4.75 to 9.09 and 9.34, and the pH of water increased to 11.96. Regenerated particles increased the pH of the shower gels from 4.75 to 5.48 and 5.76, and the pH of water increased to 7.53. Any increase in matrix pH can be compensated by incorporating various additives in the production of liquid soaps, which are already commonly used to control final product alkalinity, buffer capacity, environmental acceptability, or consumer safety, amongst other characteristics.¹⁹¹ When incorporated into a solid glycerine soap base, no visible changes were observed throughout the entire aging period for both the matrix and the particles. Particles kept at ambient conditions for 12 months maintained their characteristics throughout.

g) CLEANSING EFFICIENCY

Solid soaps containing roughly 3 wt% of natural exfoliating particles (ground walnut shells or coconut husks) were compared to soaps containing BSG particles and a control (plain soap) in terms of their cleansing efficiency (Figure 41), where cleansing efficiency is characterized by the soaps' capacities to remove waterproof eyeliner pencil from real or fake skin after a standard number of washes (10 washes, $n = 3$). All soaps containing exfoliating particles performed better than the control, with BSG particles performing similarly to other commercially available natural exfoliants. Exfoliating soaps were more effective on natural skin than on plastic "fake" skin, although replicates demonstrated a greater degree of error. This may be due to the greater adherence of water-resistant makeup products to hydrophobic plastics as opposed to natural skin. In any case, we were able to validate that BSG particles as physical exfoliants in solid soaps help remove impurities from skin with reduced visible skin irritation. From this, we interpret that BSG particles facilitate epidermal desquamation, which may prevent acne progression and lead to smoother-appearing skin.^{67, 68}

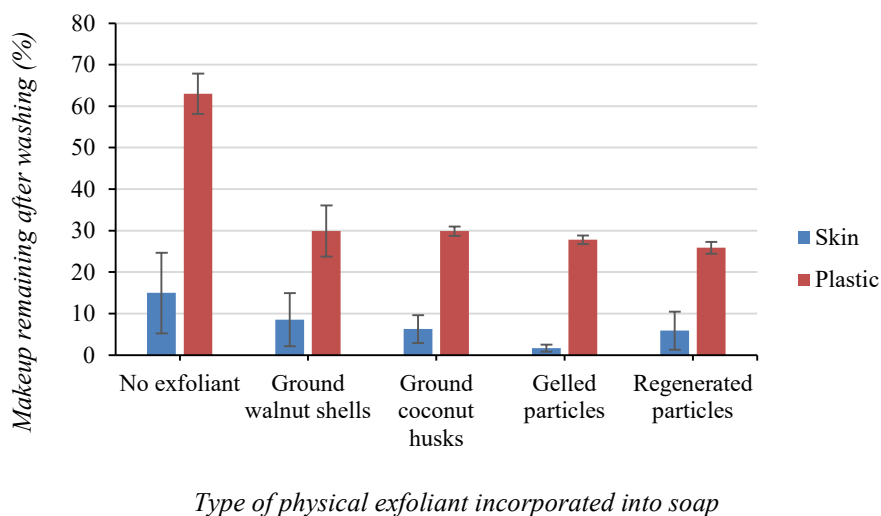


Figure 41. Cleansing efficiency of solid soap, with or without physical exfoliating particles ($n = 3$).

Soaps were equally evaluated for the number of washes it took to completely remove the eyeliner pencil from plastic “fake” skin (Figure 42) ($n = 5$). Again, all soaps containing exfoliating particles perform better than the control. BSG particle-containing soaps perform similarly to soaps containing naturally hard materials, reporting averages of 9.2 and 7.0 for gelled and regenerated particles, and 10.8 and 9.8 for ground walnut shells and ground coconut husks, respectively. More details on these assays (and example photographs) can be found in the Supporting Information.

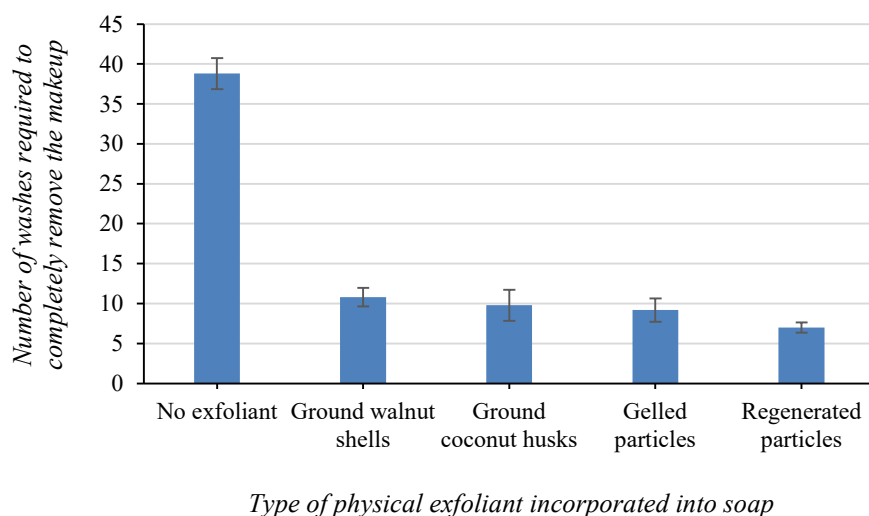


Figure 42. Cleansing efficiency of solid soap, with or without physical exfoliating particles ($n = 5$).

h) PHYTOTOXICITY

Phytotoxicity tests served as an indicator of the particles’ toxicity towards model plants (onion, *Allium fistulosum* and tomato, *Lycopersicon esculentum*) and their biodegradation in soils. Biomarker values for controls and both particles are shown in Figure 43 for onions and Figure 44 for tomatoes. Example photographs and temperature and humidity monitoring for the experiment can be found in the Supporting Information.

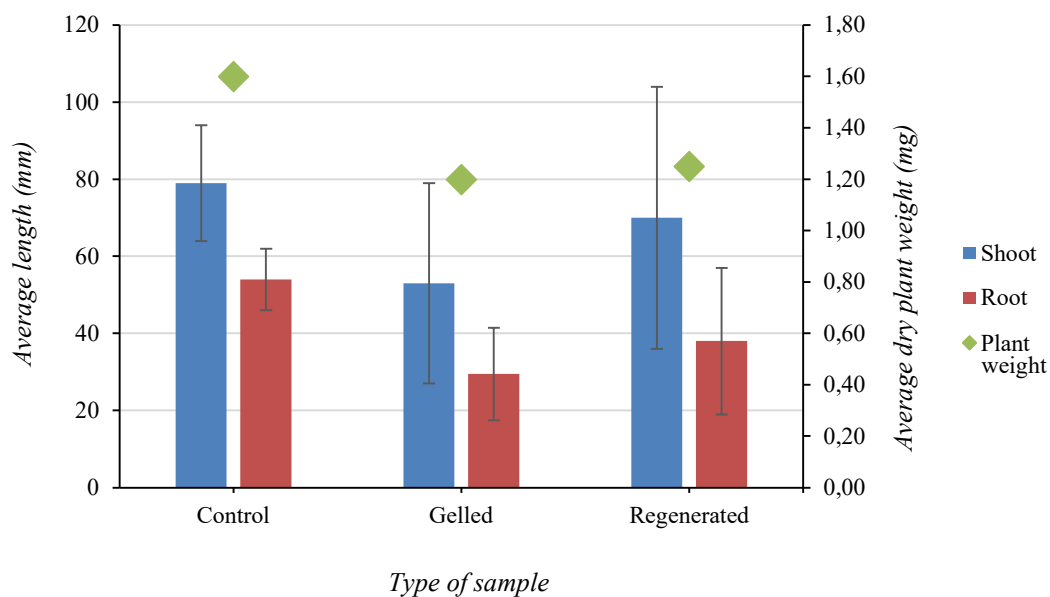


Figure 43. Comparison of onion plants (*Allium fistulosum*) grown in plain soil (control) or soil containing either gelled or regenerated BSG-particles.

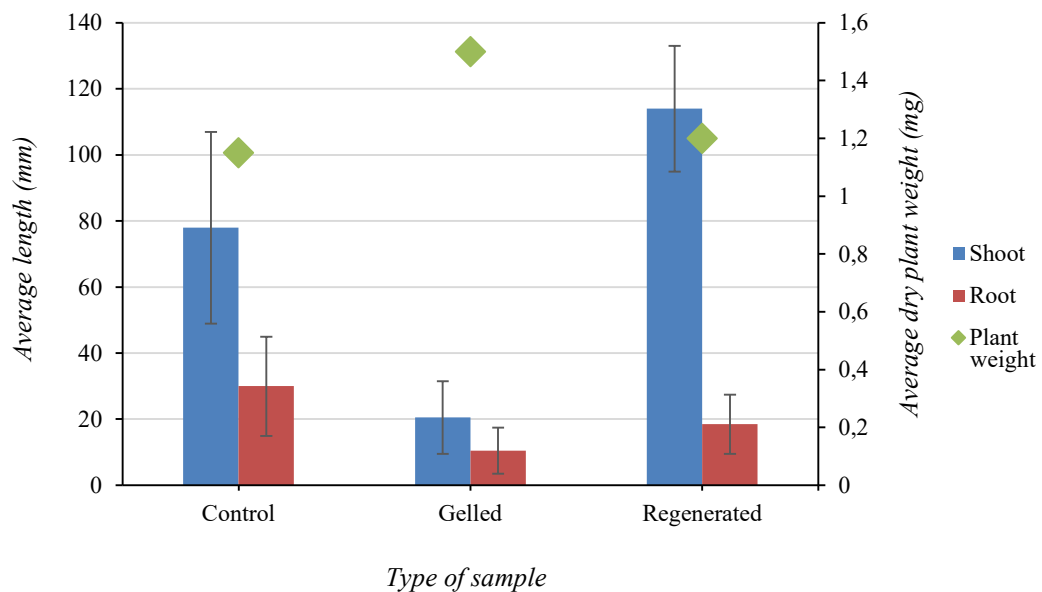


Figure 44. Comparison of tomato plants (*Lycopersicon esculentum*) grown in plain soil (control) or soil containing either gelled or regenerated BSG-particles.

Particles completely degraded in the soil over the 3-week experimental period. We did not expect to observe toxic effects from the lignocellulosic matrix of the BSG particles as biomass naturally decomposes in the environment, providing nutrients for the proliferation of other organisms.¹⁹² However, in the case of gelled particles, plants are negatively affected by the particles' high pH which raises soil pH to between 8 and 9. Onions are known to be more tolerant of alkaline soils than tomatoes, which is echoed in our experimental results.^{193, 194} For onions, seedling emergence is 55% in particle-containing samples compared to 80% for controls. With tomatoes, seedling emergence falls from 90% in controls to a mere 25% in samples. Seedling emergence rates determine n for shoot and root length measurements (i.e., 90% emergence represents $n = 18$). In gelled particle-containing samples, the biomarker values of the shoot and root lengths, as well as average dry plant weight (measured as total dry plant weight divided by the number of shoots) are consistently lower than values observed in controls (Figures 43 and 44). The only value that deviates from this trend is tomato plant average dry weight, with values of 1.50 mg despite small plant sizes (Figure 44). Theoretically, negative effects to plant growth can be attributed to changes in soil pH, although further testing may be needed to completely rule out the cellulosic fraction of the gelled particles' potential influence.

In the case of regenerated particles, no toxic effects are observed on either tomato or onion plants, although particles slightly lower soil pH (from 6.5 to 6). Seedling emergence is higher or the same as the control groups. For tomatoes, seedling emergence is at 90% for both controls and samples; for onions, controls have 80% emergence, and samples have 85%. Average dry plant mass is higher in controls than in samples with onions (1.60 mg compared to 1.20 mg, Figure 43), but the inverse is true for tomatoes (1.15 mg compared to 1.20 mg, Figure 44). Shoot and root lengths were also measured and showed similar trends (Figures 43 and 44, where n is a function of seedling emergence). Values were slightly lower in onion samples as opposed to onion controls, with shoots and roots about 10% and 30% shorter, respectively (Figure 43). As for tomato plants, shoots were about 45% longer in particle-containing samples than in controls, although roots were about 40% shorter (Figure 44).

3.2.3 Conclusion

Brewer's spent grain (BSG) was shown herein to be a promising source of natural polymers for the production of lignocellulosic materials, including particles to be used as exfoliating agents in personal hygiene products. After dilute acid hydrolysis (0.60 M HCl, 2 h, 90 °C), pretreated BSG could be dissolved up to 9 wt% (solids basis) in 3 M NaOH with 1 wt% ZnO as an additive. Solubilization of the BSG occurred at -3 °C over 24 hours, with an additional 24 hours to dissolve a subsequent addition of 2 wt% medium fiber length cellulose powder. Resulting BSG-based solutions were poured into molds, which were subsequently solidified through gelation (drying) or regeneration in a 1 M HCl bath. Dried films could be separated from the molds and cut into 1 mm² porous particles of varying thicknesses. Gelled and regenerated particles prove to be stable in solid soaps for at least three months, and for at least one year under ambient, dry conditions. However, they undergo significant delignification and NaOH leaching in liquid soaps, which reduces their mass yield over the one-month period during which this parameter is measured. They exhibit similar cleansing abilities to commercially available naturally exfoliating particles. Both gelled and regenerated particles biodegrade in soils with no toxicity to model plants. Besides BSG-based particles proving to be a promising option for exfoliating particles in personal hygiene products, the complete BSG solubilization protocol reported herein is promising in the production of further high-value materials from a readily available residual biomass.

3.2.4 Experimental Section

3.2.4.1 Materials

a) *BREWER'S SPENT GRAIN*

Brewer's spent grain (BSG) was obtained from two local Quebec microbreweries throughout this project: Le Bien le Malt (Rimouski, QC, Canada), and Ras L'Bock (La Pocatière, QC, Canada). Samples had an average humidity of 77%, determined gravimetrically before and after drying. The exact cereal composition of these samples was never specified, but the main component was always malted barley. In total, we worked with four batches of BSG from different brews to account for brewing conditions' effects on BSG's composition.

b) *OTHER MATERIALS*

Purified cellulose was obtained from a variety of sources. Celova® Cellulose Powder samples (C500, C1000, C2000) were provided by Weidmann Fiber Technology (Switzerland). Microcrystalline cellulose was purchased from Alfa Aesar (USA). Cellulose fibers (medium) and α -cellulose fiber (99.5%) were purchased from Sigma-Aldrich (USA). See Supporting Information for product specifications regarding cellulose fiber length. Non-nano zinc oxide (-200 mesh powder, 99.9%) and sodium hydroxide pellets (98%) were obtained from Alfa Aesar (USA). Hydrochloric acid (ACS grade, 36.5-38%) was purchased from VWR (USA). All materials were of the highest purity available.

3.2.4.2 Preparation of Brewer's Spent Grain Films and Particles

Humid BSG was pretreated by dilute acid hydrolysis with HCl. Accordingly, 77% humidity BSG was combined with 0.60 M HCl at a 2 : 3 mass ratio and heated at 90 °C for 2 hours. After pretreatment, the BSG-dilute acid mixture was directly solubilized by adding solid NaOH so that the overall concentration in the sample was 3 M NaOH, 1 wt% ZnO, and 2 wt% medium-DP cellulose fibers. A recirculating chilling bath was used to maintain the samples at -3 °C over 48 hours. BSG-based materials were producing by pouring the BSG-NaOH-ZnO solution into molds. The molds, which were 10 cm X 10 cm squares, allowed to produce films where thickness was a function of the volume of BSG-NaOH-ZnO solution used. We adjusted the volume to create films with an approximate wet thickness of 1 mm (dried down to about 0.25 mm). Films were either left to dry under ambient conditions (gelation) or were submersed in a tenfold (v/v) 1 M HCl batch for 12 hours (regeneration). After regeneration, the acid supernatant was gently poured away, and the remaining film was left to dry under ambient conditions. Once dry, films were separated from the molds, then cut into approximately 1 mm² particles for further characterization.

3.2.4.3 Characterization

a) BREWER'S SPENT GRAIN COMPOSITION

The molecular composition of BSG samples was determined according to a combination of NREL, ASTM, and TAPPI protocols.⁹² Each sample consisted of 100 g of dry BSG and was analysed for ash, alpha-cellulose, hemicellulose, lignin, acid-soluble lignin, and proteins. It is important to note that extractives are quantified after four successive Soxhlet extractions (hexane, toluene-ethanol, ethanol, water).

b) *DIMENSIONS OF DRIED PARTICLES*

The weight of the particles was determined using a micro-balance. Size was determined by taking pictures of particles on a clean, high-contrast surface. The images were then analyzed using ImageJ software (NIH, USA) and size was represented as Feret's diameter. The individual weights and sizes of 60 particles were taken and averaged.

c) *PARTICLE SWELLING IN WATER*

The swelling behaviour of gelled or regenerated dried BSG particles was determined by noting the changes in their dimensions after soaking in room temperature distilled water for 24 hours. After the soaking period, the particles were filtered from the water. Dried particles were photographed on a high-contrast, smooth background, and images were analyzed with ImageJ software (NIH, USA). They were then placed in room temperature distilled water. After the soaking period of 24 hours, the particles were filtered from the water. Immediately after, the size of the particles was determined by capturing photos of them on a high-contrast, smooth background, and analyzing the images with ImageJ software. The swelling degree, expressed in %-units, was calculated as a function of the total surface area occupied by particles, assuming a perfectly cubic shape.

d) *SEM-EDS*

The morphologies of gelled or regenerated dried BSG particles were examined using a scanning electron microscope (SEM), model Inspect F50 by the Field Electron and Ion Company (USA). An energy-dispersive (EDS) detector, model Octane Super-A by Edax Ametek (USA), was used to semi-quantitatively determine sample composition. Whole

particles were coated with silver and palladium using a sputter coater, then imaged at 200 X and 1000 X at an optimum accelerating voltage of 15 kV. Their elemental composition was detected at a resolution of 131.7 eV.

e) ATR-FTIR

Gelled and regenerated dried BSG particles and purified cellulose samples were analyzed by ATR-FTIR. The spectra were recorded using the ATR module of a Nicolet iS50 instrument (Thermo Scientific, USA). A total of 64 scans were realized for each sample at a resolution of 4 cm⁻¹. OMNIC spectra software (Thermo Scientific, USA) was used to normalize the spectra and investigate peaks.

f) STABILITY IN MATRICES RELEVANT TO PERSONAL HYGIENE PRODUCTS

To measure particle stability in model commercial personal hygiene products, 40 mg of gelled or regenerated dried particles were mixed in either 1 g of distilled water or one of two shower gels (Super Leaves™ Orange Leaves and Oatmeal Sensitive Extra Gentle, ATTITUDE™, Canada), or a body cream (Super Leaves™ Orange Leaves, ATTITUDE™, Canada). Herein, the shower gels are simply referred to as gel 1 and gel 2, respectively, and the body cream is described as such. Samples were prepared in triplicate for each testing period and aged in ambient conditions. After 0.5, 1, 2, 3, 7, 14, 21, and 28 days, the particles were removed from the matrices, gently rinsed with distilled water, and dried in a vacuum oven at 50 °C for 24 h to remove any residual humidity. Body cream samples were additionally rinsed with ethanol, due to the matrix's relative hydrophobicity. Dried particles were weighed, and stability (S_W) was calculated by comparing their total mass before and after soaking in the sample matrixes using the following equation (Equation 4):

Equation 4. Stability (S_W) of microbeads, determined gravimetrically

$$Stability_W (\%) = \frac{W_n}{W_0} \times 100$$

Where W_n is the weight in grams of the dried beads after n days and W_0 is the initial weight in grams of the same beads.

Stability was further characterized by analyzing the particles' dimensions using ImageJ, according to the same methods described previously, before and after soaking in the sample matrices. In this case, stability (S_A) is determined as follows (Equation 5):

Equation 5. Stability (S_A) of microbeads, determined by surface area

$$Stability_A (\%) = \frac{A_n}{A_0} \times 100$$

Where A_n is the total area in mm^2 of the dried beads after n days and A_0 is the initial total area in mm^2 of the same beads.

A further set of stability samples was prepared with 1 g of gelled or regenerated dried particles dispersed throughout 40 g of both sample body washes, water, and a solid glycerine soap base. Samples were aged in ambient conditions for three months. The pH and viscosity of each liquid matrix were taken before bead incorporation and following the three-month aging period. The pH of samples was measured using a digital pH-meter (FiveEasy Plus Benchtop FP20, Mettler-Toledo, USA) and the viscosity of samples was measured using a rotational viscometer (DV1 digital viscometer, Brookfield AMTEK, USA). Dried beads were also kept at ambient conditions for one year. Qualitative observations were noted throughout the experiment.

g) *CLEANSING EFFICIENCY*

The protocol for determining cleansing efficiency was adapted from Ju *et al.* (2021) and modified for enhanced reproducibility.⁸⁵ Approximately 0.3 g of particles or commercial natural exfoliant (ground walnut or coconut shells) were incorporated into 9 g of solid glycerine soap base. Squares of soap with and without particles were mounted on a stick attached to a swivel, which was in turn attached to a fixed surface. The word “SOAP” is written on the interior of an individual’s arm with a waterproof black eyeliner pencil, as this is a flat surface of sensitive skin with little hair. The written-on skin was gently wetted and washed by the soap at a pressure defined by the swivel/stick system for 10 seconds (passed over 10 times by the soap). Pictures are taken of the written-on skin before and after washing with the soaps and processed with ImageJ software (black-and-white contrast processing) to determine just how efficiently the makeup was removed, with cleansing efficiency defined by Equation 6 (see Supporting Information). Skin was monitored for signs of irritation. Additionally, the same experiment was performed with plastic “fake skin” as the written-on surface (ReelSkin silicone light tone sheet, UK). Both experiments were done in triplicate.

Cleansing efficiency was equally measured in terms of the total number of swivels required to completely remove the word “SOAP” written with waterproof black eyeliner from the plastic “fake skin.” The experiment was done in five replicates.

Equation 6. Cleansing efficiency of soaps

$$\text{Cleansing efficiency (\%)} = \frac{A_f}{A_i} \times 100$$

Where A_i is the total area in mm^2 of the crayon immediately following drawing on the skin and A_f is the total area in mm^2 of the remaining crayon after washing.

h) PHYTOTOXICITY

According to OECD protocol 208,¹⁹⁵ 10 onion (*Allium fistulosum*) or 10 tomato (*Lycopersicon esculentum*) seeds were planted in 60 g (dry weight) of sieved soil. Approximately 60 mg of gelled or regenerated dried BSG particles are mixed into the top layer of the soil, representing the maximum test level of 1000 mg/kg. Per type of plant, we prepared two controls, two pots with gelled particles, and two pots with regenerated particles. Plants are cultured with a 16/8 light/dark photoperiod (30-36 K lux.) at $22 \pm 2^\circ\text{C}$ with $75 \pm 15\%$ relative humidity, for 14 days after 50% seedling emergence in the controls, which contain no particles. Seeds are bottom-watered and misted with water when they are planted, then misted every 24 hours. After the germination period, seedling emergence is counted in all groups, shoots and roots length are measured and cleaned, and dried plants are weighed. Plants were also qualitatively observed for any visible signs of toxicity. (See Supporting Information.)

3.2.5 Acknowledgements

This work was supported by funding from MITACS, Canada. Special thanks to the Bien le Malt (Rimouski) and Ras L’Bock (La Pocatière) microbreweries for supplying brewer’s spent grain at no cost, Weidman Fiber Technologies (Switzerland) for donating cellulose samples to the project, as well as ATTITUDE™ (Montreal) for providing advice regarding stability testing and the required matrixes at no charge. We would also like to acknowledge the contributions of the Laboratoire des technologies de la biomasse (Université de Sherbrooke), Prof. Thierry Ghislain, and Emy Leblanc for the analysis of biomass composition, and the Laboratoire de microanalyse (Université Laval), Dr. Marc Choquette, and Suzie Côté for SEM-EDS analysis. Additional thanks to Dr. Charles Lavigne for the involvement of the Centre de développement bioalimentaire du Québec in this project and Dr. Élise Caron for her contributions to the early stages of the project. This

research was conducted thanks to the financial support of the MITACS Accelerate program, the Partenariat canadien pour l’agriculture, and the Fonds de recherche Nature et Technologies du Québec.

3.2.6 Supporting Information

3.2.6.1 Biomass Composition

The molecular composition of BSG samples was determined according to a unique combination of NREL, ASTM, and TAPPI protocols.⁹² Details of the specific protocols used can be found in Damay *et al.* 2018, sections 2.5.1 to 2.5.6. Each sample consisted of 100 g of dry BSG and was analysed for ash, alpha-cellulose, hemicellulose, lignin, acid-soluble lignin, and proteins. The complete normalized data presented in Figure 34 can be found in Table 8 below.

Table 8. Complete normalized data of the composition of BSG batches.

Brewery	Ras L’Bock		Le Bien le Malt	
Batch	July 2021	May 2021	Jan. 2021	Oct. 2020
Ash	4.58	4.37	2.65	3.99
Extractables	27.28	34.75	31.76	29.82
Alpha-cellulose	14.66	11.91	16.57	12.66
Hemicellulose	21.66	12.99	17.48	18.08
Lignin	12.11	11.58	11.12	10.00
Acid-soluble lignin	6.51	6.64	6.11	6.90
Proteins	13.21	17.77	14.31	18.55

3.2.6.2 Stability in Matrices Relevant to Personal Hygiene Products

The results of particle stability testing in model commercial personal hygiene products are presented graphically in Figures 39 and 40. Complete information for the average mass yields and average total area yields ($n = 3$) is presented in Tables 9 and 10, respectively.

Table 9. Average mass yields and associated standard deviations for stability testing of gelled and regenerated BSG-derived particles ($n = 3$).

Days	Gelled Particles			Regenerated Particles		
	Gel 1	Gel 2	Water	Gel 1	Gel 2	Water
0	100	100	100	100	100	100
0.5	33.6 ± 8.0	36.9 ± 6.4	27.5 ± 6.9	67.4 ± 11.1	57.0 ± 8.6	25.6 ± 3.4
1	35.2 ± 5.9	29.9 ± 6.9	28.3 ± 3.1	50.4 ± 16.8	44.4 ± 8.9	25.5 ± 1.7
2	30.5 ± 4.3	32.8 ± 2.0	22.2 ± 4.2	55.4 ± 7.2	55.3 ± 3.0	18.0 ± 6.2
3	34.5 ± 7.5	39.3 ± 9.5	24.5 ± 1.0	49.2 ± 6.7	38.6 ± 4.4	25.6 ± 5.5
7	33.2 ± 7.6	36.7 ± 5.1	24.8 ± 7.3	71.7 ± 10.2	53.0 ± 12.7	24.6 ± 8.0
14	30.4 ± 7.7	34.7 ± 7.6	24.1 ± 1.4	50.8 ± 15.8	46.1 ± 8.2	25.6 ± 4.6
21	31.3 ± 3.5	31.1 ± 6.5	23.4 ± 0.7	67.6 ± 3.0	53.8 ± 16.3	32.2 ± 8.9
28	34.1 ± 7.1	37.6 ± 7.1	28.4 ± 5.7	51.3 ± 22.2	47.3 ± 5.6	30.7 ± 6.3

Table 10. Average total area yields and associated standard deviations for stability testing of gelled and regenerated BSG-derived particles ($n = 3$).

Days	Gelled Particles			Regenerated Particles		
	Gel 1	Gel 2	Water	Gel 1	Gel 2	Water
0	100	100	100	100	100	100
0.5	63.3 ± 12.3	86.80 ± 0.8	79.5 ± 26.8	66.6 ± 35.2	98.0 ± 6.3	12.1 ± 3.5
1	60.4 ± 8.2	54.6 ± 3.4	45.4 ± 10.5	52.4 ± 2.7	71.5 ± 2.8	5.4 ± 1.1
2	45.9 ± 12.9	54.8 ± 5.9	41.0 ± 8.6	46.4 ± 22.8	53.0 ± 3.6	4.7 ± 1.8
3	59.4 ± 15.7	65.4 ± 8.5	60.6 ± 18.6	49.1 ± 22.0	47.7 ± 6.0	3.7 ± 1.4
7	53.0 ± 16.7	59.5 ± 4.4	45.9 ± 3.4	43.6 ± 30.8	45.5 ± 2.0	3.1 ± 1.1
14	54.0 ± 6.7	54.7 ± 10.5	34.3 ± 16.3	52.8 ± 35.6	61.6 ± 3.7	3.5 ± 1.0
21	50.2 ± 7.7	47.5 ± 10.8	50.4 ± 5.8	47.5 ± 39.9	60.9 ± 5.0	4.6 ± 0.4
28	39.9 ± 8.7	45.3 ± 17.5	42.5 ± 5.4	64.2 ± 44.1	75.5 ± 27.3	6.0 ± 2.8

3.2.6.3 Cleansing Efficiency

Cleansing efficiency evaluated the capacity of soaps formulated with or without exfoliating particles for their capacity to remove a model pollutant, a black waterproof eye pencil, from real and fake skin. The word “SOAP” was written on the model surface, which was then gently wetted and washed by the soap samples. Pictures were taken of the written-on skin before and after washing with the soaps and processed with ImageJ software (black-and-white contrast processing) to determine just how efficiently the makeup was removed, with cleansing efficiency defined by Equation 6:

Equation 6. Cleansing efficiency of soaps

$$\text{Cleansing efficiency (\%)} = \frac{A_f}{A_i} \times 100$$

Where A_i is the total area in mm^2 of the crayon immediately following drawing on the skin and A_f is the total area in mm^2 of the remaining crayon after washing.

Alternatively, cleansing efficiency was measured in terms of the total number of washes required to completely remove the word from the model surface. Examples of photos used to determine cleansing efficiency are pictured below (Figures 45 and 46).

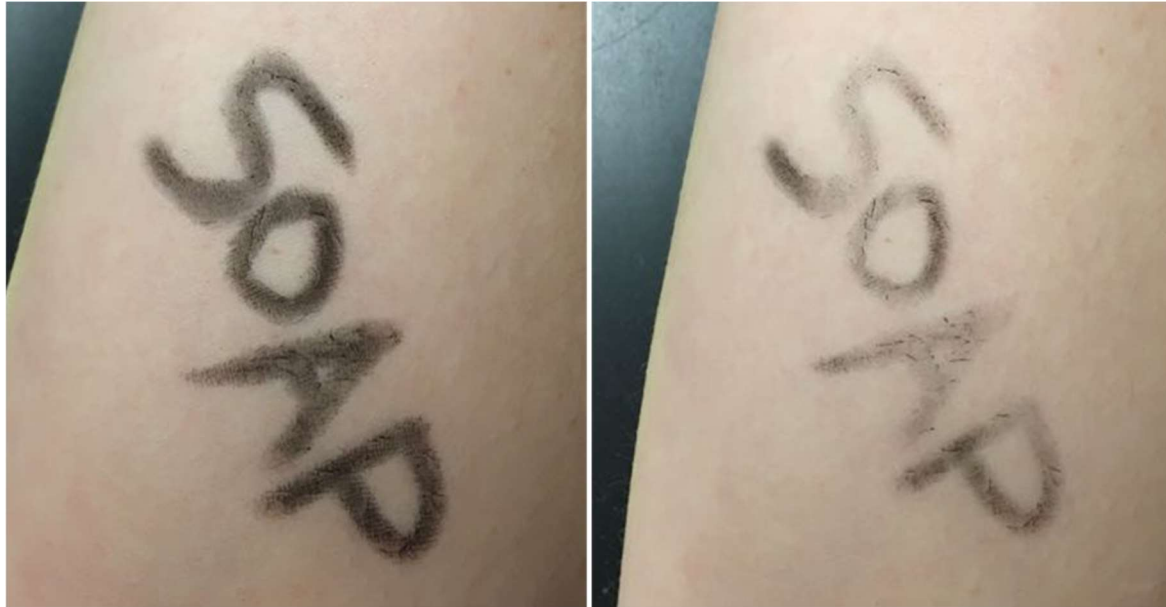


Figure 45. Eye pencil on skin before (left) and after (right) washing with a soap containing no exfoliating particles.



Figure 46. Eye pencil on skin before (left) and after (right) washing with a soap containing gelled BSG particles.

3.2.6.4 Phytotoxicity

Phytotoxicity tests, realized according to OECD protocol 208,¹⁹⁵ modelled the biodegradation of the particles in soils and their effects on two model plant species: onion (*Allium fistulosum*) and tomato (*Lycopersicon esculentum*). We counted 10 seeds of each species and planted them (separately) in 60 g (dry weight) of sieved soil for each sample. Approximately 60 mg of gelled or regenerated dried BSG particles are mixed into the top layer of the soil, representing the maximum test level of 1000 mg/kg. Per type of plant, we prepared two controls, two pots with gelled particles, and two pots with regenerated particles. Plants are cultured with a 16/8 light/dark photoperiod (30-36 K lux.) at $22 \pm 2^\circ\text{C}$ with $75 \pm 15\%$ relative humidity, for 14 days after 50% seedling emergence in the controls, which contain no particles. Seeds are bottom-watered and misted with water when they are planted and misted every 24 hours. After the germination period, seedling emergence is counted in all groups, shoots and roots length are measured and cleaned, and dried plants are weighed. Besides measuring and weighing the resulting plants, shoots were characterized visually for signs of toxicity and photographs of the plants were taken throughout the experiment (Figures 47 and 48). The experiments were realized in a controlled environment, where temperature and humidity were continuously monitored throughout the experiment (Figure 49).



Figure 47. Example photographs of onion (*Allium fistulosum*) plants after phytotoxicity tests: control (left), gelled particles (center), and regenerated particles (right).



Figure 48. Example photographs of tomato (*Lycopersicon esculentum*) plants after phytotoxicity tests: control (left), gelled particles (center), and regenerated particles (right).

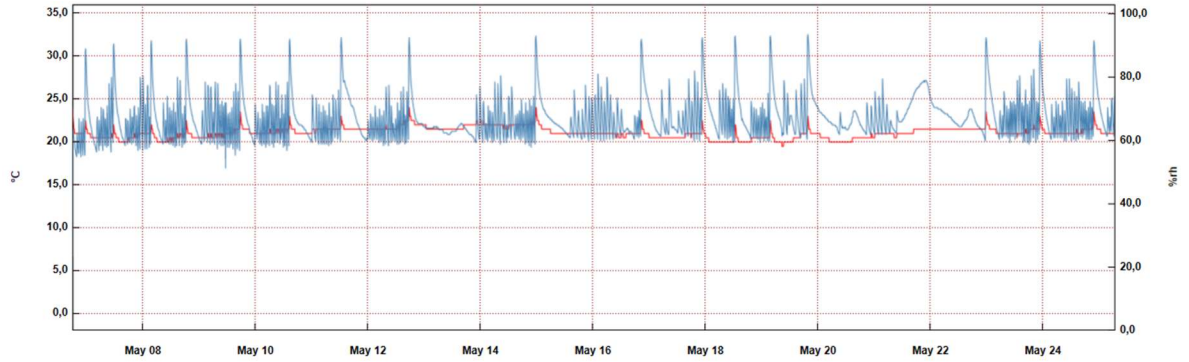


Figure 49. Temperature (red) and humidity (blue) tracking throughout phytotoxicity testing.

3.2.6.5 Cellulose Fiber Length

Product specifications for the various cellulose powders provided indicated their DP (Table 11). Screen analysis revealed that 15-25% and 65-75% of C2000 were retained on 1000 and 63 μm sieves respectively, indicating high DP. For C1000, 2-10% was retained on a 500 μm sieve, while the remaining 70-90% was retained on a 32 μm sieve. Samples C500 and medium cellulose fiber have similar DP, each with 5-15% retained on a 125 μm sieve and the remaining 60-75% on a 32 μm sieve. For α -cellulose powder, average DP was slightly lower, with 35% on a 200 μm sieve, 50% on a 100 μm sieve, and 20% on a 32 μm sieve. Microcrystalline cellulose's average DP of 350 was provided directly from the manufacturer.

Table 11. Screen analysis of the various cellulose powders used, as provided by the manufacturers.

Sample	1000 μm (%)	500 μm (%)	200 μm (%)	100 μm (%)	63 μm (%)	32 μm (%)
C2000	15-25	-	-	-	65-75	-
C1000	-	2-10	-	-	-	70-80
C500	-	-	5-15	-	-	60-75
Cellulose fibers (medium)	-	-	5-15	-	-	60-75
α-cellulose fiber	-	-	35	50	-	20

CHAPTER 4

INDUSTRIAL FEASIBILITY OF THE METHODS

4.1 SCALE-UP OF THE PROTOCOL FOR BSG-BASED MICROBEAD PRODUCTION

4.1.1 Introduction

As is the case with any chemical process – or any business endeavour for that matter – planning and realizing the scale-up process is one of the most critical tools in proving industrial feasibility. Scale-ups of chemical mechanisms are highly complex, extending far beyond simply running the same transformations or reactions in larger quantities.¹⁹⁶ Typically, this process regroups chemists, chemical engineers, health and safety or environmental specialists, and businesspeople, who each contribute to distinct aspects of the operation.

Many parameters need to be considered when realizing the scale-up of a chemical process. At larger scales, health and safety risks need to be even more carefully considered,¹⁹⁶ as greater production volumes represent the capacity to do more substantial harm. Raw materials and equipment need to be chosen in a manner that minimizes potential dangers, both at human and environmental levels. These parameters are also required to ensure reliable results in a cost-effective way. Design of Experiments and Process Analytical Technologies are commonly employed to model the scale-up's plan, ensuring optimization.¹⁹⁷ At a general level, algorithmic tools such as these allow for a better understanding of reaction kinetics and thermodynamics, heat transfer, mixing, and potential impurities' formation. For more precise synthetic strategies, these can also help predict crystallization and polymerization mechanisms, among others. When the scale-up process

is properly realized, a high-quality product is obtained through a safe, reliable, reproducible, cost-efficient, and profitable mechanistic strategy.

In this section, we present the results of laboratory and pilot scale-up of the production of brewer's spent grain-based (BSG-based) microbeads (Chapter 2). As is the case with lab-scale optimization, process scale-up needs to account for the variable humidity and molecular composition of the biomass,¹² which is addressed by using different samples of BSG obtained from different brews. Our lab-scale results demonstrate that the process is particularly sensitive to temperature, requiring the scale-up process to emphasize optimal heat transfer and mixing. Moreover, as initial scale-up tests were to be realized by hand, we needed to pay particular attention to health and safety concerns.

4.1.2 Results & Discussion

Original samples were all prepared with 50 mL total of BSG-based solutions, allowing to produce approximately 3.2 g of dried microbeads. Samples were pretreated using a stirring, heating plate (Magnetic Hotplate, VWR®, USA), which could heat samples to 100 °C. Then, samples were solubilized in a polystyrene cooler placed atop a multi-spot stirring plate, cooled by a serpentine cooling coil attached to a recirculating chilling bath (1196 D Refrigerated Circulating Bath, VWR®, USA) containing a 2 : 3 mixture of ethylene glycol and water. Using this system setup, samples could be cooled to a temperature of -15 °C.

The process was scaled-up in the lab setting for the solubilization of up to 500 mL of BSG-based solutions. This process was realized using the same experimental setup, and no modifications of the protocol were required to obtain homogenous BSG solutions. At 500 mL of BSG-based solutions, a theoretical yield of 32 g of dried microbeads could be produced.

The scale-up process was then extended to much larger volumes of BSG-based solution using a different experimental setup. A stainless-steel double-jacket reservoir (unknown model and manufacturer) was used to pre-treat and dissolve BSG. It was equipped with a motorized stirrer and had an approximate maximum capacity of 500 L. As the HCl used for pretreatment is incompatible with stainless-steel, it was understood that the equipment would be damaged throughout this process.¹⁹⁸ For pretreatment, the system was heated by circulating low pressure, hot water vapour through the double-jacket of the reservoir; for grain solubilization, the system was cooled by circulating cold water (cooled using an ethylene glycol-based refrigerating system) through the double-jacket of the reservoir. Maximum temperatures that could be reached using this non-pressurized system were around 120 °C, while minimum cooling temperatures were around 1 °C. Although this did not interfere with pretreatment, which only required 75 °C, temperatures required for complete grain solubilization at lab-scale were observed to be between -3 and -1 °C.

Initial tests using this system attempted to produce 100 L of BSG solution using the same optimal parameters used for lab-scale production (reported in Chapter 2). When attempts failed to adequately solubilize BSG for this production volume – despite raising pretreatment temperature, pretreatment acid concentration, or NaOH concentration for solubilization – we dropped our aim to producing 25 L of solution. At this reduced volume, we initially did not observe an acceptable degree of BSG solubilization, although there was an improvement compared to our first tests at 100 L (Figure 50, comparison between lots 1 and 2). Then, after having slightly raised pretreatment temperature to 80 °C instead of 75 °C, we were able to dissolve about 90% of BSG over a period of four days (Figure 50, lot 3). This increase in temperature did not affect grain yields, indicating that the system's actual temperatures may be lower than indicated. Besides increasing pretreatment temperature and doubling the required duration of the solubilization step, no other system parameters changed. Subsequently, we scaled our batch volume up to 50 L of solution, again noting about 90% of BSG solubilization over four days (Figure 50, lot 4). This volume would yield around about 2.85 kg of dried microbeads, in theory, accounting for

the incomplete grain dissolution. However, it is worth noting that greater process time represents decreased industrial feasibility.

As sub-samples of these batches could be completely dissolved using our lab-scale experimental setup, we determined that discrepancies in sample temperature, no matter how slight, influence BSG's solubilization. This would explain why we could not adequately solubilize grain with increasing production volumes: larger quantities of BSG-NaOH-ZnO-water are more difficult to chill in a uniform manner. We assume that had the system had the capacity to cool the BSG solutions to below freezing, we may not have necessarily needed to increase pretreatment temperature nor the duration of grain solubilization. Furthermore, we may have been able to observe complete BSG solubilization at 25 L, 50 L, or even larger volumes.



Figure 50. Photographs of various scale-up tests in the stainless-steel reservoir: lot 1, 100 L (left); lot 2, 25 L (center left); lot 3, 25 L (center right); lot 4, 50 L (right).

After these tests, having realized that the reservoir would not be able to be cooled to the required temperatures of -3 to -1 °C, we designed a new experimental setup for the production of up to 4 L of BSG-based solution (Figure 51). This new setup involved placing a culinary stand mixer (Precision Stand Mixer, Cuisinart, USA) in a blast chiller whose temperature could be easily controlled, cooling BSG-solutions to the required

temperatures. Pretreatment was still performed at 80 °C in the stainless-steel reservoir used in the previous tests, as this system was only designed for cooling.

With this new system, we began by attempting to dissolve 1 L of BSG-solution. We observed slightly improved grain solubilization over four days (around 95%), while sub-samples could be completely dissolved in our lab-scale chilling bath in 48 hours (original duration). When a few additional attempts at these volumes did not show any improvement, we scaled-up to 2, 3, and 4 L volumes of BSG-solution, noting the same observations.

Using this system, we were consequently able to solubilize up to 4 L of BSG-solution with near-complete solubilization achieved after four days. This volume would yield around about 253 g of dried microbeads, in theory. Unfortunately, we were not able to produce microbeads from these solutions to experimentally validate these predicted yields. Samples required constant stirring, so that temperature and grain dispersion throughout the solution would remain as uniform as possible. However, even the lowest speed setting on the stand mixer was too high, frothing the BSG-solution and rendering it incompatible with the dropping technique for microbead production. The flat beater attachment for the stand mixer significantly “whipped” the BSG-solutions, while the dough-hook attachment visibly reduced this phenomenon (Figure 51).



Figure 51. Photographs of various scale-up tests in the stand mixer: stand mixer placed in the blast chiller (left), 1 L of “whipped” BSG solution (center), 1 L of BSG solution (right).

It is important to note that microbeads produced throughout the scale-up process were not characterized. It is reasonable to believe that with incomplete solubilization of the grain, the materials' mechanical characteristics may deviate from our observations during lab-scale production, as presented in Chapter 2.

4.1.3 Conclusion

Although scale-up results were deemed acceptable, there is still obvious room for improvement. At volumes of 25 L or above, maximum grain solubility was around 90%, which decreased with increasing production volumes. Despite having raised pretreatment temperature by 5 °C and doubled the solubilization period's duration (compared to our lab-scale method, Chapter 2), we were hindered by the minimal possible temperature of the system of 1 °C and poor control over system mixing. As the minimal possible temperature is 3 °C higher than the optimal temperature, it is unsurprising that we were unable to achieve complete grain solubilization. At volumes of 4 L or less, maximum grain solubility was improved but remained incomplete. Although the setup used to this effect allowed to achieve lower temperatures, it still lacked the precision required to ensure reliable heat transfer. Ideally, with a greater budget, we would have been able to procure high-precision heating and chilling reactors that would provide better control over system temperatures and heat transfer through mixing, likely yielding better results. More than anything, these tests further demonstrate the necessity of the optimal BSG solubilization temperatures, as even a few degrees higher drastically diminishes the ability to dissolve the grain. We did not characterize any microbeads produced during the scale-up process and suspect that incomplete grain solubilization may hinder the strong mechanical properties we observed at a smaller scale, in Chapter 2. Even so, having used less-than-ideal equipment, this work helps to demonstrate the industrial feasibility of the method as we were still able to achieve acceptable solubilization results. This provides a great starting point for any future work on industrial scale-up of the method.

4.1.4 Experimental Section

4.1.4.1 Brewer's Spent Grain

Brewer's spent grain (BSG) was obtained from two local Quebec microbreweries throughout this project: Le Bien le Malt (Rimouski, QC, Canada), and Ras L'Bock (La Pocatière, QC, Canada). Samples had an average humidity of 77% as determined gravimetrically. The exact cereal composition of these samples was never specified, but the main component was always malted barley. We worked with four batches of BSG obtained from different brews to account for the effects brewing conditions may have on BSG's composition.

4.1.4.2 Other Materials

Purified cellulose used in scale-up experiments was Celova® Cellulose Powder C500, provided by Weidmann Fiber Technology (Switzerland). Non-nano zinc oxide (purity unknown) was obtained from Botanic Planet (Canada). Sodium hydroxide pellets (97%) and hydrochloric acid (32%) was purchased from Univar Solutions (USA).

4.1.4.3 Preparation of Brewer's Spent Grain Microbeads

Humid BSG was pretreated by dilute acid hydrolysis with HCl. Accordingly, 77% humidity BSG was combined with dilute acid at a 1 : 4 mass ratio and heated at 80 °C for 2 hours. After pretreatment, BSG was isolated from the liquid hydrolysate by filtering over a 1 mm sieve. Pretreated grain was rinsed with water until it had a neutral pH using the same 1 mm sieve, then dissolved (9 wt% dry solids' basis, upon agitation with a motorized stirrer) using an aqueous solution of 2 M NaOH and 1 wt% ZnO, alongside 2 wt% medium-DP cellulose fibers. At volumes of 25 L or more, a stainless-steel reservoir, cooled by water

circulated through its double-jacket, was used to maintain the samples at 1 °C over 96 hours. At volumes of 4L or less, a stand mixer placed within a blast chiller was able to maintain the samples at -2 °C over 96 hours. The resulting BSG solution was filtered over a 1 mm sieve to remove undissolved impurities. The shaping of the beads and the regeneration of the polymeric structure was completed using the dropping/extrusion technique. The BSG-NaOH-ZnO solution was introduced, drop by drop, into a tenfold (v/v) acidic regenerating solution, at a drop height of 2 cm. The BSG solution was extruded through syringes equipped with needles of various sizes with the smallest compatible needle size being 26 G. As for the acid bath, 1 M HCl at ambient temperature yielded the best results. Following a minimum regeneration period of 12 h, the supernatant was poured away. Beads were filtered from the remaining solution and dried at in an oven at 50 °C. Once dry, beads were stored in a closed vessel for later characterization.

4.2 TECHNOECONOMIC ASSESSMENT OF THE METHODS

Novel chemical processes that present green alternatives to pre-existing products or methods need to be profitable to be adopted industrially. A rudimentary technoeconomic assessment was realized for the protocols described herein (Chapter 2, BSG-based microbeads; Chapter 3, BSG-based gelled and regenerated particles). A similar technoeconomic assessment was realized for a pre-existing protocol for the production of purified cellulose microbeads, reported by Mohamed *et al.* (2015).⁸⁸ This method relies on an aqueous solution of NaOH-ZnO-urea to dissolve purified cellulose, which may then be extruded drop-by-drop into an acid bath to produce spherical, porous microbeads. Of all microbead-production protocols found in the literature, this study was the closest to the methods elaborated from the present research.

To best estimate the costs for microbead or particle production, each method was extrapolated from their lab-scale protocols to the production of 1 kg of final product (including possible residual humidity) (Tables 12, 13, 14, and 15). Data for BSG-based microbead production (Chapter 2) can be deemed more robust than that of the others, as the pilot scale-up process realized for this method provided some experimental observations as well. Conversely, the data for cellulose microbead production is the least rigorous, as the assessment was extrapolated from the information described in the published article in which this protocol is found.⁸⁸

Table 12. Raw materials associated with producing 1 kg of BSG-based microbead production.

Pretreatment					
	BSG	Water	HCl [32%]		
Quantity (kg)	10	38.5	1.625		
Solids (kg)	2.3		0.52		
Humidity (%)	77		68		
Filtration					
	Pretreated BSG	Liquid Hydrolysate			
Quantity (kg)	7.5	- 42.625			
Solids (kg)	1.115				
Humidity (%)	85	96			
Rinsing					
	Water	Liquid Hydrolysate			
Quantity (kg)	12.5	- 13.6			
Solids (kg)					
Humidity (%)		99			
Solubilisation					
	Pretreated BSG	Water	NaOH [97%]	ZnO	Cellulose
Quantity (kg)	6.4	7.25	1	0.125	0.25
Solids (kg)	0.96		0.97	0.125	0.25
Humidity (%)	85		3		
Microbead Shaping & Solidification					
	BSG Solution	Water	HCl [32%]		
Quantity (kg)	15	54.125	5.875		
Solids (kg)	2.305		1.88		
Humidity (%)	84.7		68		
Filtration					
	Wet BSG Beads	Acid Filtrate			
Quantity (kg)	2.5	- 72.5			
Solids (kg)	1.55				
Humidity (%)	62				
Dried Microbeads					
	BSG Beads	Evaporated Water			
Quantity (kg)	1	- 1.5			
Solids (kg)	0.95				
Humidity (%)	5				

Legend: green, added; yellow, maintained from previous step; red, eliminated.

Table 13. Raw materials associated with producing 1 kg of BSG-based gelled particles.

Pretreatment					
	BSG	Water	HCl [32%]		
Quantity (kg)	1.633	2.302	0.147		
Solids (kg)	0.376		0.047		
Humidity (%)	77		68		
Solubilisation					
	Pretreated BSG- HCl solution	Water	NaOH [97%]	ZnO	Cellulose
Quantity (kg)	4.082	0.459	0.408	0.051	0.102
Solids (kg)	0.423		0.372	0.051	0.102
Humidity (%)			3		
Particle Shaping & Solidification					
BSG Solution					
Quantity (kg)	5.102				
Solids (kg)	4.102				
Humidity (%)	80.4				
Dried Particles					
	BSG Particles	Evaporated Water			
Quantity (kg)	1	- 4.102			
Solids (kg)	0.948				
Humidity (%)	5				

Legend: green, added; yellow, maintained from previous step; red, eliminated.

Table 14. Raw materials associated with producing 1 kg of BSG-based regenerated particles.

Pretreatment					
	BSG	Water	HCl [32%]		
Quantity (kg)	1.587	2.238	0.143		
Solids (kg)	0.365		0.046		
Humidity (%)	77		68		
Solubilisation					
	Pretreated BSG	Water	NaOH [97%]	ZnO	Cellulose
Quantity (kg)	3.968	0.446	0.397	0.050	0.100
Solids (kg)	0.411		0.361	0.050	0.100
Humidity (%)			3		
Particle Shaping & Solidification					
	BSG Solution	Water	HCl [32%]		
Quantity (kg)	4.96	17.183	1.865		
Solids (kg)	0.922		0.597		
Humidity (%)	80.4		68		
Filtration					
	Wet BSG Particles	Acid Filtrate			
Quantity (kg)	4.762	- 19.246			
Solids (kg)	1.000				
Humidity (%)	79				
Dried Particles					
	BSG Particles	Evaporated Water			
Quantity (kg)	1	- 3.822			
Solids (kg)	0.94				
Humidity (%)	6				

Legend: green, added; yellow, maintained from previous step; red, eliminated.

Table 15. Raw materials associated with producing 1 kg of cellulose microbeads, according to Mohamed *et al.* (2015).

Solubilisation					
	Water	NaOH [97%]	Urea	ZnO	Cellulose
Quantity (kg)	15.1	1.4	2.4	0.1	1
Solids (kg)		1.358	2.4	0.1	1
Humidity (%)		3			
Microbead Shaping & Solidification					
	Cellulose Solution	Water	HCl [32%]		
Quantity (kg)	20	64.62	15.38		
Solids (kg)	4.858		4.922		
Humidity (%)	75.71		68		
Filtration					
	Wet Cellulose Beads	Ethanol	Filtrate		
Quantity (kg)	1	10	99		
Dried Microbeads					
	Cellulose Beads				
Quantity (kg)	1				

Legend: green, added; yellow, maintained from previous step; red, eliminated.

Based off the abovementioned tabulated data, we then estimated the costs associated with the raw materials used in the production of BSG-based microbeads and particles, and cellulose-based microbeads. Minimum and maximum predicted costs (in CAD) were estimated using information sourced from chemical manufacturing companies, multiplied by the amount of the substance required by the protocol. For BSG, only one value is used, which is \$50 per tonne of raw biomass, as reported by the literature.³⁰ Minimum costs for HCl and NaOH came from Univar Solutions (USA).¹⁹⁹ For ZnO, the value came from Botanic Planet (Canada).²⁰⁰ Weidmann Fiber Technologies (Switzerland) graciously provided a quote for purified cellulose fibers.²⁰¹ The minimum cost associated with ethanol was estimated from the Business Insider markets tool,²⁰² while the value used for urea was

determined based on the Canadian base market price for the material.²⁰³ All maximum costs were sourced from Sigma Aldrich (USA) and were for analytical grade chemicals,²⁰⁴ hence the significant price differences (higher purity, greater cost). It can be assumed that actual method costs would fall somewhere between the presented minima and maxima. Costs associated with labor and electricity are not included in these rough estimates of economic feasibility, nor are those associated with water use, although we assume that they would be of the same order of magnitude for each of the methods. However, these factors are important to understand to better evaluate the environmental and economic impact of the methods. Future life cycle analysis work could fill this gap in the knowledge. Approximate method costs are broken down in Figure 52, below.

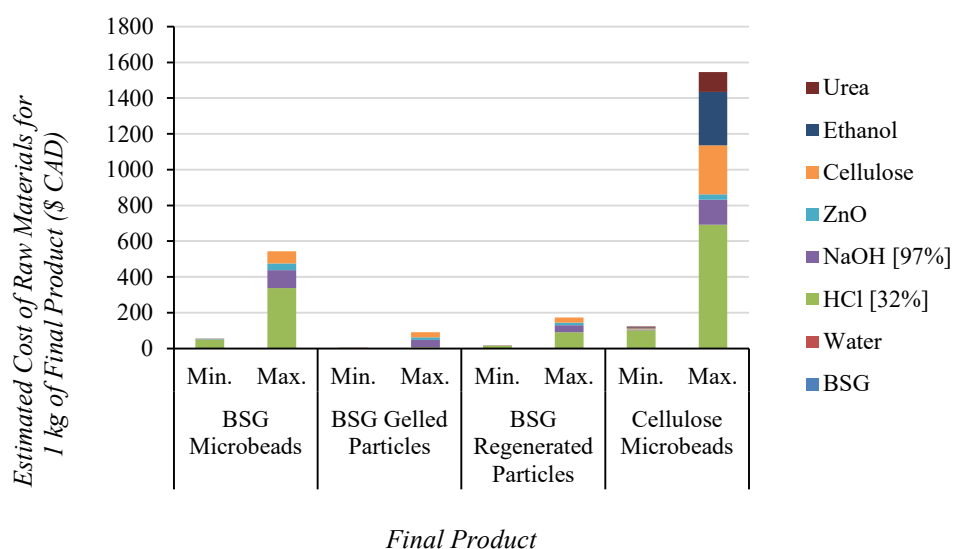


Figure 52. Costs (\$ CAD) associated with the raw materials required for the production of 1 kg of BSG- and cellulose-based microbeads and particles.

As is evidenced by the figure above, the cost of production for BSG-based materials is significantly less than that associated with the production of cellulose aerogel beads. Moreover, the costs associated with the production of microbeads is greater than that of particles, likely due to the reduced number of steps required to yield the latter. The costs

associated with purified cellulose obviously make up for significant differences between the methods: while cellulose microbeads rely solely on purified cellulose for their solids content, BSG-based materials are mostly based off of inexpensive spent grains, commonly sold for \$50 (CAD) per tonne.³⁰ The ethanol required for the rinsing of cellulose microbeads also increases the costs associated with their production, as this step is not required for the production of BSG-based materials. The same can be said of urea, used as an additive in purified cellulose's solubilization, albeit to a lesser extent. Hydrochloric acid, associated with all methods, is the mostly costly of the required raw materials. This explains why BSG-based gelled particles are the least expensive to produce of the four materials, as this protocol does not require using an acid bath for the material's generation. When high purity acid is used, as is the case for the reported maxima, costs are significantly increased. However, as high purity acid is not a requirement for the fabrication of BSG- or cellulose-based materials, we can assume that realistic costs would fall closer to the lower end of the predicted scale.

As for the equipment required for the realization of a proper scale-up of the method, or the production of 10 kg of final product, total costs would likely fall between \$45,500 and \$69,500 (CAD). These estimated values are based on the types of equipment required for the realization of the protocols and their associated prices from various vendors. Like raw materials cost, equipment costs are presented as a rough estimate.

All methods would require a heating reactor for pretreatment resistant to HCl (ideally made from glass or titanium or coated with polytetrafluoroethylene).¹⁹⁸ If the heating reactor were to be made from stainless-steel, costs associated with the equipment would likely be lower, but HCl would have to be swapped for HNO₃. The process also requires a cooling reactor for BSG solubilization, ideally made from stainless steel,¹⁹⁸ cooled with an ethylene glycol solution or other refrigerant. If HCl were swapped for HNO₃ for the pretreatment step, a stainless-steel dual heating-cooling reactor could be used for both steps. This would reduce the space occupied by the various equipment but would not necessarily reduce cost.

Between pretreatment and solubilization steps, the method for microbead production (Chapter 2) requires filtering and rinsing the pretreated grain. This can be done by hand, which is a very time-consuming process, or automated using a filter-press. The cost of this equipment largely depends on the size of the filter bed.

The remaining equipment depends on the chosen method for microbead or particle production. Microbeads would ideally be produced using automated equipment, which vary in cost according to the specific technique used. As for particles, they can be cut from BSG-based films, ideally using automated equipment. Robotic cutters would be able to cut these films into particles of specific and reproducible dimensions. Otherwise, BSG-solutions could be theoretically poured into custom silicone molds of the desired dimensions. Silicone molds would likely be significantly less costly than automated cutters, but it would be more difficult to obtain particles of smaller sizes.

CHAPTER 5

GENERAL CONCLUSION

5.1 REVIEW OF THE OBJECTIVES

Primarily, this research set out to develop an efficient method for the production of exfoliating microbeads from brewer's spent grain (BSG) (Objective 1). As a second objective, we aimed to valorize whole raw, undried BSG in this application, minimizing the generation of process-specific co-products (Objective 2). We envisioned a new application for BSG as a feedstock in the production of exfoliating microbeads for personal hygiene products, which have conventionally been made from petrochemical polymers associated with environmental pollution and negative effects on marine life. Through the development of a biodegradable alternative to a class of petrochemical primary microplastics using undervalued biowaste, these objectives have a strong underlying theme of environmental conscientiousness. We reinforced this motif by respecting the other principles of Green chemistry throughout the project's elaboration (Objective 3). The guiding objectives of this work are outlined in greater detail in section 1.4.

This work ended up yielding two distinct protocols: the first describes the valorization of BSG in the production of biodegradable, spherical microbeads (Chapter 2) while the second focuses on the one-pot pretreatment and complete solubilization of spent grains (Chapter 3). The first method sacrifices the complete valorization of the grain in the name of obtaining homogenous batches of exfoliating microbeads that meet industry requirements for such materials. A fraction of the pretreated grain (52.5%) is used in the production of the beads; we produce lignin degradation product- (LDP) and sugar-rich acid hydrolysate as a by-product. By fractionating the biomass, we can produce BSG-based microbeads that are highly stable in sample personal hygiene product matrices and provide

improved cleansing efficiencies compared to two types of commercially-available physical exfoliants. Consequently, although we meet Objective 1, the components of Objectives 2 and 3 that refer to complete BSG valorization and minimizing process-specific co-products are not respected.

On the other hand, the second method (Chapter 3) solubilizes and uses the entirety of the undried grain in the production of materials that may be used as physical exfoliating agents in personal hygiene products, but whose dimensions are not as spherical or uniform. These results respect Objectives 2 and 3 by valorizing the entirety of the grain through a process that respects the principles of Green Chemistry and avoids generating any process-specific co-products. This method also meets Objective 1 by demonstrating that the BSG solutions can be used to produce BSG-based particles. Despite deviating from ideal microbead dimensions, these particles proved to be stable in personal hygiene products, with similar or improved cleansing efficiencies when compared to soaps containing other types of physical exfoliant.

However, it remained clear that the microbeads produced according to the first method exhibited superior mechanical properties to the particles produced according to the second. This serves to demonstrate how the two methods are complementary yet distinct in their potential applications and to justify the compromise made between unique aspects of the objectives defined at the beginning of this work.

5.2 FUTURE WORK

Method 1 (Chapter 2) notably leaves room for improvement in terms of the valorization of the acid hydrolysate obtained as a co-product in microbead production. By investigating a cascade valorization strategy, both solid and liquid fractions could serve in high added-value applications. Several previous studies have investigated the dilute acid hydrolysis of BSG with other final applications in mind. With these methods, the pretreated solids are disposed of as waste, while the acid hydrolysate serves in the production of second-generation biofuels, natural sugar alcohols, or other platform chemicals.^{27, 35, 39, 45} Basic HPLC analysis of the acid hydrolysate obtained in our method showed, at minimum, the presence of LDPs that may serve in the synthesis of valuable chemicals.

Otherwise, based on what we know of BSG's composition before and after pretreatment, the hydrolysate contains elements that are useful for soil remediation or in improving agricultural crop quality. Just as raw BSG or compost derived from BSG may be used as a fertilizer,^{12, 26} further research may reveal that the hydrolysate could be neutralized and equally used as such. Moreover, as the pH of the dilute acid used in the hydrolysis pretreatment is more important than the nature of the acid itself, HCl could theoretically be swapped for nitrogen-containing HNO₃, as nitric and hydrochloric acids completely dissociate in aqueous solutions (no pK_a). An HNO₃-based hydrolysate could be neutralized with nitrogen-containing ammonia, providing a sugar-rich solution of ammonium nitrate that could potentially be used as an even more potent fertilizer. At the very least, future research could investigate if the acid hydrolysate's pH could be readjusted with fresh acid to realize several subsequent pretreatment cycles, improving the method's sustainability and profitability. This work could help reinforce the second and third objectives regarding the first method.

Besides exploring a cascade valorization approach regarding the method described in Chapter 2, I hope that further work will continue the microbead production scale-up that I began as a part of this project (Chapter 4.1). Using automated or semi-automated

equipment, larger volumes of BSG will be able to be solubilized, allowing to produce greater quantities of microbeads in shorter periods. Furthermore, automated techniques for microbead production will provide greater control over the beads' dimensions. They will be able to be made bigger or smaller, depending on if they are to be incorporated into soaps to be used on the body (mean diameter of 419 μm) or the face (mean diameter of 197 μm).⁶² Automation will also help ensure uniform batches, which provides reliable product performance and an aesthetic value that consumers have been accustomed to with conventional plastic precedents. Pushing the technoeconomic assessment out of the theoretical will also provide a better sense of the method's profitability compared to those used in the production of other exfoliating particles (Chapter 4.2). All of this will help to eventually commercialize BSG microbeads for use in personal hygiene products.

The research presented in Chapter 3 (Method 2) could be furthered by investigating the use of the BSG solutions in the production of other types of materials. Future research could look into using solutions obtained from whole, raw BSG to produce high-texture paper products (i.e., napkins, cardboard), wood products (i.e., particleboard or fiberboard), or composite materials (mixed with conventional or bio-based plastics). Alternatively, BSG-derived pulps may potentially replace a fraction of purified cellulose commonly used in the manufacture of these products. If BSG solutions demonstrated similar or improved performance in these applications, they may be able to relieve some of the burdens on the forestry industry, which currently supplies necessary feedstocks. This would also provide a new objective, potentially replacing Objective 1 regarding the production of uniform, spherical microbeads that this protocol failed to fully meet. Other future research could look into extending the method to the one-pot solubilization of other agri-food wastes, especially other cereal wastes of similar molecular composition.

Both methods will benefit from more long-term stability testing, ensuring the BSG microbeads and particles maintain their stabilities in various matrices over a minimum of a year. Furthermore, although other data presented herein indicate the biodegradability of the materials, evaluating the samples according to OECD Test No. 301 (Ready

Biodegradability)²⁰⁵ or No. 306 (Biodegradability in Seawater)²⁰⁶ would irrefutably affirm or contradict these arguments (Objective 3, design for degradation). While there are many OECD-normalized tests for evaluating biodegradability, Test No. 301 looks at a material's decomposition over a relatively short period (faster biodegradability indicates reduced environmental impacts) and Test No. 306 best imitates the expected end-of-life conditions of our BSG-based exfoliants. When applying either of these protocols, the theoretical Biochemical Oxygen Demand (BOD) of the materials would need to be determined beforehand.

5.3 FINAL REMARKS

By realizing the goals this project set out to accomplish, this research makes a few notable contributions to the scientific understanding of BSG and its possible applications. The production of exfoliating microbeads from this biomass is a novel and innovative application whose commercialization I anticipate in the coming years. This will help relieve the environmental burden of conventional plastic microbeads in personal hygiene products, and/or the use of purified molecules from coveted biomass in the production of biodegradable alternatives. The realization of the complete solubilization of raw, undried BSG is equally exciting, especially given the little pre-existing knowledge surrounding one-pot processes for its transformation. I hope that with this original contribution to the field, future research will demonstrate the ability to produce a wide variety of fibrous, polymeric, or composite materials from whole BSG solutions, extending far beyond physical exfoliants in personal hygiene products.

BIBLIOGRAPHY

1. Colen, L., & Swinnen, J. (2015). Economic Growth, Globalisation and Beer Consumption. *Journal of Agricultural Economics*, 67(1), 186-207. doi:10.1111/1477-9552.12128
2. Kirin Holdings Company. (2022). *Beer Consumption by Country (Year)*. Retrieved from Tokyo: https://www.kirinholdings.com/en/newsroom/release/2022/0127_04.html
3. Ritchie, H., & Roser, M. (2018, 2022). Alcohol Consumption. Retrieved from <https://ourworldindata.org/alcohol-consumption>
4. The Earth Observatory. (2001). Niagara Falls. Retrieved from <https://earthobservatory.nasa.gov/images/1437/niagara-falls>
5. Cabras, I., & Higgins, D. M. (2016). Beer, brewing, and business history. *Business History*, 58(5), 609-624. doi:10.1080/00076791.2015.1122713
6. Sewell, S. L. (2014). The Spatial Diffusion of Beer from its Sumerian Origins to Today. In M. Patterson & N. Hoalst-Pullen (Eds.), *The Geography of Beer: Regions, Environment, and Societies* (pp. 212). Dordrecht: Springer Science & Business Media.
7. Araus, J. L., Ferrio, J. P., Voltas, J., Aguilera, M., & Buxo, R. (2014). Agronomic conditions and crop evolution in ancient Near East agriculture. *Nature Communications*, 5. doi:10.1038/ncomms4953
8. Guido, L. F., & Moreira, M. M. (2013). Malting. In R. Guiné & P. Correia (Eds.), *Engineering Aspects of Cereal and Cereal-Based Products* (pp. 51-70). Florida: CRC Press.
9. Aubert, M. K., Coventry, S., Shirley, N. J., Betts, N. S., Würschum, T., Burton, R. A., & Tucker, M. R. (2018). Differences in hydrolytic enzyme activity accompany natural variation in mature aleurone morphology in barley (*Hordeum vulgare* L.). *Scientific Reports*, 8, 11025. doi:10.1038/s41598-018-29068-4
10. Yahya, H., Linforth, R. S. T., & Cook, D. J. (2014). Flavour generation during commercial barley and malt roasting operations: a time course study. *Journal of Food Chemistry*, 145, 378-387. doi:10.1016/j.foodchem.2013.08.046
11. Capece, A., Rossana, R., Gabriella, S., & Patrizia, R. (2018). Conventional and non-conventional yeasts in beer production. *Fermentation*, 4(2). doi:10.3390/fermentation4020038
12. Mussatto, S. (2014). Brewer's spent grain: a valuable feedstock for industrial applications. *Journal of the Science of Food and Agriculture*, 94, 1264-1275. doi:10.1002/Jsfa.6486
13. Lynch, K. M., Steffen, E. J., & Arendt, E. K. (2016). Brewer's spent grain: a review with an emphasis on food and health. *Journal of the Institute of Brewing*, 122(4), 553-568. doi:10.1002/jib.363

14. Macneil, P., & Bellamy, M. (2006). Brewing Industry in Canada. In B. Graves (Ed.), *The Canadian Encyclopedia*. Toronto: Historica Canada.
15. Association des Brasseurs du Québec. (2022). Les membres. Retrieved from <https://brasseurs.qc.ca/membres/>
16. Eberts, D. (2014). Neolocalism and the branding and marketing of place by Canadian microbreweries. In M. Patterson & N. Hoalst-Pullen (Eds.), *The Geography of Beer: Regions, Environment, and Societies* (Vol. 9789400777873, pp. 189-199). Dordrecht: Springer Science & Business Media.
17. Weersink, A., Probyn-Smith, K., & Von Massow, M. (2017). The Canadian craft beer sector. In C. Garavaglia & J. Swinnen (Eds.), *Economic Perspectives on Craft Beer: A Revolution In the Global Beer Industry* (pp. 89-113). London: Palgrave Macmillan Cham.
18. Labelle, V. (2018). *Mise en valeur des drêches de microbrasserie et outil d'aide à la décision pour les spécialistes en environnement*. (Maîtrise en environnement). Université de Sherbrooke, Sherbrooke.
19. Montembeault, M. (2022, June 14). 80 % des drêches des brasseries Molson-Coors et Labatt exportées aux États-Unis. *Radio-Canada*.
20. Association des Microbrasseries du Québec. (2022). Statistiques. Retrieved from <https://ambq.ca/fr/quebec-1>
21. Québec residual materials management policy, 35.1 C.F.R. (2011).
22. Aliyu, S., & Bala, M. (2011). Brewer's spent grain: A review of its potentials and applications. *African Journal of Biotechnology*, 10(3), 324-331. doi:10.5897/AJBx10.006
23. Mussatto, S., Dragone, G., & Roberto, I. C. (2006). Brewer's spent grain: generation, characteristics and potential applications. *Journal of Cereal Science*, 43(1), 1-14. doi:10.1016/j.jcs.2005.06.001
24. Filipowska, W., Jaskula-Goiris, B., Ditych, M., Bustillo Trueba, P., De Rouck, G., Aerts, G., Powell, C., Cook, D., & De Cooman, L. (2021). On the constitution of malt quality and the malting process to the formation of beer staling aldehydes: a review. *Institute of Brewing*, 127(2). doi:10.1002/jib.644
25. Mussatto, S. (2009). Biotechnological Potential of Brewing Industry By-Products. In P. Singh & P. A. (Eds.), *Biotechnology for Agro-Industrial Residues Utilization* (pp. 313-326). Dordrecht: Springer.
26. Bachmann, S. A. L., Calvete, T., & Féris, L. A. (2022). Potential applications of brewery spent grain: Critical an overview. *Journal of Environmental Chemical Engineering*, 10(1). doi:10.1016/j.jece.2021.106951
27. Mussatto, S., & Roberto, I. C. (2005). Acid hydrolysis and fermentation of brewer's spent grain to produce xylitol. *Journal of the Science of Food and Agriculture*, 85, 2453-2460. doi:10.1002/jsfa.2276
28. Moriel, P. (2014). Wet brewers grains an option for beef heifers. *Feedstuffs*, 86(47).
29. Shen, Y., Abeynayake, R., Sun, X., Ran, T., Li, J., Chen, L., & Yang, W. (2019). Feed nutritional value of brewer's spent grain residue resulting from protease aided protein removal. *Journal of Animal Science and Biotechnology*, 10(78). doi:10.1186/s40104-019-0382-1

30. Buffington, J. (2014). The Economic Potential of Brewer's Spent Grain (BSG) as a Biomass Feedstock. *Advances in Chemical Engineering and Science*, 4(3), 308-318. doi:10.4236/aces.2014.43034
31. Northcott, A. (2020, December 25). Turning beer into bread, a Montreal co-op takes on food waste. *CBC News*. Retrieved from <https://www.cbc.ca/news/canada/montreal/belle-gueule-beer-bread-1.5835898>
32. Viens, M.-C. (2021, March 10) *Les craquelins Malterre font leur entrée sur le marché Louperivois/Interviewer: M. Rivard*. Même fréquence, Radio-Canada, Montreal.
33. Madsen, S. K., Thulsen, E. T., & Mohammadifar, M. A. (2021). Development of a yoghurt alternative, based on plant-adapted lactic acid bacteria, soy drink and the liquid fraction of brewer's spent grain. *FEMS Microbiology Letters*, 368(15). doi:10.1093/femsle/fnab093
34. Take Two Foods. (2022). Barley is Better. *Take Two*. Retrieved from <https://taketwofoods.com/>
35. Rojas-Chamorro, J. A., Romero, I., Lopez-Linares, J. C., & Castro, E. (2020). Brewer's spent grain as a course of renewable fuel through optimized dilute acid pretreatment. *Renewable Energy*, 148, 81-90. doi:10.1016/j.renene.2019.12.030
36. Nkeumaleu, A. T., Benetti, D., Haddadou, I. D. M., M., Ouellet-Plamondon, C. M., & Rosei, F. (2022). Brewery spent grain derived carbon dots for metal sensing. *RSC Advances*, 12, 11621-11627. doi:10.1039/D2RA00048B
37. Lorente, A., Remon, J., Budarin, V., Sanchez-Verdu, P., Moreno, A., & Clark, J. H. (2019). Analysis and optimization of a novel "bio-brewery" approach: Production of bio-fuels and bio-chemicals by microwave-assisted, hydrothermal liquefaction of brewers' spent grains. *Energy Conversion and Management*, 185, 410-430. doi:10.1016/j.enconman.2019.01.111
38. Guarda, E. C., Oliveira, A. C., Antunes, S., Freitas, F., Castro, P. M. L., Duque, A. F., & Reis, M. A. M. (2021). A Two-Stage Process for Conversion of Brewer's Spent Grain into Volatile Fatty Acids through Acidogenic Fermentation. *Applied Sciences*, 11, 3222-3238. doi:10.3390/app11073222
39. Bonifacio-Lopes, T., Teixeira, J. A., & Pintado, M. (2019). Current extraction techniques towards bioactive compounds from brewer's spent grain - A review. *Critical Reviews in Food Science and Nutrition*. doi:10.1080/10408398.2019.1655632
40. Ishiwaki, N., Murayama, H., Awayama, H., Kanauchi, O., & Sato, T. (2000). Development of high value uses of spent grain by fractionation technology. *Technical Quarterly - Master Brewers Association of America*, 37, 261-265.
41. Deshwal, G. K. P., N.R., & Alam, T. (2019). An overview of paper and paper based food packaging materials: health safety and environmental concerns. *Journal of Food Science and Technology*, 56(10). doi:10.1007/s13197-019-03950-z
42. Wool, R. P., & Sun, X. S. (2005). *Bio-Based Polymers and Composites*. Cambridge: Academic Press.
43. Mishra, P. K., Gregor, T., & Wimmer, R. (2017). Utilising Brewer's Spent Grain as a Source of Cellulose Nanofibres Following Separation of Protein-based Biomass. *BioResources*, 12(1), 107-116. doi:10.15376/biores.12.1.107-116

44. Matebie, B. Y., Tizazu, B. Z., Kadhem, A. A., & Prabhu, S. V. (2021). Synthesis of Cellulose Nanocrystals (CNCs) from Brewer's Spent Grain Using Acid Hydrolysis: Characterization and Optimization. *Journal of Nanomaterials*, 2021, 7133154. doi:10.1155/2021/7133154
45. Liu, Y., Nie, Y., Lu, X., Zhang, X., He, H., Pan, F., Zhou, L., Liu, X., Ji, X.-J., & Zhang, S. (2019). Cascade utilization of lignocellulosic biomass to high-value products. *Green Chemistry*, 21, 3499-3535. doi:10.1039/c9gc00473d
46. Ritter, S. K. (2008). Lignocellulose: A Complex Biomaterial. *Chemical & Engineering News*, 86(49).
47. Robertson, J. A., Castro-Marinhas, L., Collins, S. R. A., Faulds, C. B., & Waldron, K. W. (2011). Enzymatic and Chemical Treatment Limits on the Controlled Solubilization of Brewer's Spent Grain. *Journal of Agricultural and Food Chemistry*, 59, 11019-11025. doi:10.1021/jf202814j
48. Thakur, M., Sharma, A., Chandel, M., & Pathania, D. (2021). Modern applications and current status of green nanotechnology in environmental industry. In U. H. Shanker, C.M. & M. Rani (Eds.), *Micro and Nano Technologies* (Vol. Green Functionalized Nanomaterials for Environmental Applications). Amsterdam: Elsevier.
49. Ibrahim, N. I., Shahar, F. S., Sultan, M. T. H., Shah, A. U. M., Safri, S. N. A., & Mat Yazik, M. H. (2021). Overview of Bioplastic Introduction and Its Applications in Product Packaging. *Coatings*, 11. doi:10.3390/coatings11111423
50. Kupikowska-Stobba, B., & Lewinska, D. (2020). Polymer microcapsules and microbeads as cell carriers for *in vivo* biomedical applications. *Biomaterials Science*, 8, 1536-1574. doi:10.1039/c9bm01337g
51. Nam, H. C., & Park, W. H. (2019). Eco-friendly poly(lactic acid) microbeads for cosmetics via melt electrospraying. *International Journal of Biological Macromolecules*, 157, 734-742. doi:10.1016/j.ijbiomac.2019.11.240
52. Mostafa, N. A., Farag, A. A., Abo-dief, H. M., & Tayeb, A. M. (2018). Production of biodegradable plastic from agricultural wastes. *Arabian Journal of Chemistry*, 11(4), 546-553.
53. Thielen, M. (2014). *Bioplastics: Plants and crops, raw materials, products*. Gülzow-Prüzen: Federal Republic of Germany
54. Cotton Incorporated. (2022). Cotton Morphology and Chemistry. *Cotton for Nonwovens Technical Guide*. Retrieved from [https://www.cottoninc.com/quality-products/nonwovens/cotton-fiber-tech-guide/cotton-morphology-and-chemistry/#:~:text=After%20scouring%20and%20bleaching%2C%20cotton,of%20water%20\(glycoside%20bonds\)](https://www.cottoninc.com/quality-products/nonwovens/cotton-fiber-tech-guide/cotton-morphology-and-chemistry/#:~:text=After%20scouring%20and%20bleaching%2C%20cotton,of%20water%20(glycoside%20bonds).).
55. Mülhaupt, R. (2013). Green Polymer Chemistry and Bio-based Plastics: Dreams and Reality. *Macromolecular Chemistry and Physics*, 214, 159-174. doi:10.1001/macp.201200439
56. Agarwal, S. (2020). Biodegradable Polymers: Present Opportunities and Challenges in Providing a Microplastic-Free Environment. *Macromolecular Chemistry and Physics*, 221. doi:10.1002/macp.202000017
57. Rhodes, C. J. (2018). Plastic pollution and potential solutions. *Science Progress*, 101(3), 207-260. doi:10.3184/003685018X15294876706211

58. Rhodes, C. J. (2019). Solving the plastic problem: From cradle to grave, to reincarnation. *Science Progress*, 102(3), 218-248. doi:10.1177/0036850419867204
59. Hoang, T. C., & Felix-Kim, M. (2020). Microplastic consumption and excretion by fathead minnows (*Pimephales promelas*): Influence of particles size and body shape of fish. *Science of the Total Environment*, 704. doi:10.1016/j.scitotenv.2019.135433
60. Geyer, R., Jambeck, J. R., & Law, K. L. (2017). Production, use, and fate of all plastics ever made. *Science Advances*, 3(7). doi:10.1126/sciadv.1700782
61. Leslie, H. A., van Velzen, M. J. M., Brandsma, S. H., Vethaak, A. D., Garcia-Vallejo, J. J., & Lamoree, M. H. (2022). Discovery and quantification of plastic particle pollution in human blood. *Environment International*, 163. doi:10.1016/j.envint.2022.107199
62. Sun, Q., Ren, S.-Y., & Ni, H.-G. (2020). Incidence of microplastics in personal care products: An appreciable part of plastic pollution. *Science of the Total Environment*, 742. doi:10.1016/j.scitotenv.2020.140218
63. Bayo, J., Rojo, D., & Olmos, S. (2019). Abundance, morphology and chemical composition of microplastics in sand and sediments from a protected coastal area: The Mar Menor lagoon (SE Spain). *Environmental Pollution*, 252, 1357-1366. doi:10.1016/j.envpol.2019.06.024
64. King, C. A., Shamshine, J. L., Zavgorodnya, O., Cutfield, T., Block, L. E., & Rogers, R. D. (2017). Porous Chitin Microbeads for More Sustainable Cosmetics. *ACS Sustainable Chemistry & Engineering*, 5, 11660-11667. doi:10.1021/acssuschemeng.7b03053
65. Nam, H. C., & Park, W. H. (2020). Aliphatic Polyester-Based Biodegradable Microbeads for Sustainable Cosmetics. *ACS Biomaterials Science & Engineering*, 6, 2440-2449. doi:10.1021/acsbmaterials.0c00017
66. Prata, J. C., Silva, A. L. P., Costa, J. P. d., Mouneyrac, C., Walker, T. R., Duarte, A. C., & Rocha-Santos, T. (2019). Solutions and Integrated Strategies for the Control and Mitigation of Plastic and Microplastic Pollution. *International Journal of Environmental Research and Public Health*, 16. doi:10.3390/ijerph16132411
67. Decker, A., & Graber, E. M. (2012). Over-the-counter Acne Treatments. *The Journal of Clinical and Aesthetic Dermatology*, 5(5), 32-40.
68. Draelos, Z. D. (2017). Astringents, masks, and ancillary skin care products. In R. Baran & H. Maibach (Eds.), *Textbook of Cosmetic Dermatology* (4 ed., pp. 192-195). New York: Informa Healthcare.
69. Li, J., Qu, X., Su, L., Zhang, W., Yang, D., Kolandhasamy, P., Li, D., & Shi, H. (2016). Microplastics in mussels along the coastal waters of China. *Environmental Pollution*, 214, 177-184. doi:10.1016/j.envpol.2016.04.012
70. Iyare, P. U., Ouki, S. K., & Bond, T. (2020). Microplastics Removal in Wastewater Treatment Plants: A Critical Review. *Environmental Science: Water Research & Technology*, 6, 2664-2675. doi:10.1039/D0EW00397B
71. Wang, X., Bolan, N., Tsang, D. C. W., Sarkar, B., Bradney, L., & Li, Y. (2021). A review of microplastics aggregation in aquatic environment: Influence factors, analytical methods, and environmental implications. *Journal of Hazardous Materials*, 402. doi:10.1016/j.jhazmat.2020.123496

72. Scudo, A., Liebmann, B., Corden, C., Tyrer, D., Kreissig, J., & Warwick, O. (2017). *Intentionally added microplastics in products*. Retrieved from London: <https://ec.europa.eu/environment/chemicals/reach/pdf/39168%20Intentionally%20added%20microplastics%20-%20Final%20report%2020171020.pdf>
73. Government of Canada. (2018). *Microbeads*. Health Canada: Government of Canada Retrieved from <https://www.canada.ca/en/health-canada/services/chemical-substances/other-chemical-substances-interest/microbeads.html>
74. Habib, R. Z., Salim Abdoon, M. M., Al Megbaali, R. M., Ghebremedhin, F., Elkashlan, M., Kittaneh, W. F., Cherupurakal, N., Mourad, A.-H. I., Thiemann, T., & Al Kindi, R. (2020). Analysis of microbeads in cosmetic products in the United Arab Emirates. *Environmental Pollution*, 258, 113831. doi:10.1016/j.envpol.2019.113831
75. Baek, S., Moon, S.-K., Kang, R., Ah, Y., Kim, H., & Choi, S.-W. (2018). One-Step Fabrication of Uniform Biodegradable Microbeads with Unimodal and Bimodal Porous Structures Using Spontaneous Microphase Separation. *Macromolecular Materials and Engineering*, 303. doi:10.1002/mame.201800139
76. Munoz-Bonilla, A., Echeverria, C., Sonseca, A., Arrieta, M. P., & Fernandez-Garcia, M. (2019). Bio-Based Polymers with Antimicrobial Properties towards Sustainable Development. *Materials*, 12, 641-691. doi:10.3390/ma12040641
77. Green, D. S., Boots, B., Sigwart, J., Jiang, S., & Rocha, C. (2016). Effects of conventional and biodegradable microplastics on a marine ecosystem engineer and sediment nutrient cycling. *Environmental Pollution*, 208, 426-434. doi:10.1016/j.envpol.2015.10.010
78. Elieh-Ali-Komi, D., & Hamblin, M. (2016). Chitin and Chitosan: Production and Application of Versatile Biomedical Nanomaterials. *International Journal of Advanced Research*, 4(3), 411-427.
79. Govindasamy, S., Syafiq, I. M., Amirul, A. A., Amin, R. M., & Bhubalan, K. (2019). Dataset on controlled production of polyhydroxyalkanoate-based microbead using double emulsion solvent evaporation technique. *Data in Brief*, 23, 103675. doi:10.1016/j.dib.2019.01.023
80. OBrien, J. C., Torrente-Murciano, L., Mattia, D., & Scott, J. L. (2017). Continuous Production of Cellulose Microbeads via Membrane Emulsification. *ACS Sustainable Chemistry & Engineering*, 5, 5931-5939. doi:10.1021/acssuschemeng.7b00662
81. Sescousse, R., & Budtova, T. (2009). Influence of processing parameters on regeneration kinetics and morphology of porous cellulose from cellulose-NaOH-water solutions. *Cellulose*, 16, 417-426. doi:10.1007/s10570-009-9287-z
82. Rosenberg, P., Rom, M., Janicki, J., & Fardim, P. (2008). New Cellulose Beads from Biocelsol Solution. *Cellulose Chemistry and Technology*, 42(7-8), 293-305.
83. Jha, A. K., & Bhattacharya, A. (2009). Preparation and evaluation of sweet potato starch-blended sodium alginate microbeads. *Asian Journal of Pharmaceutics*(4), 299-303. doi:10.4103/0973-8398.59955
84. Kozłowska, J., Prus, W., & Stachowiak, N. (2019). Microparticles based on natural and synthetic polymers for cosmetic applications. *International Journal of Biological Macromolecules*, 129, 952-956. doi:10.1016/j.ihbiomac.2019.02.091

85. Ju, S., Shin, G., Lee, M., Koo, J. M., Jeon, H., Ok, Y. S., Hwang, D. S., Hwang, S. Y., Oh, D. X., & Park, J. (2021). Biodegradable chito-beads replacing non-biodegradable microplastics for cosmetics. *Green Chemistry*, 23, 6953-6965. doi:10.1039/d1gc01588e
86. Gericke, M., Trygg, J., & Fardim, P. (2013). Functional Cellulose Beads: Preparation, Characterization, and Applications. *Chemical Reviews*, 113, 4812-4836. doi:10.1021/cr300242j
87. Statista. (2022). Market value for natural and organic beauty worldwide 2018-2027. In *Consumer Goods & FMCG* (Feb 2, 2022 ed.). Hamburg: Statista Research Department.
88. Mohamed, S. M. K., Ganesan, K., Milow, B., & Ratke, L. (2015). The effect of zinc oxide (ZnO) addition on the physical and morphological properties of cellulose aerogel beads. *Royal Society of Chemistry Advances*, 5. doi:10.1039/c5ra17366c
89. Gabov, K., Oja, T., Deguchi, T., Fallarero, A., & Fardim, P. (2016). Preparation, characterization and antimicrobial application of hybrid cellulose-lignin beads. *Cellulose*, 24(2), 641-658. doi:10.1007_s10570-016-1172-y
90. Anastas, P. T., & Warner, J. C. (1998). *Green Chemistry: Theory and Practice*. New York: Oxford University Press.
91. Budtova, T., & Navard, P. (2016). Cellulose in NaOH-water based solvents: a review. *Cellulose, Springer Verlag*, 23(1), 5-55. doi:10.1007/s10570-015-0779-8
92. Damay, J., Duret, X., Ghislain, T., Lalonde, O., & Lavoie, J.-M. (2018). Steam explosion of sweet sorghum stems: Optimisation of the production of sugars by response surface methodology combined with the severity factor. *Industrial Crops and Products*, 111, 482-493. doi:10.1016/j.indcrop.2017.11.006
93. Yang, D., Gao, T., & Mao, Z. (2019). Study on the Nitric Acid Pulping, Delignification Course, and Waste-Liquid Recovery. *BioResources*, 14(4), 8892-8903.
94. Mussatto, S., Rocha, G. J. M., & Roberto, I. C. (2008). Hydrogen peroxide bleaching of cellulose pulps obtained from brewer's spent grain. *Cellulose*, 15, 641-649. doi:10.1007/s10570-008-9198-4
95. Väisänen, S., Kosonen, H., Ristolainen, M., & Vuorinen, T. (2021). Cellulose dissolution in aqueous NaOH-ZnO: effect of pulp pretreatment at macro and molecular levels. *Cellulose*, 28, 4385-4396. doi:10.1007/s10570-021-03779-w
96. Trygg, J., & Fardim, P. (2011). Enhancement of cellulose dissolution in water-based solvent via ethanol-hydrochloric acid pretreatment. *Cellulose*, 18. doi:10.1007/s10570-011-9550-y
97. Trygg, J., Fardim, P., Gericke, M., Mäkilä, E., & Salonen, J. (2013). Physicochemical design of the morphology and ultrastructure of cellulose beads. *Carbohydrate Polymers*, 93, 291-299. doi:10.1016/j.carbpol.2012.03.085
98. Nadiruzzahra, S., & Tristantini, D. (2020). Cellulose acetate from oil palm empty fruit bunches waste as biodegradable microbeads for making scrubs. *AIP Conference Proceedings*, 2223(1).
99. Park, S., Oh, Y., Yun, J., Yoo, E., Jung, D., Oh, K. K., & Lee, S. H. (2020). Cellulose/biopolymer/Fe₃O₄ hydrogel microbeads for dye and adsorption. *Cellulose*, 27(5), 2757-2773. doi:10.1007/s10570-020-02974-5

- 100.Scott, J. L., & Edler, K. (2017). Biodegradable Microbeads and Microspheres. Retrieved from <https://researchportal.bath.ac.uk/en/projects/biodegradable-microbeads-and-microspheres-2/datasets/>
- 101.Singh, P., Duarte, H., Alves, L., Antunes, F., Le Moigne, N., Dormanns, J., Duchemin, B., Staiger, M. P., & Medronho, B. (2015). From Cellulose Dissolution and Regeneration to Added Value Applications - Synergism Between Molecular Understanding and Material Development. In M. Poletto & H. L. O. Junior (Eds.), *Cellulose - Fundamental Aspects and Current Trends*: IntechOpen.
- 102.Zhang, J., Wu, J., Yu, J., Zhang, X., He, J., & Zhang, J. (2017). Application of ionic liquids for dissolving cellulose and fabricating cellulose-based materials: state of the art and future trends. *Materials Chemistry Frontiers*, *1*, 1273-1290. doi:10.1039/c6qm00348f
- 103.Sobue, H., Kiessig, H., & Hess, K. (1939). The cellulose-sodium hydroxide-water system as a function of the temperature. *Z Physik Chem B*, *43*, 309-328.
- 104.Wang, Y. (2008). *Cellulose Fiber Dissolution in Sodium Hydroxide Solution at Low Temperature: Dissolution Kinetics and Solubility Improvement*. (PhD). Georgia Institute of Technology, Atlanta, Georgia.
- 105.Zhou, J., & Zhang, L. (2000). Solubility of Cellulose in NaOH/Urea Aqueous Solution. *Polymer Journal*, *32*(10), 866-870. doi:10.1295/polymj.32.866
- 106.Zhang, L., Ruan, D., & Gao, S. (2002). Dissolution and Regeneration of Cellulose in NaOH/Thiourea Aqueous Solution. *Journal of Polymer Science*, *40*, 1521-1529. doi:10.1002/polb.10215
- 107.Hu, G., Fu, S., & Liu, H. (2013). Hemicellulose in pulp affects paper properties and printability. *Appita*, *66*(2), 139-144.
- 108.Bajpai, P. (2018). Wood and Fiber Fundamentals. In P. Bajpai (Ed.), *Biermann's Handbook of Pulp and Paper* (Third ed.). Amsterdam: Elsevier.
- 109.Xu, H., Huang, L., Xu, M., Qi, M., Mo, Q., Zhao, H., Huang, C., Wang, S., & Liu, Y. (2020). Preparation and Properties of Cellulose-Based Films Regenerated from Waste Corrugated Cardboards Using [Amim]Cl/CaCl₂. *ACS Omega*, *5*(37), 23743-23754. doi:10.1021/acsomega.0c02713
- 110.Woo, H. L., & Hazen, T. C. (2018). Enrichment of Bacteria From Eastern Mediterranean Sea Involved in Lignin Degradation via the Phenylacetyl-CoA Pathway. *Frontiers in Microbiology*, *9*. doi:10.3389/fmicb.2018.00922
- 111.Grethelin, H. E. (1985). The effect of pore size distribution on the enzymatic hydrolysis of cellulosic substrates. *Bio/Technology*, *3*(2), 155-160. doi:10.1038/nbt0285-155
- 112.Jackson, M. G. (1977). Review article: The alkali treatment of straws. *Animal Feed Science and Technology*, *2*(2), 105-130. doi:10.1016/0377-8401(77)90013-X
- 113.Ma, X., Zheng, X., Yang, H., Wu, H., Cao, S., Chen, L., & Huang, L. (2016). A perspective on lignin effects on hemicelluloses dissolution for bamboo pretreatment. *Industrial Crops and Products*, *94*, 117-121. doi:10.1016/j.indcrop.2016.08.025
- 114.Ladisich, M. R., Lin, K. W., Voloch, M., & Tsao, G. T. (1983). Process considerations in the enzymatic hydrolysis of biomass. *Enzyme and Microbial Technology*, *5*(2), 82-102. doi:10.1016/0141-0229(83)90042-X

115. Sawada, T., Nakamura, Y., Kobayashi, F., Kuwahara, M., & Watanabe, T. (1995). Effects of fungal pretreatment and steam explosion pretreatment on enzymatic saccharification of plant biomass. *Biotechnology and Bioengineering*, *48*(6), 719-724. doi:10.1002/bit.260480621
116. Comunian, T. A., & Favaro-Trindade, C. S. (2016). Microencapsulation using biopolymers as an alternative to produce food enhanced with phytosterols and omega-3 fatty acids: A review. *Food Hydrocolloids*, *61*, 442-457. doi:10.1016/j.foodhyd.2016.06.003
117. Nguyen, T. T. U., Zuratul, A. A. H., Nguyen, X. T. T., & Nurasreena, A. (2020). Fabrication of alginate microspheres for drug delivery: A review. *International Journal of Biological Macromolecules*, *153*, 1035-1046. doi:10.1016/j.ijbiomac.2019.10.233
118. Moreno-Castilla, C. (2016). Colloidal and micro-carbon spheres derived from low-temperature polymerization reactions. *Advances in Colloid and Interface Science*, *236*, 113-141. doi:10.1016/j.cis.2016.08.003
119. Cheng, H., Yin, Y., Wang, B., Zhu, J., & Wang, C. (2021). Facile fabrication of highly conductive poly(styrene-co-methacrylic acid)/ poly(aniline) microspheres based on surface carboxylation modification. *Journal of Applied Polymer Science*. doi:10.1002/app.50190
120. Ge, X., Zhao, H., Chen, J., Xu, J., & Luo, G. (2016). Microfluidic technology for multiphase emulsions morphology adjustment and functional materials preparation. *Chinese Journal of Chemical Engineering*, *24*, 677-692. doi:10.1016/j.cjche.2016.02.009
121. Tapia-Hernandez, J. A., Torres-Chavez, P. I., Ramirez-Wong, B., Rascon-Chu, A., Plascencia-Jatomea, M., Barreras-Urbina, C. G., Rangel-Vazquez, N. A., & Rodriguez-Felix, F. (2015). Micro- and Nanoparticles by Electrospray: Advances and Applications in Foods. *Journal of Agricultural and Food Chemistry*, *63*, 4699-4707. doi:10.1021/acs.jafc.5b01403
122. Paraskevopoulou, P., Chriti, D., Raptopoulos, G., & Anyfantis, G. C. (2019). Synthetic Polymer Aerogels in Particulate Form. *Materials*, *12*, 1543. doi:10.3390/ma12091543
123. Timilsena, Y. P., Akanbi, T. O., Khald, N., Adhikari, B., & Barrow, C. J. (2019). Complex coacervation: Principles, mechanisms and applications in microencapsulation. *International Journal of Biological Macromolecules*, *121*, 1276-1286. doi:10.1016/j.ijbiomac.2018.10.144
124. Perrier, E., & Hart, J. (2005). Smart Vectorization. In M. R. Rosen (Ed.), *Delivery System Handbook for Personal Care and Cosmetic Products*. Norwich, New York: William Andrew Inc.
125. Petrusic, S., & Koncar, V. (2016). Controlled release of active agents from microcapsules embedded in textile structures. In V. Koncar (Ed.), *Smart Textiles and Their Applications*. Amsterdam: Elsevier.
126. Bock, N., Dargaville, T. R., & Woodruff, M. A. (2012). Electrospraying of polymers with therapeutic molecules: State of the art. *Progress in polymer science*, *37*, 1510-1551. doi:10.1016/j.progpolymsci.2012.03.002

127. Qian, L., & Zhang, H. (2011). Controlled freezing and freeze drying: a versatile route for porous and micro-/nano-structured materials. *Journal of Chemical Technology and Biotechnology*, 86, 172-184. doi:10.1002/jctb.2495
128. Alkayyali, T., Cameron, T., Haltli, B., Kerr, R. G., & Ahmadi, A. (2019). Microfluidic and cross-linking methods for encapsulation of living cells and bacteria - A review. *Analytica Chimica Acta*, 1053, 1-21. doi:10.1016/j.aca.2018.12.056
129. Jithendra, T., Reddy, O. S., Sunbha, M. C. S., & Rao, K. C. (2020). Fabrication of drug delivery system for controlled release of curcumin, intercalated with magnetite nanoparticles through sodium alginate/polyvinylpyrrolidone-co-vinyl acetate semi IPN microbeads. *International Journal of Advanced Pharmaceutics*, 12(5), 249-257. doi:10.22159/ijap.2020v12i5.37761
130. Schwalm, R. (2001). Photoinitiators and Photopolymerization. In K. H. Jürgen Buschow, R. W. Cahn, M. C. Flemings, B. Ilshner, E. J. Kramer, S. Mahajan, & P. Veysière (Eds.), *Encyclopedia of Materials: Science and Technology*. Amsterdam: Elsevier.
131. Tedesco, M., Lisa, D. D., Massobrio, P., Colistra, N., Pesce, M., Catelani, T., Dellacasa, E., Raiteri, R., Martinoia, S., & Pastorino, L. (2018). Soft chitosan microbeads scaffold for 3D functional neuronal networks. *Biomaterials*, 156, 159-171. doi:10.1016/j.biomaterials.2017.11.043
132. Pawar, H. A., Lalitha, K. G., & Ruckmani, K. (2015). Alginate beads of Captopril using galactomannan containing Senna tora gum, guar gum and locust bean gum. *International Journal of Biological Macromolecules*, 76, 119-131. doi:10.1016/j.ijbiomac.2015.02.026
133. Markovic, G., Marinovic-Cincovic, M., Jovanovic, V., Samarzija-Jovanovic, S., & Budinski-Simendic, J. (2016). Polymer characterization (II). In A. Mendez-Vilas & A. Solano-Martin (Eds.), *Polymer science: research advances, practical applications and educational aspects* (pp. 397-403). Spain: Formatex Research Center.
134. Wang, Y., Li, Y., Liu, S., & Li, B. (2015). Fabrication of chitin microspheres and their multipurpose application as catalyst support and adsorbent *Carbohydrate Polymers*, 120, 53-59. doi:10.1016/j.carbpol.2014.12.005
135. Sari, M. M., Armutcu, C., Bereli, N., Uzun, L., & Denizli, A. (2011). Monosize microbeads for pseudo-affinity adsorption of human insulin. *Colloids and Surfaces B: Biointerfaces*, 84, 140-147. doi:10.1016/j.colsurfb.2010.12.025
136. Benhalima, T., & Ferfera-Harrar, H. (2019). Eco-friendly porous carboxymethyl cellulose/dextran sulfate composite beads as reusable and efficient adsorbents of cationic dye methylene blue. *International Journal of Biological Macromolecules*, 132, 126-141. doi:10.1016/j.ijbiomac.2019.03.164
137. Wang, M., Ji, N., Li, M., Li, Y., Dai, L., Zhou, L., Xiong, L., & Sun, Q. (2020). Fabrication and characterization of starch beads formed by a dispersion-inverse gelation process for loading polyphenols with improved antioxidation. *Food Hydrocolloids*, 101, 105565. doi:10.1016/j.foodhyd.2019.105565
138. Hashide, R., Yoshida, K., Hasebe, Y., Takahashi, S., Sato, K., & Anzai, J. (2012). Insulin-containing layer-by-layer films deposited on poly(lactic acid) microbeads for

- pH-controlled release of insulin. *Colloids and Surfaces B: Biointerfaces*, 89, 242-247. doi:10.1016/j.colsurfb.2011.09.023
139. Höflinger, G. (2013). Brief Introduction to Coating Technology for Electron Microscopy. Retrieved from <https://www.leica-microsystems.com/science-lab/brief-introduction-to-coating-technology-for-electron-microscopy/#:~:text=Sputter%20coating%20prevents%20charging%20of,the%20signal%20to%20noise%20ratio>.
 140. Hari, B. N. V., Praneetha, T., Prathyusha, T., Mounika, K., & Devi, D. R. (2012). Development of Starch-Gelatin Complex Microspheres as Sustained Release Delivery System. *Journal of Advanced Pharmaceutical Technology & Research*, 3(3). doi:10.4103/2231-4040.101015
 141. Crnivec, I. G. O., Istenic, K., Skrt, M., & Ulrih, N. P. (2020). Thermal protection and pH-gated release of folic acid in microparticles and nanoparticles for food fortification. *Food & Function*, 11, 1467-1477. doi:10.1039/c9fo02419k
 142. Dutra, L., Nele, M., & Pinto, J. C. (2018). A Novel Approach for the Preparation of Poly(Butylene Succinate) Microparticles. *Macromolecular Symposia*, 381, 1800118. doi:10.1002/masy.201800118
 143. Okunlola, A., Odeku, O. A., & Patel, R. P. (2012). Formulation optimization of floating microbeads containing modified Chinese yam starch using factorial design. *Journal of Excipients and Food Chemicals*, 3(1), 19-25.
 144. Gore, P. M., Khurana, L., Dixit, R., & Balasubramanian, K. (2017). Keratin-Nylon 6 engineered microbeads for adsorption of Th (IV) ions from liquid effluents. *Journal of Environmental Chemical Engineering*, 5, 5655-5667. doi:10.1016/j.jece.2017.10.048
 145. Godoy, V., Martin-Lara, M. A., Calero, M., & Blazquez, G. (2019). Physical-chemical characterization of microplastics present in some exfoliating products from Spain. *Marine Pollution Bulletin*, 139, 91-99. doi:10.1016/j.marpolbul.2018.12.026
 146. Jakes, J. E., & Stone, D. S. (2021). Best Practices for Quasistatic Berkovich Nanoindentation of Wood Cell Walls. *Forests*, 12. doi:10.3390/f12121696
 147. West, B. F., Hottle, B. T., Jakes, J. E., Considine, J. M., Rowlands, R. E., & Turner, K. T. (2008). *Nanoindentation Studies of Paper*. Paper presented at the Conference for Progress in Paper Physics Otaniemi, Finland.
 148. Kim, S., Lee, S.-M., Lee, S. S., & Shin, D.-S. (2019). Microfluidic Generation of Amino-Functionalized Hydrogel Microbeads Capable of On-Bead Bioassay. *Micromachines*, 10, 527-536. doi:10.3390/mi10080527
 149. Azhar, U., Ahmed, Q., Alwahabi, Z., & Dai, S. (2020). Synthesis and spectroscopic study of dual self-encoded polymer microbeads with Raman scattering and surface-enhanced Raman scattering. *Journal of Raman Spectroscopy*, 51, 910-918. doi:10.1002/jrs.5863
 150. Mani, T., Blarer, P., Storck, F. R., Pittroff, M., Wernicke, T., & Burkhardt-Holm, P. (2019). Repeated detection of polystyrene microbeads in the Lower Rhine River. *Environmental Pollution*, 245, 634-641. doi:10.1016/j.envpol.2018.11.036
 151. Raddadi, N., & Fava, F. (2019). Biodegradation of oil-based plastics in the environment: Existing knowledge and needs of research and innovation. *Science of the Total Environment*, 679, 148-158. doi:10.1016/j.scitotenv.2019.04.419

152. Tristantini, D., & Yunan, A. (2018). Advanced characterization of microbeads replacement from cellulose acetate base on empty fruit branches and dried jackfruit leaves. *E3S Web of Conferences*, 67. doi:10.1051/e3sconf/20186704045
153. Choi, S.-H., Lee, K.-P., Kang, H.-D., & Park, H. G. (2004). Radiolytic Immobilization of Lipase on Poly(glycidyl methacrylate)-grafted Polyethylene Microbeads. *Macromolecular Research*, 12(6), 586-592. doi:10.1007/BF03218448
154. Robertson, I. (2020). *Attenuated Total Reflectance (ATR) Measurements into the Far-Infrared Spectral Region on a Multi-range FT-IR Spectrometer*. Retrieved from Seer Green, United Kingdom: https://resources.perkinelmer.com/labsolutions/resources/docs/APP_68164-Spectrum3.pdf
155. Zalasiewicz, J., Waters, C. N., Ivar do Sul, J. A., Corcoran, P. L., Barnosky, A. D., Cearreta, A., Edgeworth, M., Galuszka, A., Jeandel, C., Leinfelder, R., McNeill, J. R., Steffen, W., Summerhayes, C., Wagemann, M., Williams, M., Wolfe, A. P., & Yonah, Y. (2016). The geological cycle of plastics and their use as a stratigraphic indicator of the Anthropocene. *Anthropocene*, 13, 4-17. doi:10.1016/j.ancene.2016.01.002
156. MacLeod, M., Arp, H. P. H., Tekman, M. B., & Jahnke, A. (2021). The global threat from plastic pollution. *Science*, 373(6550), 61-65. doi:10.1126/science.abg5433
157. Barrett, J., Chase, Z., Zhang, J., Banaszak Holl, M. M., Willis, K., Williams, A., Hardesty, B. D., & Wilcox, C. (2020). Microplastic Pollution in Deep-Sea Sediments From the Great Australian Bight. *Frontiers in Marine Science*, 7. doi:10.3389/fmars.2020.576170
158. Cole, M., Lindeque, P., Halsband, C., & Galloway, T. S. (2011). Microplastics as contaminants in the marine environment: A review. *Marine Pollution Bulletin*, 62(12), 2588-2597. doi:10.1016/j.marpolbul.2011.09.025
159. Teuten, E. L., Saquing, J. M., Knappe, D. R. U., Barlaz, M. A., Jonsson, S., Bjarn, A., Rowland, S. J., Thompson, R. C., Galloway, T. S., Yamashita, R., Ochi, D., Watanuki, Y., Moore, C., Viet, P. H., Tana, T. S., Prudente, M., Boonyatumanond, R., Zakaria, M. P., Akkhavong, K., Ogata, Y., Hirai, H., Iwasa, S., Mizukawa, K., Hagino, Y., Imamura, M. S., & Takada, H. (2009). Transport and release of chemicals from plastics to the environment and to wildlife. *Philosophical Transactions of the Royal Society B: Biological Sciences*, 364, 2027-2045. doi:10.1098/rstb.2008.0284
160. Joint Group of Experts on the Scientific Aspects of Marine Environmental Protection. (2015). *Sources, Fate and Effects of Microplastics in the Marine Environment: a Global Assessment*. Retrieved from London: https://ec.europa.eu/environment/marine/good-environmental-status/descriptor-10/pdf/GESAMP_microplastics%20full%20study.pdf
161. Zitko, V., & Hanlon, M. (1991). Another source of pollution by plastics: Skin cleaners with plastic scrubbers. *Marine Pollution Bulletin*, 22(1), 41-42. doi:10.1016/0025-326X(91)90444-W
162. Fendall, L. S., & Sewell, M. A. (2009). Contributing to marine pollution by washing your face: Microplastics in facial cleansers. *Marine Pollution Bulletin*, 58, 1225-1228. doi:10.1016/j.marpolbul.2009.04.025

163. Duis, K., & Coors, A. (2016). Microplastics in the aquatic and terrestrial environment: sources (with a specific focus on personal care products), fate and effects. *Environmental Sciences Europe*, 28(2). doi:10.1186/s12302-015-0069-y
164. Murphy, F., Ewins, C., Carbonnier, F., & Quinn, B. (2016). Wastewater Treatment Works (WwTW) as a source of microplastics in the aquatic environment. *Environmental Science and Technology* 50, 5800-5808. doi:10.1021/acs.est.5b05416
165. Watkins, E., Schweitzer, J.-P., Leinala, E., & Börkey, P. (2019). *Policy Approaches to Incentivise Sustainable Plastic Design*. Retrieved from Paris: https://www.oecd-ilibrary.org/environment/policy-approaches-to-incentivise-sustainable-plastic-design_233ac351-en
166. *Cellulose Solvents: For Analysis, Shaping and Chemical Modification*. (2010). Washington, DC: American Chemical Society.
167. Frangville, C., Rutkevicius, M., Richter, A. P., Velez, O. D., Stoyanov, S. D., & Paunov, V. N. (2012). Fabrication of Environmentally Biodegradable Lignin Nanoparticles. *ChemPhysChem*, 13, 4235-4243. doi:10.1002/cphc.201200537
168. Österberg, M., Sipponen, M. H., Mattos, B. D., & Rojas, O. J. (2020). Spherical lignin particles: a review on their sustainability and applications. *Green Chemistry*, 22, 2712-2733. doi:10.1039/d0gc00096e
169. Luo, X., & Zhang, L. (2010). Creation of regenerated cellulose microspheres with diameter ranging from micron to millimeter for chromatography applications. *Journal of Chromatography A*, 1217, 5922-5929. doi:10.1016/j.chroma.2010.07.026
170. Roy, C., Budtova, T., & Navard, P. (2003). Rheological properties and gelation of aqueous cellulose - NaOH solutions. *Biomacromolecules*, 4(2), 259-264. doi:10.1021/bm020100s
171. Kjeldahl, J. (1883). Neue Methode zur Bestimmung des Stickstoffs in organischen Körpern. *Zeitschrift für analytische Chemie*, 22(1), 366-383.
172. Waters, D. M., Jacob, F., Titze, J., Arendt, E. K., & Zannini, E. (2012). Fibre, protein, and mineral fortification of wheat bread through milled and fermented brewer's spent grain enrichment. *European Food Research and Technology*, 235, 767-778. doi:10.1007/s00217-012-1805-9
173. Miao, P., Han, K., Tang, Y., Wang, B., Lin, T., & Cheng, W. (2015). Recent advances in carbon nanodots: synthesis, properties and biomedical applications. *Nanoscale*, 7, 1586-1595. doi:10.1039/c4nr05712k
174. El Korhani, O., Zaouk, D., Cerneaux, S., Khoury, R., Khoury, A., & Cornu, D. (2013). Synthesis and performances of bio-sourced nanostructured carbon membranes elaborated by hydrothermal conversion of beer industry wastes. *Nanoscale Research Letters*, 8, 121. doi:10.1186/1556-276X-8-121
175. Li, L., & Dong, T. (2018). Photoluminescence tuning in carbon dots: surface passivation or/and functionalization, heteroatom doping. *Journal of Materials Chemistry C*, 6, 7944-7970. doi:10.1039/c7tc05878k
176. El-Sakhawy, M., Kamel, S., Salama, A., & Sarhan, H.-A. (2018). Preparation and infrared study of cellulose based amphiphilic materials. *Cellulose Chemistry and Technology*, 52(3-4), 193-200. doi:10.1155/2014/575969

177. Oh, S. Y., Yoo, D. I., Shin, Y., Kim, H. C., Kim, H. Y., Chung, Y. S., Park, W. H., & Youk, J. H. (2005). Crystalline structure analysis of cellulose treated with sodium hydroxide and carbon dioxide by means of X-ray diffraction and FTIR spectroscopy. *Carbohydrate Research*, *340*, 2376-2391. doi:10.1016/j.carres.2005.08.007
178. Hill, S. J., Kirby, N. M., Mudie, S. T., Hawley, A., Ingham, B., Franich, R., & Newman, R. H. (2010). Effect of drying and rewetting of wood on cellulose molecular packing. *Holzforschung*, *64*(4), 421-427. doi:10.1515/HF.2010.065
179. Jee, A.-Y., & Lee, M. (2010). Comparative analysis on the nanoindentation of polymers using atomic force microscopy. *Polymer Testing*, *29*(1), 95-99. doi:10.1016/j.polymertesting.2009.09.009
180. Li, W., Zhai, Z. H., Pang, Q., Kong, Z. R., & Zhou, Z. R. (2013). Influence of exfoliating facial cleanser on the bio-tribological properties of human skin. *Wear*, *301*(1-2), 353-361. doi:10.1016/j.wear.2012.11.073
181. Manas, D., Ovsik, M., Mizera, A., Manas, M., Hylova, L., Bednarik, M., & Stanek, M. (2018). The Effect of Irradiation on Mechanical and Thermal Properties of Selected Types of Polymers. *Polymers*, *10*(2), 158. doi:10.3390/polym10020158
182. Kaupp, G., & Maimi-Jamal, M. R. (2011). Nutshells' mechanical response: from nanoindentation and structure to bionics models. *Journal of Materials Chemistry*, *21*, 8389-8400. doi:10.1039/C0JM03713C
183. Dong, B.-Y., Chen, Y.-F., Zhao, C.-C., Zhang, S.-J., Guo, X.-W., & Xiao, D.-G. (2013). Simultaneous Determination of Furfural, Acetic Acid, and 5-Hydroxymethylfurfural in Corn cob Hydrolysates Using Liquid Chromatography with Ultraviolet Detection. *Journal of AOAC International*, *96*(6), 1239-1244. doi:10.5740/jaoacint.12-290
184. Fillaudeau, L., Blanpain-Avet, P., & Daufin, G. (2006). Water, wastewater and waste management in brewing industries. *Journal of Cleaner Production*, *14*, 463-471. doi:10.1016/j.jclepro.2005.01.002
185. De Buck, V., Polanska, M., & Van Impe, J. (2020). Modeling Biowaste Biorefineries: A Review. *Frontiers in Sustainable Food Systems*, *14*(11). doi:10.3389/fsufs.2020.00011
186. Hejna, A., Formela, K., Barczewski, M., Kuang, T., & Saeb, M. R. (2022). Enhanced aging resistance of poly(ϵ -caprolactone)/brewers' spent grain composites. *Polymer/Polymers*, *67*(1), 3-12. doi:10.14314/POLIMERY.2022.1.1
187. Ji, X.-J., Huang, H., Nie, Z.-K., Qu, L., Xu, Q., & Tsao, G. T. (2012). Fuels and Chemicals from Hemicellulose Sugars. *Advances in Biochemical Engineering/Biotechnology*, *128*, 199-224. doi:10.1007/10_2011_124
188. Sahin, H. T. (2011). Evaluation of paper two sidedness with SEM/AFM microscope technique. *Wood Research*, *56*(2), 203-212.
189. Infrared Spectroscopy Lab. (2013). IR spectrum of sodium hydroxide. In *Transmission spectrum*. Woburn, MA.: Analytical Answers, Inc.
190. Shahabazuddin, M., Sarat Chandra, T., Meena, S., Sukumaran, R. K., Shetty, N. P., & Mudliar, S. N. (2018). Thermal assisted alkaline pretreatment of rice husk for enzymatic saccharification: Physico-chemical and structural characterization. *Bioresource Technology*, *263*, 199-206. doi:10.1016/j.biortech.2018.04.027

191. Chupa, J., Misner, S., Sachdev, A., & Smith, G. A. (2003). Soap, Fatty Acids, and Synthetic Detergents. In J. A. Kent (Ed.), *Riegel's Handbook of Industrial Chemistry* (pp. 1694-1741). Boston, MA: Springer.
192. Juma, N. G. (1999). *The Pedosphere and Its Dynamics: A Systems Approach to Soil Science*. (Vol. Volume 1: Introduction to soil science and soil resources). Sherwood Park, Canada: Salman Productions, University of Alberta.
193. Sideman, R. Growing Vegetables: Tomatoes [fact sheet]. *Agriculture & Gardens*. Retrieved from <https://extension.unh.edu/resource/growing-vegetables-tomatoes-fact-sheet-1#:~:text=Tomato%20plants%20will%20grow%20well,foliage%20but%20little%20fruit%20production>.
194. Tong, C. (2020). Growing onions in home gardens. *Yard and garden - Vegetables*. Retrieved from <https://extension.umn.edu/vegetables/growing-onions#:~:text=Onions%20grow%20best%20in%20well,according%20to%20soil%20test%20recommendations>
195. OECD. (2006). Test No. 208: Terrestrial Plant Test: Seedling Emergence and Seedling Growth Test. In *OECD Guidelines for the Testing of Chemicals, Section 2* (pp. 21). London: OECD.
196. Hitchin, J. R. (2022). The scale up of chemical reactions. *Nature Reviews Methods Primers*, 2. doi:10.1038/s43586-022-00116-8
197. Mettler Toledo. (2022). Chemical Process Development & Scale-Up: Creating Safe, Efficient Processes from Lab to Plant. *Applications*. Retrieved from https://www.mt.com/gb/en/home/applications/L1_AutoChem_Applications/L2_ProcessDevelopment.html
198. Hayward Flow Control. (2022). Chemical Resistance Guide. In *Technical Information* (pp. 195-206). Clemmons, USA: Hayward Industries, Inc.
199. Univar Solutions. (2021). Product Catalog. Retrieved from <https://www.univarsolutions.com/product-catalog>
200. Botanic Planet. (2022). Raw Materials for Cosmetics. Retrieved from <https://www.botanicplanet.ca/raw-materials-canada-usa>
201. Weidmann Fiber Technology. (2022). What are cellulose powders? *Product Specification*. Retrieved from <https://weidmannfibertechnology.com/products/#CellulosePowders>
202. Business Insider. (2022). *Ethanol*. Retrieved from: <https://markets.businessinsider.com/commodities/ethanol-price>
203. Index Mundi. (2022). *Urea Monthly Price - Canadian Dollar per Metric Ton*. Retrieved from: <https://www.indexmundi.com/commodities/?commodity=urea&months=60¤cy=cad>
204. Sigma Aldrich. (2022). Analytical Reagents. *Products*. Retrieved from <https://www.sigmaaldrich.com/CA/en/products/analytical-chemistry/analytical-reagents>
205. OECD. (1992). Test No. 301: Ready Biodegradability. In *OECD Guidelines for the Testing of Chemicals, Section 3* (pp. 62). London: OECD.

206.OECD. (1992). Test No. 306: Biodegradability in Seawater. In *OECD Guidelines for the Testing of Chemicals, Section 3* (pp. 27). London: OECD.

